

**AD-753 650**

# **Development of Composite Constructions with Improved Rain Erosion Resistance**

**Hughes Aircraft Co.**

**prepared for  
Naval Air Systems Command**

**JANUARY 1973**

**Distributed By:**



**National Technical Information Service  
U. S. DEPARTMENT OF COMMERCE**

AD 758650  
**DEVELOPMENT OF COMPOSITE CONSTRUCTIONS  
WITH IMPROVED RAIN EROSION RESISTANCE**

BY  
BOYCE G. KIMMEL  
HUGHES AIRCRAFT COMPANY  
AEROSPACE GROUP

JANUARY 1973

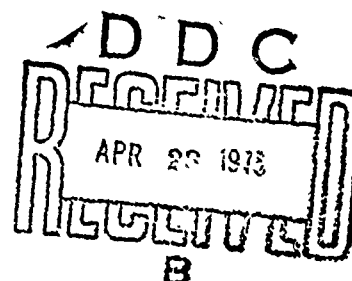
FINAL SUMMARY REPORT

Prepared Under  
Naval Air Systems Command  
Contract No. N00019-72-C-0257  
Materials and Processes Branch  
Washington, D.C. 20360

Report No. 1000  
NATIONAL TECHNICAL  
INFORMATION SERVICE  
U.S. GOVERNMENT

Details of illustrations in  
this document may be better  
studied on microfiche

APPROVED FOR PUBLIC RELEASE;  
DISTRIBUTION UNLIMITED



**UNCLASSIFIED**

Security Classification

**DOCUMENT CONTROL DATA - R & D**

(Security classification of title, body of abstract and indexing annotation must be entered when the overall report is classified)

1 ORIGINATING ACTIVITY (Corporate author) Hughes Aircraft Company Culver City, California 90230		2a. REPORT SECURITY CLASSIFICATION Unclassified
2b. GROUP		
3 REPORT TITLE Development of Composite Constructions with Improved Rain Erosion Resistance		
4. DESCRIPTIVE NOTES (Type of report and inclusive dates) Final Summary Report, 1 December 1971 to 31 December 1972		
5 AUTHOR(S) (First name, middle initial, last name) Boyce G. Kimmel		
6 REPORT DATE January 1973		7a. TOTAL NO. OF PAGES <del>114</del> 126
8a. CONTRACT OR GRANT NO N00019-72-C-0257		7b. NO. OF REFS 0
b. PROJECT NO.		9a. ORIGINATOR'S REPORT NUMBER(S) P73-43
c.		9b. OTHER REPORT NO(S) (Any other numbers that may be assigned this report)
d.		
10 DISTRIBUTION STATEMENT Approved for public release; distribution unlimited		
11 SUPPLEMENTARY NOTES Details of institutions on this document may be better studied on microfiche		12 SPONSORING MILITARY ACTIVITY Naval Air Systems Command Washington, D.C. 20360
13 ABSTRACT  This report describes the continued investigation of composite constructions with improved rain erosion resistance. The studies included the effect on the rain erosion resistance as determined by whirling arm tests of such variables as matrix, reinforcement, reinforcement configuration, fiber loading, impact angle and fiber angle. Matrices evaluated included rigid epoxies, flexibilized epoxies, polyurethanes, polyphenylene oxide, polybutadiene and polyimide. Reinforcements included ECG glass, SCG glass, Nomex and Dacron. Most of the work involved the evaluation of reinforcements in unidirectionally reinforced, end-oriented composites. However, a limited effort was also expended in evaluating multi-dimensional fabrics. The test results show that, with respect to rain erosion resistance, polymeric fibers are superior to glass fibers, high fiber loadings are superior to low fiber loadings, one polymeric multidimensional construction to be far superior to several tested.		

**Best  
Available  
Copy**

**UNCLASSIFIED**

Security Classification

14. KEY WORDS	LINK A		LINK B		LINK C	
	ROLE	WT	ROLE	WT	ROLE	WT
Rain erosion						
Composites erósin						
Plastics erosion						
End-oriented composites						
Three-dimensional composites						

REPORT NO. P73-43  
HAC REF. NO. C6212

# DEVELOPMENT OF COMPOSITE CONSTRUCTIONS WITH IMPROVED RAIN EROSION RESISTANCE

BY  
BOYCE G. KIMMEL  
HUGHES AIRCRAFT COMPANY  
AEROSPACE GROUP

JANUARY 1973

FINAL SUMMARY REPORT

Prepared Under  
Naval Air Systems Command  
Contract No. N00019-72-C-0257  
Materials and Processes Branch  
Washington, D.C. 20380

Approved By: L. B. Keller  
L. B. KELLER  
Manager, Materials and Processes Laboratory  
Equipment Engineering Divisions  
Culver City, California

APPROVED FOR PUBLIC RELEASE;  
DISTRIBUTION UNLIMITED

## FOREWORD

The work described in this report was performed by Hughes Aircraft Company, Equipment Engineering Divisions, Culver City, California under Contract N00019-72-C-0257 under the technical management of Mr. Maxwell Stander, Materials and Processes Branch, Code AIR-52032D, Naval Air Systems Command, Washington, D.C. 20360.

This report covers work from 1 December 1971 to 31 December 1972. Previous work on this program was performed under Contracts N00019-70-C-0315 and N00019-71-C-0167 covering the period from 1 April 1970 to 1 November 1971.

The assistance of Mr. J. R. Shackleton of Ground Systems Group, Hughes Aircraft Company, Fullerton, California in preparing the scanning electron micrographs and Mr. A. A. Castillo in preparing the composite moldings is gratefully acknowledged.

## CONTENTS

ABSTRACT . . . . .	1
SUMMARY . . . . .	3
INTRODUCTION . . . . .	5
EXPERIMENTAL . . . . .	7
Rain Erosion Testing . . . . .	7
Specimen Preparation . . . . .	8
Impregnation of Reinforcements . . . . .	8
Plasma Etching of Reinforcements . . . . .	9
Molding Procedure . . . . .	10
Machining of Specimens . . . . .	10
Determination of Composition and Void Content . . . . .	14
Rain Erosion Test Results . . . . .	14
Effect of Matrix . . . . .	14
Effect of Reinforcement . . . . .	15
Reinforcement Configuration . . . . .	15
Effect of Hardener Concentration . . . . .	15
Effect of Fiber Loading (Nomex-Epon 828/MPDA) . . . . .	109
Effect of the Fiber Angle and Impact Angle . . . . .	109
Effect of Glass Finish and Dielectric Filler . . . . .	110
Electrical Properties . . . . .	110
AFML Whirling Arm Test Results . . . . .	111
Radome Fabrication . . . . .	113

## LIST OF ILLUSTRATIONS

Figure		Page
1	Roving Wound on Frame .....	9
2	Frame Assembly with Impregnated Roving in Place .....	11
3	Molding of Unidirectional Composite .....	12
4	Composite Bar Cured in Channel Mold.....	13
5	ECG Glass Roving - P13N Polyimide, End-oriented (Reinforcement Content - 66.9 volume-percent).....	17
6	ECG Glass Roving - Epon 825/Versamid 140 (65/35), End-oriented (Reinforcement Content = 77.0 volume-percent) .	18
7	ECG Glass Roving - Epon 825/Versamid 140 (55/45), End- oriented (Reinforcement Content = 74.7 volume-percent). . . .	19
8	Scanning Electron Micrographs of Specimen EP-9A (ECG-Epon 825/Versamid 140, 55/45, end-oriented) .....	20
9	ECG Glass Roving - Epon 825/Versamid 140 (80/20), End- oriented (Reinforcement Content = 77.1 volume-percent). . . .	27
10	ECG Glass Roving - Uralane 5716, End-oriented (Reinforcement Content = 73.7 volume-percent).....	28
11	ECG Glass Yarn, A174 Sizing-FCR 1261-TM303 Polybutadiene, End-oriented (Reinforcement Content = 77.3 volume-percent) .....	29
12	Quartz Roving, 9073 Sizing-FCR 1261-TM303 Polybutadiene, End-oriented (Reinforcement Content = 75.1 volume-percent) .....	30
13	ECG Glass Roving - 534-801 Polyphenylene Oxide, End- oriented (Reinforcement Content = 74.2 volume-percent). . . .	31
14	ECG Glass Roving - 534-801 Polyphenylene Oxide Cross- linked with Benzenetrisulfonyl Chloride, End-oriented (Reinforcement Content = 79.1 volume-percent). . . .	32
15	ECG Glass Roving - Epon 828/Hycar/piperidine, End- oriented (Reinforcement Content = 75.3 volume-percent). . . .	33

## LIST OF ILLUSTRATIONS (Continued)

Figure	Page
16 Nomex 1200 Denier Yarn - Epon 828/MPDA, End-oriented (Reinforcement Content = 78.6 volume-percent) . . . . .	35
17 Nomex 1200 Denier Yarn - Epon 828/Versamid 140, End-oriented (Reinforcement Content = 78.5 volume-percent) . . . . .	36
18 Scanning Electron Micrographs of Specimen N-3A (Nomex-Epon 825/Versamid 140, end-oriented) . . . . .	37
19 Nomex 1200 Denier Yarn - Epon 828/Menthane Diamine/MPDA/BDMA, End-oriented (Reinforcement Content = 79.5 volume-percent) . . . . .	41
20 Scanning Electron Micrographs of Specimen N-6B (Nomex-Epon 825/Menthane Diamine/MPDA/BDMA, end-oriented) . . .	42
21 Nomex 1200 Denier Yarn - Epon 828/Hycar/piperidine, End-oriented (Reinforcement Content = 78.6 volume-percent) . . . . .	45
22 Scanning Electron Micrographs of Specimen N-8B (Nomex-Epon 828/Hycar/piperidine, end-oriented) . . . . .	46
23 PRD-49 Type I, 400 Denier Yarn - Epon 828/MPDA, End-oriented (Reinforcement Content = 65.6 volume-percent) . . . . .	52
24 PRD-49 Type I, 400 Denier Yarn (Plasma-treated) - Epon 825/Versamid 140, End-oriented (Reinforcement Content - 76.8 volume-percent) . . . . .	53
25 Dacron 1100 Denier Yarn - Epon 828/MPDA, End-oriented (Reinforcement Content = 75.3 volume-percent) . . . . .	54
26 Scanning Electron Micrographs of Specimen DA-1B (Dacron-Epon 828/MPDA, end-oriented) . . . . .	55
27 Dacron 1100 Denier Yarn - Epon 828/MPDA, End-oriented (Reinforcement Content = 38.6 volume-percent) . . . . .	58
28 Dacron 1100 Denier Yarn (Plasma-treated) - Epon 828/MPDA, End-oriented (Reinforcement Content = 73.6 volume-percent) . . . . .	59
29 Omniweave 341-52BA (3-D Fabric) (SCG Glass, Type S1014) - Epon 828/MPDA (Reinforcement Content = 42.3 volume-percent)	61
30 Omniweave 337-04AA (3-D Fabric) (Nomex 1200 Denier Yarn) - Epon 828/MPDA (Reinforcement Content = 53.8 volume-percent)	62
31 Nomex Fabric Type 3105-Epon 825/Versamid 140 (55/45) (Reinforcement Content = 60.7 volume-percent, not end-oriented)	63
32 Omniweave 337-04AA (3-D Fabric) (Nomex 1200 Denier Yarn) - Epon 825/Versamid 140 (Reinforcement Content = 49.6 volume-percent) . . . . .	64

## LIST OF ILLUSTRATIONS (Continued)

Figure		Page
33	PRD-49 Type III 3-D Orthogonal Construction (Plasma-treated) - Epon 828/MPDA . . . . .	65
34	PRD-49 Type III 3-D Orthogonal Fabric - Epon 828/ Menthane Diamine (Reinforcement Content = 57.3 volume-percent) . . . . .	66
35	ECG Glass Roving - Epon 828/MPDA (Fresh, 1.4 times stoichiometric), End-oriented (Reinforcement Content = 75.0 volume-percent) . . . . .	68
36	ECG Glass Roving - Epon 828/MPDA (Fresh, Stoichiometric), End-oriented (Reinforcement Content = 73.1 volume-percent) . . . . .	69
37	ECG Glass Roving - Epon 828/MPDA (Fresh, 1.6 times Stoichiometric), End-oriented (Reinforcement Content = 75.0 volume-percent) . . . . .	70
38	ECG Glass Roving - Epon 828/MPDA (Fresh, 1.2 times Stoichiometric), End-oriented (Reinforcement Content = 75.7 volume-percent) . . . . .	71
39	ECG Glass Roving - Epon 828/MPDA (Old, 1.4 times Stoichiometric), End-oriented (Reinforcement Content = 74.8 volume-percent) . . . . .	72
40	ECG Glass Roving - Epon 828/MPDA (Old, Stoichiometric), End-oriented (Reinforcement Content = 69.6 volume- percent) . . . . .	73
41	ECG Glass Roving - Epon 828/MPDA (Fresh, Stoichiometric), End-oriented (Reinforcement Content = 75.8 volume- percent) . . . . .	74
42	Nomex 1200 Denier Yarn - Epon 828/MPDA, End- oriented (Reinforcement Content = 64.0 volume-percent) . . . . .	77
43	Scanning Electron Micrographs of Specimen N-4A (Nomex Epon 828/MPDA, end-oriented) . . . . .	78
44	Nomex 1200 Denier Yarn - Epon 828/MPDA, End-oriented (Reinforcement Content = 52.4 volume-percent) . . . . .	82
45	Nomex 1200 Denier Yarn - Epon 828/MPDA, End-oriented (Reinforcement Content = 80.3 volume-percent) . . . . .	83
46	Nomex 1200 Denier Yarn - Epon 828/MPDA, End-oriented (Reinforcement Content = 35.3 volume-percent) . . . . .	84
47	Nomex 1200 Denier Yarn - Epon 828/MPDA, End-oriented (Reinforcement Content = 41.2 volume-percent) . . . . .	85

## LIST OF ILLUSTRATIONS (Continued)

Figure		Page
48	Nomex 1200 Denier Yarn - Epon 828/MPDA, End-oriented (Reinforcement Content = 45.4 volume-percent) . . . . .	86
49	Nomex 1200 Denier Yarn (Plasma-treated) - Epon 828/MPDA, End-oriented (Reinforcement Content = 41.2 volume- percent) . . . . .	87
50	Nomex 1200 Denier Yarn (Plasma-treated) - Epon 828/MPDA, End-oriented (Reinforcement Content = 76.8 volume- percent) . . . . .	88
51	ECG Glass Roving - Epon 828/MPDA, End-oriented (Reinforcement Content = 76.1 volume-percent). . . . .	90
52	ECG Glass Roving - Epon 828/MPDA, End-oriented (Reinforcement Content = 76.1 volume-percent). . . . .	91
53	ECG Glass Roving - Epon 828/MPDA, End-oriented (Reinforcement Content = 76.1 volume-percent). . . . .	92
54	ECG Glass Roving - Epon 828/MPDA, End-oriented (Reinforcement Content = 76.1 volume-percent). . . . .	93
55	ECG Glass Roving - Epon 828/MPDA, End-oriented (Fiber Angle = 90°). . . . .	94
56	ECG Glass Roving - Epon 828/MPDA, End-oriented (Fiber Angle = 60°) . . . . .	95
57	ECG Glass Roving - Epon 828/MPDA, End-oriented (Fiber Angle = 45°). . . . .	96
58	ECG Glass Roving - Epon 828/MPDA, End-oriented (Fiber Angle = 30°). . . . .	97
59	Nomex 1200 Denier Yarn - Epon 828/MPDA, End-oriented (Average Reinforcement Content = 35.3 volume-percent). . . .	99
60	Nomex 1200 Denier Yarn - Epon 828/MPDA, End-oriented (Average Reinforcement Content = 35.3 volume-percent). . . .	100
61	Nomex 1200 Denier Yarn - Epon 828/MPDA, End-oriented (Average Reinforcement Content = 40.6 volume-percent). . . .	101
62	Nomex 1200 Denier Yarn - Epon 828/MPDA, End-oriented (Average Reinforcement Content = 40.6 volume-percent). . . .	102
63	Nomex 1200 Denier Yarn - Epon 828/MPDA, End-oriented (Reinforcement Content = 45.8 volume-percent). . . . .	103
64	Nomex 1200 Denier Yarn - Epon 828/MPDA, End-oriented (Reinforcement Content = 45.8 volume-percent) . . . . .	104

## LIST OF ILLUSTRATIONS (Continued)

Figure		Page
65	ECG 37 1/0 Glass Yarn, Starch-oil Sizing with Epon 828/MPDA, End-oriented (Reinforcement Content = 77.0 volume-percent) . . . . .	106
66	ECG Glass Roving, 801 Sizing with Epon 828/MPDA, End-oriented (Reinforcement Content = 77.1 volume-percent) . . . . .	107
67	ECG Glass Roving, Epon 828/MPDA, Filled with Titanium Dioxide, End-oriented (Reinforcement Content = 77.3 volume-percent) . . . . .	108
68	PRD-49 Type III, Epon 828/Methane Diamine (AFML Airfoil Specimens) . . . . .	112
69	Experimental Radome Structures Fabricated from 3-D PRD-49/epoxy . . . . .	114

## LIST OF TABLES

Table	Page
1 Relative Rain Erosion Resistance of Various Matrices (Unidirectional, End-oriented ECG, SCG or Quartz Roving) . . . . .	16
2 Relative Rain Erosion Resistance of Various Matrices (Unidirectional, End-oriented Nomex Yarn) . . . . .	34
3 Relative Rain Erosion Resistance of Various Reinforcements (Epon 828/MPDA, Unidirectional, End-oriented) . . . . .	51
4 Relative Rain Erosion Resistance of Various Reinforcement Configurations (Matrix: Epon 828/MPDA, Except as Noted; Reinforcement SCG Glass, Nomex or PRD-49) . . . . .	60
5 Relative Rain Erosion Resistance of Epon 828/MPDA-ECG Glass Roving, End-oriented Composites with Various Hardener Contents (All Specimens Exposed 30 Seconds at 333 Meters/Second) . . . . .	67
6 Relative Rain Erosion Resistance of Epon 828/MPDA- Nomex, End-oriented Composites with Various Fiber Loadings (All Specimens Tested at 333 Meters/Second). . . . .	75
7 Effect of Fiber Angle and Impact Angle on Relative Rain Erosion Resistance of Epon 828/MPDA-ECG Glass, End- oriented Composites (All Specimens Tested at 300 Meters/Second) . . . . .	89
8 Effect of Fiber Angle and Impact Angle on Relative Rain Erosion Resistance of Epon 828/MPDA-Nomex, End-oriented Composites (All Specimens Tested at 333 Meters/Second) . . . . .	98
9 Effect of Glass Cloth Finish and Dielectric Filler on Rain Erosion Resistance of End-oriented, Fiber-reinforced Composites (ECG-Epon 828/MPDA) . . . . .	105
10 Dielectric Properties of Unidirectional, Fiber-reinforced Plastics Composites (Frequency = 9.28 GHz). . . . .	111

## ABSTRACT

This report describes the continued investigation of composite constructions with improved rain erosion resistance. The studies included the effect on the rain erosion resistance as determined by whirling arm tests of such variables as matrix, reinforcement, reinforcement configuration, fiber loading, impact angle and fiber angle. Matrices evaluated included rigid epoxies, flexibilized epoxies, polyurethanes, polyphenylene oxide, polybutadiene and polyimide. Reinforcements included ECG glass, SCG glass, Nomex and Dacron. Most of the work involved the evaluation of reinforcements in unidirectionally reinforced, end-oriented composites. However, a limited effort was also expended in evaluating multidimensional fabrics. The test results show that, with respect to rain erosion resistance, polymeric fibers are superior to glass fibers and high fiber loadings are superior to low fiber loadings. One polymeric multidimensional construction was shown to be far superior to several others tested.

## SUMMARY

This technical report covers the third year's effort in the development of fiber-reinforced composites with improved resistance to rain erosion at near-sonic or supersonic speeds. The development of improved composite constructions and their successful application in aircraft radome structures will allow substantial cost savings through less frequent repair and replacement.

The program consisted of the determination of the relative rain erosion resistance of a large number of fiber-reinforced plastics composites by whirling arm tests conducted at Dornier Systems, GmbH, West Germany. The variables evaluated included matrix, reinforcement, reinforcement configuration, fiber loading, impact angle and fiber angle. The following types of specimens were evaluated:

- A standard epoxy matrix combined with various unidirectional reinforcements including ECG glass, SCG glass, Nomex, Dacron and PRD-49.
- A standard epoxy matrix combined with various multidimensional constructions.
- ECG glass, SCG glass or quartz fibers combined with various matrices.
- Nomex fibers combined with various epoxy matrices.
- Glass fiber-reinforced, end-oriented epoxy composites at various impact angles and fiber angle with respect to the specimen surface.
- Nomex fiber-reinforced, end-oriented epoxy composites at various impact angles and fiber angles.

In addition, the dielectric constant and loss tangent at 9.28 gHz were calculated from resonant cavity electrical measurements made on several composite systems which showed promising rain erosion resistance.

The results of the rain erosion tests showed that rain erosion resistance is substantially increased by the use of polymeric fibers such as Nomex or Dacron, high fiber loadings and flexibilized matrices such as flexibilized epoxies or polyurethanes. End-oriented composites reinforced with Nomex fibers were found to have excellent rain erosion resistance for brittle, rigid or flexibilized matrices. One multidimensional construction woven from Nomex was found to be fairly rain erosion resistant, far more so than a corresponding construction woven from S glass.

## INTRODUCTION

Rain erosion tests performed for the U. S. Navy by the University of Cincinnati\* have demonstrated the superior rain erosion resistance of end-oriented fiber-reinforced plastics composites when compared with the conventional, fabric-reinforced composites.

Further study of end-oriented plastic composites at Hughes Aircraft Company under Navy Contracts N00019-70-C-0315 and N00019-71-C-0167 has confirmed the superior rain erosion resistance of end-oriented plastics. On the other hand, highly directionally reinforced composites fabricated from three-dimensional fabrics and directional fabrics so as to contain a large fraction of end-oriented fibers were found to be no more rain erosion resistant than conventional, fabric-reinforced composites.

Degree of fiber loading was found to have a profound effect on the rain erosion resistance of unidirectionally-reinforced, end-oriented, epoxy-glass composites. Epoxy-glass composites with high fiber loadings (greater than 70 volume-percent) were found to be highly rain erosion resistant, though apparently subject to localized erosion by spallation.

Lower fiber loadings are permissible for polymeric fibers such as Nomex (polyaromatic nylon) or Dacron (polyethylene terephthalate). End-oriented composites containing these fibers are not subject to spallation as are the end-oriented composites reinforced with glass fibers.

Tough, flexibilized matrices were found to be more rain erosion resistant than rigid matrices when reinforced with glass fibers. Nomex fibers, on the other hand, appear to give composites with good rain erosion resistance whether combined with rigid or tough, flexibilized matrices.

---

\*Progress Report, Dept. of Mechanical Engineering, University of Cincinnati, "Testing of Rain Erosion Resistance," 19 September 1968.

Based on the results of the previous work at Hughes, further activities were concentrated on composites containing polymeric fibers, lower fiber loadings consistent with those achievable in radome structures, fiber finishes for polymeric fibers, and the effect of fiber angle and impact angle on Nomex-reinforced composites.

## EXPERIMENTAL

### RAIN EROSION TESTING

Most of the rain erosion tests were run in the whirling arm facility operated by Dornier System GmbH, Friedrichshafen, West Germany.

Dornier's apparatus consists essentially of a rotor driven by a powerful electric motor. The rotor is contained inside a chamber which may be partially evacuated as required for high testing speeds. Water drops of the required size and quantity are injected into the chamber at eight points around the periphery. The specimen holder can be adjusted to allow impact angles ranging from 15 to 90 degrees.

The specimens consist of circular discs 16.75 mm (0.660 inch) in diameter by 5.08 mm (0.200 inch) maximum thickness. The specimen is secured to a specimen holder at the end of the rotor by means of a retaining ring. During the test, one face of the specimen is subjected to simulated rain erosion under controlled test conditions. All of the specimens evaluated during this reporting period were tested under the following conditions:

- Velocity - 300 or 333 meters/second
- Droplet diameter - 1.2 mm
- Impact angle - 30 to 90 degrees
- Exposure time - 10 to 120 seconds
- Rain density -  $1.2 \times 10^{-5}$  (equivalent to a rainfall rate of 7.5 inches per hour)

Prior to testing, the weight and thickness of each specimen are measured and recorded. The responses measured for a given exposure time are weight loss and erosion depth. In addition, the specimens are examined visually, with specimens of particular interest also being examined with the

aid of a scanning electron microscope. Repeated weight loss measurements of the same specimen are not made for various exposure times. Instead, one or more sets of specimens machined from the same composite are subjected to different exposure times.

Rain erosion tests were also run on one material of interest in the whirling arm facility at AFML. The test conditions used were a velocity of 500 mph, and a simulated rainfall rate of one inch/hour with an average rain-drop diameter of 1.8 mm.

## SPECIMEN PREPARATION

### Impregnation of Reinforcements

The 3-D (three-dimensional) fabrics were pre-impregnated with the epoxy resin system using a vacuum-pressure impregnation process. Prior to impregnation, a piece of the fabric was encased in a closely fitting shell of polycarbonate film by vacuum forming. After cutting a number of slits in the film to allow resin penetration, the encased fabric was placed in a small container and subjected to vacuum (pressure - 0.02 torr) for one hour to remove residual volatiles. The Epon 828-MPDA mixture, preheated to 140°F, was added under vacuum until the fabric was immersed in resin. The vacuum was released and the pressure was increased to 90 psig and held for two hours. The resin was allowed to gel for 16 hours at 175°F and was cured for two hours at 325°F. After chipping away the excess resin, the polycarbonate parting film was removed. The final composition and void content of the glass reinforced composites were determined by resin burnoff and density measurements made on a small section of the cured composite. The composition of the Nomex 3-D composites was calculated from the known density of the unimpregnated 3-D fabric with the assumption that the packing function of this material is not changed by the impregnation and curing procedure.

A procedure was developed to allow the impregnation of rovings or yarns after winding on a series of frames. A specified number of turns of roving is wound on each of several frames as shown in Figure 1. During winding, the portions of the fibers nearest the frame spools are coated with RTV silicone rubber, leaving a 4-inch long uncoated center section. After

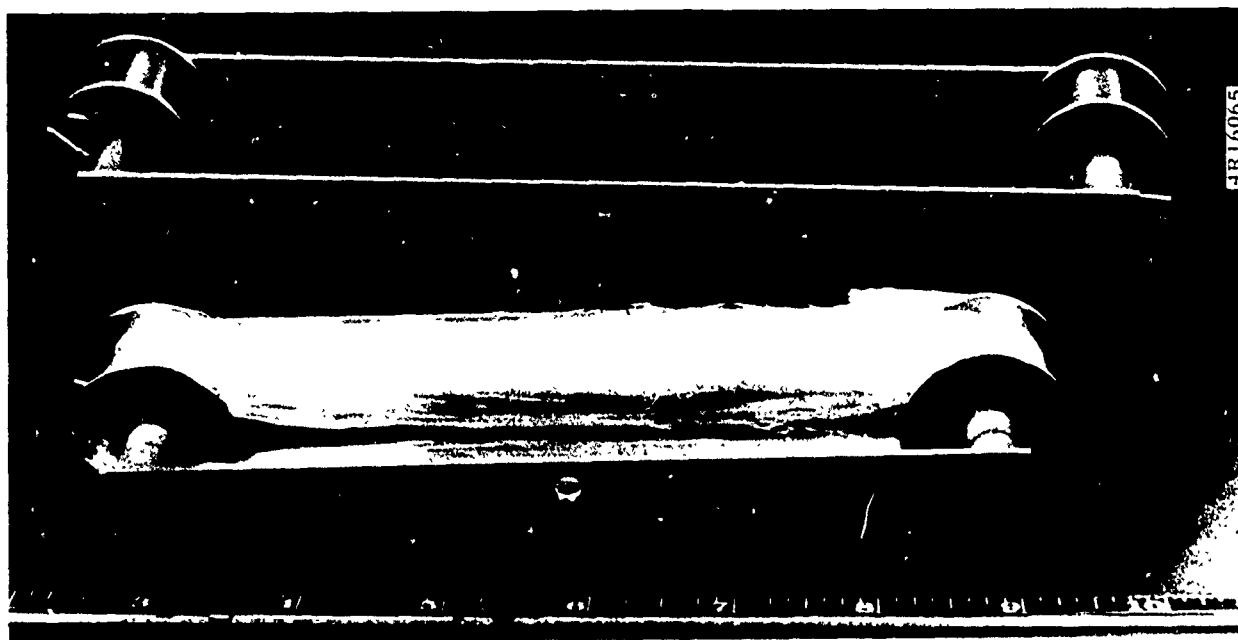


Figure 1. Roving wound on frame.

curing the RTV, the fiber loops are removed from the frames and vacuum-pressure impregnated with the resin system. In practice, the fiber loops are bent into a U-shape and placed, with the uncoated portion of the fibers downward, in a small beaker. The vacuum-pressure impregnation consists of covering the fiber loops with the resin while under vacuum and then increasing the pressure to 90-100 psig. Some very viscous resins with short pot lives cannot be heated to lower the viscosity and do not penetrate to the center of the fiber bundles. In this case, the fibers are spread and the resin is applied manually with a small brush to aid in wetting the fibers. This hand application of resin supplements the vacuum-pressure impregnation and may be performed before or after.

#### Plasma Etching of Reinforcements

Three polymeric fibers (in the form of roving or 3-D fabric), Nomex, Dacron and PRD-49, were subjected to a low pressure plasma in an attempt to promote adhesion between the fiber and the matrix. The apparatus consists essentially of a small, glass chamber containing a low pressure gas which is continuously subjected to radio frequency by electrodes located outside the

vacuum chamber. The resulting plasma reacts with the surface layers of the material being treated, usually resulting in improved bondability of typical organic polymers. The device (International Plasma Corporation's "Plasma Machine") is equipped to allow plasma treatment with different gases. The Nomex, Dacron and PRD-49 fibers were etched for 2 minutes with air at a pressure of 2 torr and 15 minutes with helium at a pressure of 15 torr. Each reinforcing material was etched immediately after winding and before impregnation with the epoxy resin.

#### Molding Procedure

The loops of impregnated fibers are then secured by wire hooks in a frame assembly as shown in Figure 2. Tension is applied by a spring on the stem of the eye loop on the outside of the frame. The tension is adjusted by the nut on the stem to approximately 40 pounds.

After the impregnated roving is centered in the mold cavity, the frame is unclamped from the press. The punch is positioned in the cavity and the press closed to apply pressure to the layup as shown in Figure 3. Usually, shims are placed between the cavity and the punch to allow the molding of a composite of closely controlled thickness and composition. The mold shown in Figure 3 has more rigid sides than a previously used mold, eliminating movement of the fibers between the cavity walls and punch which sometimes occurred with the previous mold. The cavity of the present mold is much deeper, permitting loading of high bulk materials.

A typical molded composite bar is shown immediately after being removed from the mold (Figure 4). The center molded portion is nominally 3 inches long with a cross section approximately three-quarters of an inch square.

#### Machining of Specimens

The excess material is cut away from the molded composite leaving an oblong bar approximately 3 inches long. After cutting a quarter-inch section from each end and discarding, a half-inch long piece is then cut from the remaining material for determination of density and resin content.



Figure 2. Frame assembly with impregnated roofing felt being applied.

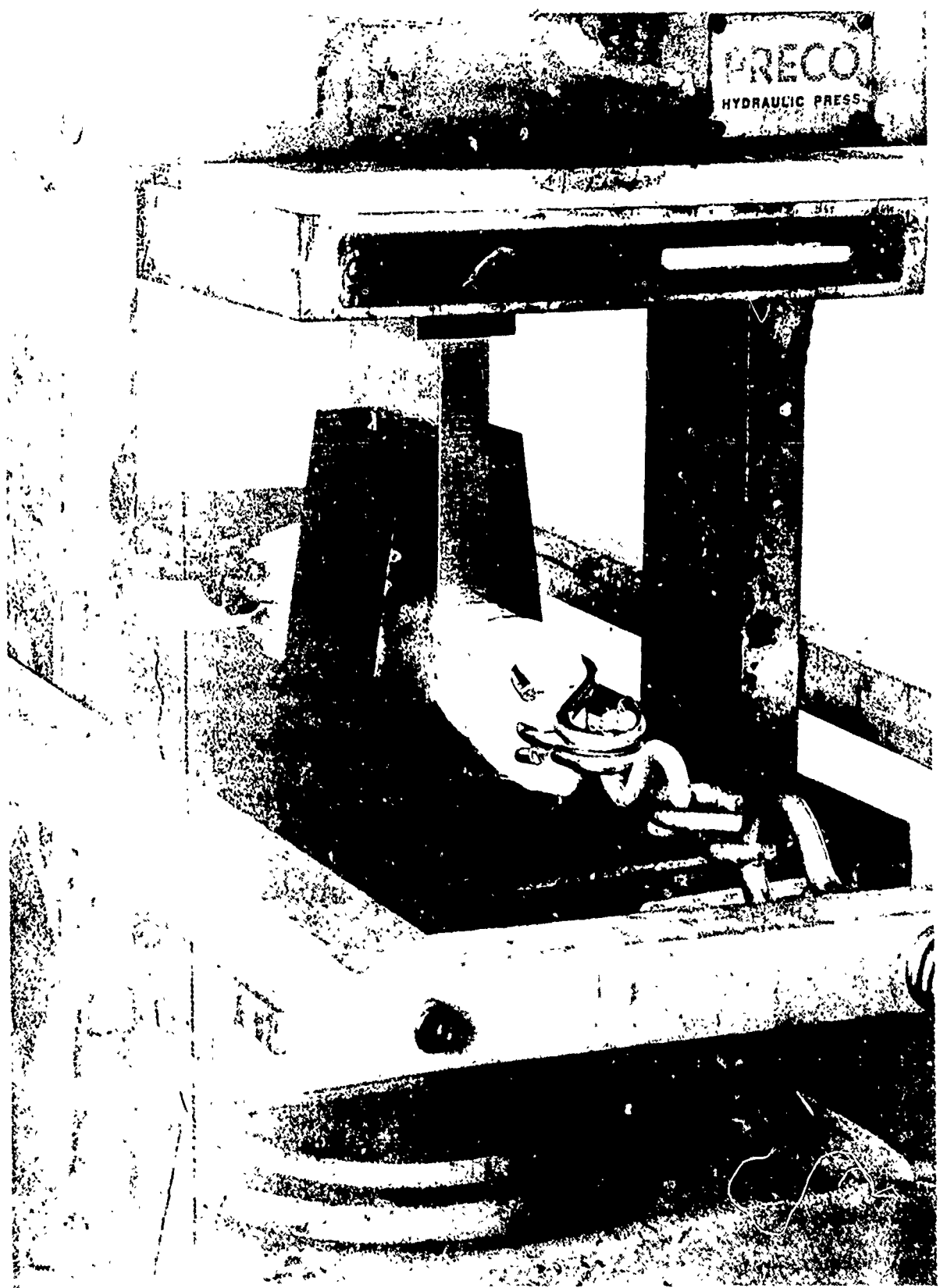


Fig. 8 unidirectional composite (scale 1:2).

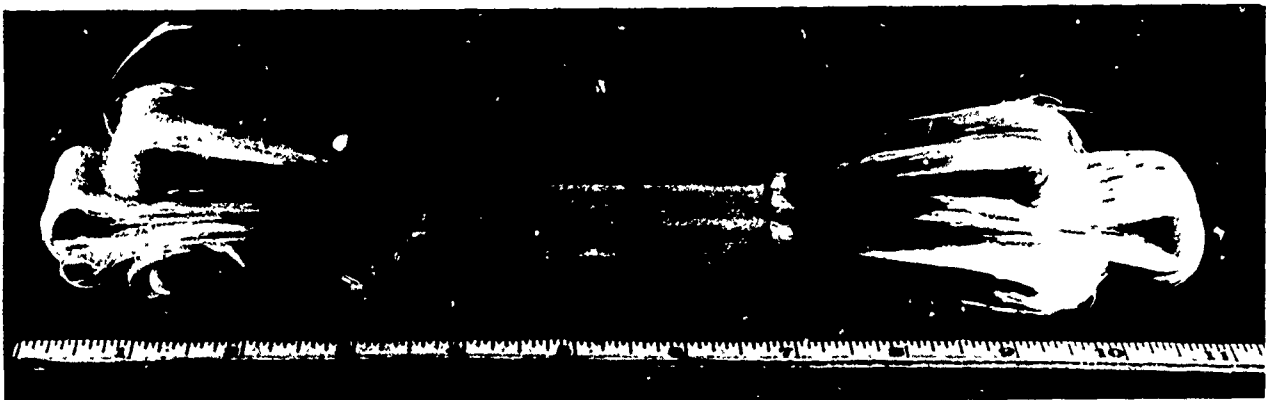


Figure 4. Composite bar cured in channel mold.

The remaining material is chucked in a lathe and ground to a diameter of 0.660 inch. Individual specimens are cut off with a diamond saw mounted in a tool post grinder. Finally, one surface of each specimen is surface ground to obtain the final thickness of 0.200 inch. Profilometer inspection has shown the surface roughness to vary from 11 to 14 microinches.

Specimens are machined from composites prepared from the 3-D fabrics with the specimen face parallel to the original surface of the tape. Sufficient material is machined from the surface layer to remove any fabric construction details present at or near the surface resulting in a specimen surface with the maximum degree of end-oriented fibers corresponding to the construction details of the interior of the fabric. Of course the reinforcing fibers in such composites are only partially end-oriented. In addition, the angle interlock fabrics give composites in which the fibers intersect the surface at angles considerably less than 90 degrees. Nevertheless, composites prepared from such reinforcements can be considered to be end-oriented.

Prior to submission for rain erosion testing, the thickness and weight of each specimen are measured and recorded. The nominal weight of most of the glass-epoxy specimens is approximately 2 grams prior to testing.

Relatively large, unidirectionally reinforced moldings (1-1/8 inches thick by 3 inches by 6 inches) were also made for electrical measurements in a resonant cavity dielectrometer. Moldings were made successfully from Epon 828-MPDA reinforced, respectively, with E glass, Nomex, Dacron and PRD-49 fibers.

Airfoil specimens were also made from PRD-49 Type III 3-D fabric and epoxy resin for rain erosion tests conducted by AFML in their whirling arm apparatus. The fabrication process consisted of vacuum bagging and curing a wet layup of the fabric and resin system in a female epoxy splash mold.

#### Determination of Composition and Void Content

The composition of each molded, unidirectional composite is controlled closely to the desired value by molding to a fixed volume impregnated roving or yarn with a known weight per unit length for the unimpregnated reinforcement. The actual composition of the composites containing siliceous reinforcements is determined by ignition analysis. This composition and the densities of the composite, reinforcement and cured matrix are used to calculate the void content.

### RAIN EROSION TEST RESULTS

The results of the rain erosion tests performed by Dornier are summarized in Tables 1 through 9. The figure references in each table refer to photographs and/or scanning electron micrographs (SEMs) of exposed test specimens. Test results along with photographs and SEMs are included for a large number of test specimens submitted under the preceding contract. Although weight loss data received from Dornier was previously reported, the exposed test specimens were not available for examination until after the period of performance of the preceding contract.

The following conclusions have been drawn from the test results and from examination of the exposed test specimens.

#### Effect of Matrix

Only the epoxies (rigid or flexibilized) and a polyurethane were found to have fair to good rain erosion resistance when combined with end-oriented glass fibers. Other matrices which had poor rain erosion resistance included a polyimide, a polybutadiene, a polyphenylene oxide, a cross-linked polyphenylene oxide and an epoxy containing a carboxy terminated butadiene-acrylonitrile copolymer (B. F. Goodrich's Hycar CBTN) as a toughening agent.

Several matrices were shown to have good rain erosion resistance when combined with end-oriented Norlex fibers. These included, besides the standard Epon 828/MPDA, Epon 825/Versamid 140, Epon 828/menthane diamine/MPDA/BDMA and Epon 828/Hycar/piperidine. The various Nomex-reinforced composites varied substantially in the degree to which cracking occurred. The Epon 828/MPDA specimens (Figures 16, 42, 45, 46, 47 and 48) appeared slightly deformed, possibly from the high centrifugal loads imposed during the test. In some cases (e.g., specimen No. N-2A, Figure 16), dimensional changes prevented removal of the specimen from the specimen holder without severely damaging it.

#### Effect of Reinforcement

Three polymeric fibers, Dupont's Nomex, Dacron and PRD-49, are compared in the form of end-oriented, fiber-reinforced composites in Table 3. The weight loss of the Dacron-reinforced composite was comparable to that of the Nomex composite. However, the Dacron specimens (Figure 25) were only slightly cracked near the edges compared with extensive cracking of the Nomex specimen (Figure 16). The PRD-49 specimens were moderately eroded with most of the erosion occurring in the region of a number of fine cracks which covered the specimens prior to rain erosion testing.

#### Reinforcement Configuration

The results obtained on Omniweave multidimensional constructions woven from Nomex and S glass showed the Nomex (Figure 30) to be far superior to the S glass (Figure 29) when combined with the standard Epon 828/MPDA matrix. A composite consisting of the Nomex Omniweave combined with a flexibilized epoxy (Figure 32) also had relatively good erosion resistance. A conventional laminate consisting of Nomex fabric combined with a flexibilized epoxy (Figure 31) was deeply eroded after a 30 second exposure.

#### Effect of Hardener Concentration

Figures 35-41 show the results obtained from end-oriented, epoxy-glass specimens made from various Epon 828/MPDA formulations (previous

TABLE I. RELATIVE RAIN EROSION RESISTANCE OF VARIOUS MATRICES  
(UNIDIRECTIONAL, END-ORIENTED ECG, SCG OR QUARTZ ROVING)

Specimen Code	Matrix-Roving	Reinforcement Content, volume-percent	Void Content, percent	Velocity, meters/sec	Exposure Time, sec	Weight Loss, mg	Erosion Depth, mils	Appearance	Figure Refs.
PL-1A PL-1B	P13N polyimide-ECG, 801 sizing	66.9	0.5	333	30	567	-	Extremely eroded	5
EP-8A EP-8B	Epon 825/Versamid 140 (65/45)-ECG, 801 sizing	77.0	0.8	333	30	192	0.4	Deeply eroded	6
EP-9A EP-9B	Epon 825/Versamid 140 (55/45)-ECG, 801 sizing	74.7	0	333	30	249	0.2	Scattered pitting Deeply eroded	7, 8
EP-11A EP-11A	Epon 825/Versamid 140 (80/20)-ECG, 801 sizing	77.1	1.0	333	30	126	0.5	Deeply eroded	9
U-2A U-2B	Uralane 5716-ECG, 801 sizing	73.3	0	333	60	589	3.3	Extremely eroded	10
PB-1A PB-1B	FCR 1261-TM 303 polybutadiene-ECG, A174 sizing	77.3	0.4	333	60	147	0.5	Slightly eroded Locally Deeply eroded Locally	11
PB-2A PB-2B	FCR 1261-TM 303 polybutadiene-quartz 9073 sizing	75.1	1.8	300	30	507	14.9	Extremely eroded Extremely eroded; broken in half	11
PO-1A	Polyphenylene oxide 534-801-ECG, 801 sizing	74.2	5.8	333	30	536	22.9	Broken into many pieces Broken into many pieces	12
PO-1B	PFO 534-801 cross-linked with benzene trisulfurylchloride-ECG, 801 sizing	79.1	4.1	333	10	*	-	Specimen completely eroded away	13
PO-2A	PFO 534-801				30	*	-	Specimen completely eroded away	14
PO-2B					10	-	-	Extremely eroded	
EP-10A EP-10B	Epon 828/Hycar/piperidine-ECG, 801 sizing	75.3	0	333	30	82	0.1	Deeply eroded	15

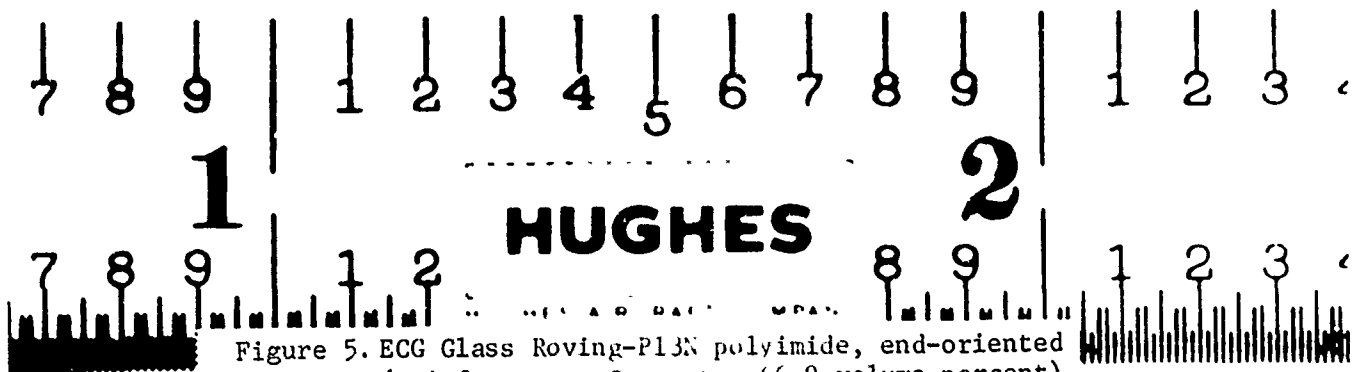
<sup>a</sup>Weight loss could not be determined.



a. Specimen No. PI-1A, 30 seconds  
at 333 meters/second



b. Specimen No. PI-1B, 30 seconds  
at 333 meters/second





a. Specimen No. EP-8A, 30 seconds  
at 333 meters/second



b. Specimen No. EP-8B, 60 seconds  
at 333 meters/second



c. Unexposed Control

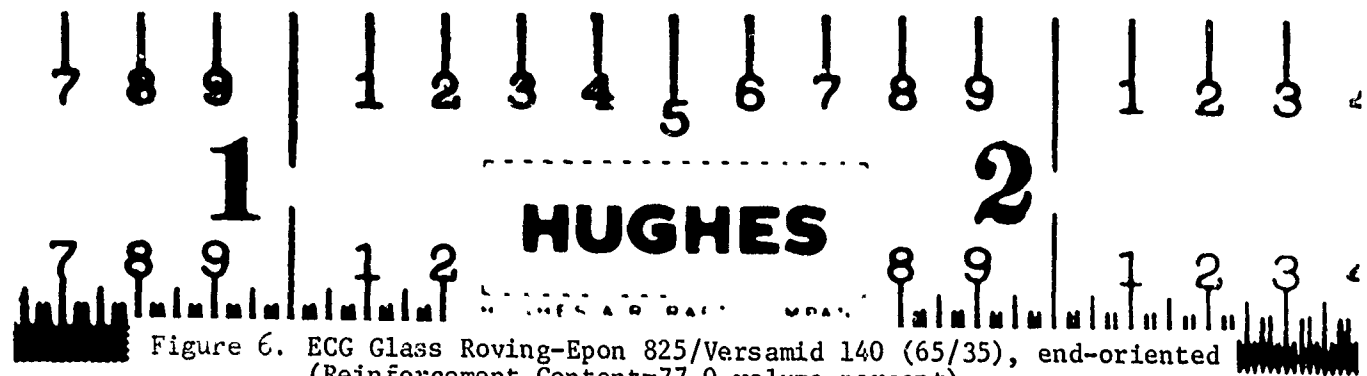
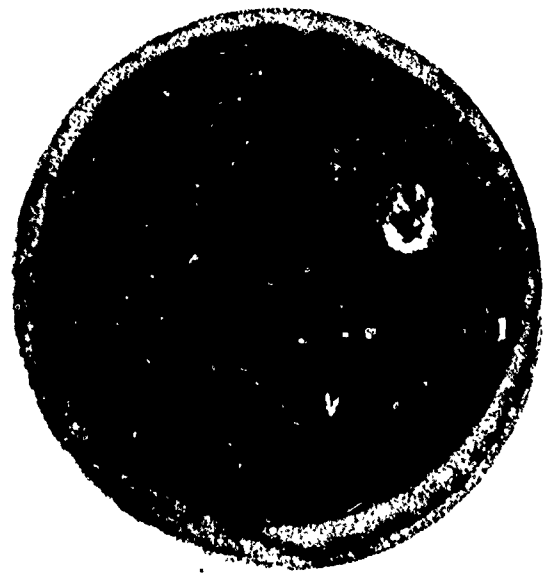


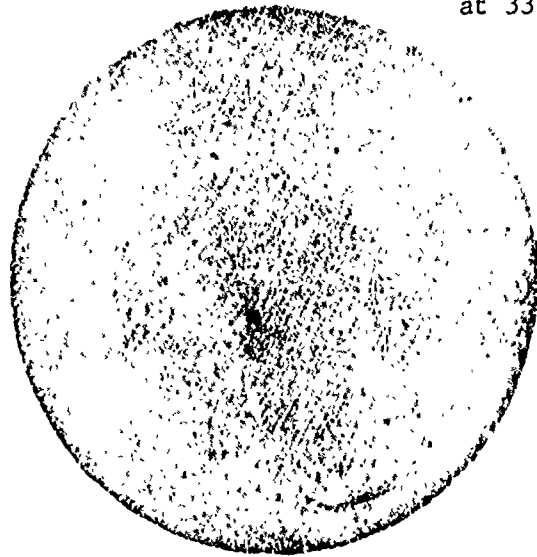
Figure 6. ECG Glass Roving-Epon 825/Versamid 140 (65/35), end-oriented  
(Reinforcement Content=77.0 volume-percent)



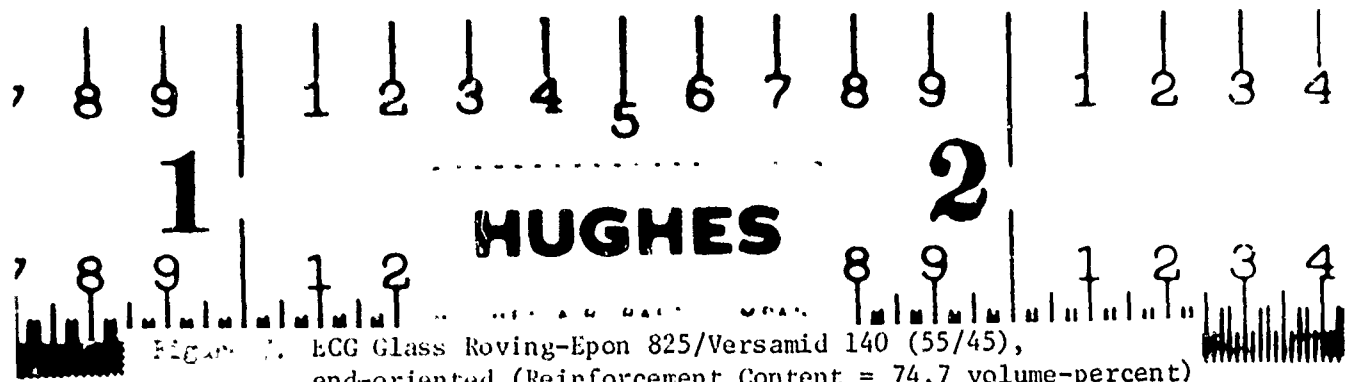
a. Specimen No. EP-9A, 30 seconds  
at 333 meters/second



b. Specimen No. EP-9B, 60 seconds  
at 333 meters/second



c. Unexposed Control



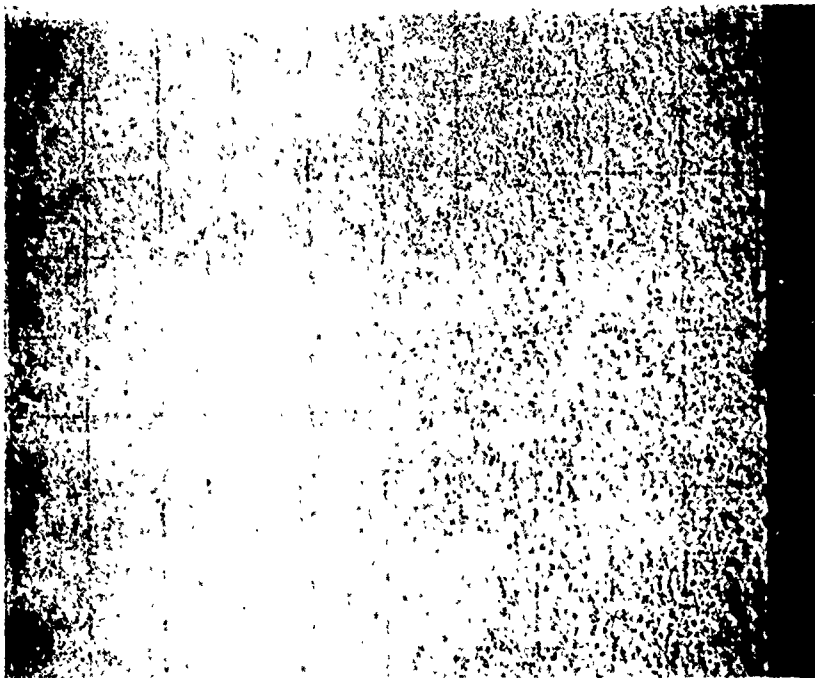
SET DATA

2017-1-21

SPECTRUM  $\propto t^{-1 - \gamma/4}$

DATE 28 Ma

**OPERATOR**



Magnification 100 X

Angle of View 45°

Inv. No.        Sec.

Coating Am

### Operating Conditions

Accel. Potent. 25

### Condenser Lets

Obj. Lens \_\_\_\_\_

Detector Type

## Settings

Massachusetts and

area and uneroded  
area



NEG I DENT A (

Magnification 100 $\times$

Angle of View 45°

Det. Mode Suz

#### Operating Conditions:

Accel Patent 25

#### Condenser Lens

#### Obi Lens

Detector Type

## Settings

Petroleum

area

**Figure 8**

**Micrographs of Specimen EP-9A  
(in the  $\beta$ -transformation-undifferentiated)**

NEG IDENT AZ

SEM DATA

REQUEST # 7215  
SPECIMEN EP-9A

DATE 28 Mar  
OPERATOR JLS



Magnification 5000  
Angle of View 45°  
Det. Mode sec  
Coating Ar

Operating Conditions:  
Accel. Potent. 25 kv  
Condenser Lens \_\_\_\_\_  
Obj. Lens \_\_\_\_\_  
Detector Type \_\_\_\_\_  
Settings \_\_\_\_\_

Erosion in pit



NEG IDENT A3  
Magnification 2500  
Angle of View 45°  
Det. Mode sec  
Coating Ar

Operating Conditions:  
Accel. Potent. 25 kv  
Condenser Lens \_\_\_\_\_  
Obj. Lens \_\_\_\_\_  
Detector Type \_\_\_\_\_  
Settings \_\_\_\_\_

Erosion in pit

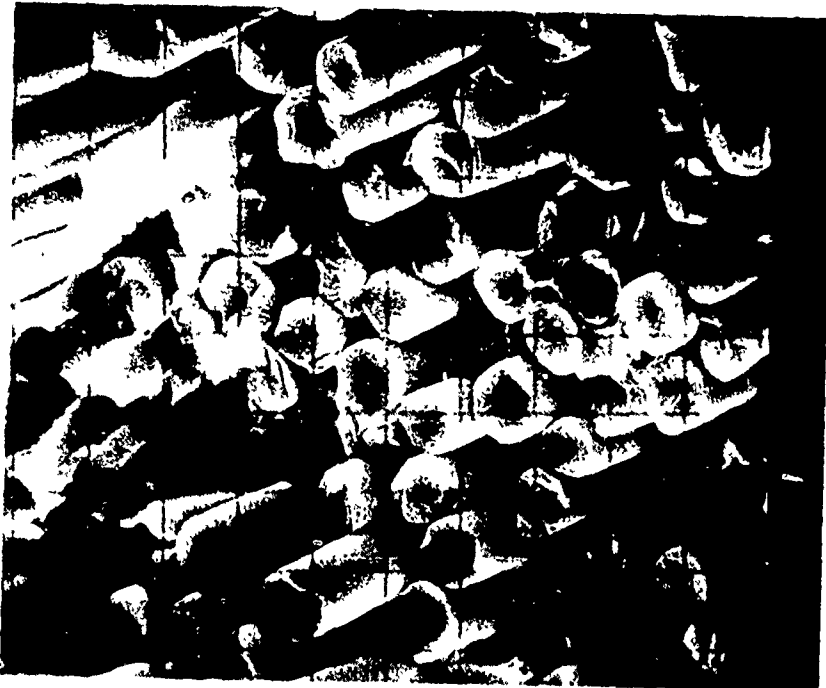
NEG IDENT A4

Figure 8. Scanning electron Micrographs of specimen EP-9A  
(Cont.) (ECG-Epon 825/Versamid 140, 55/45, end-oriented)

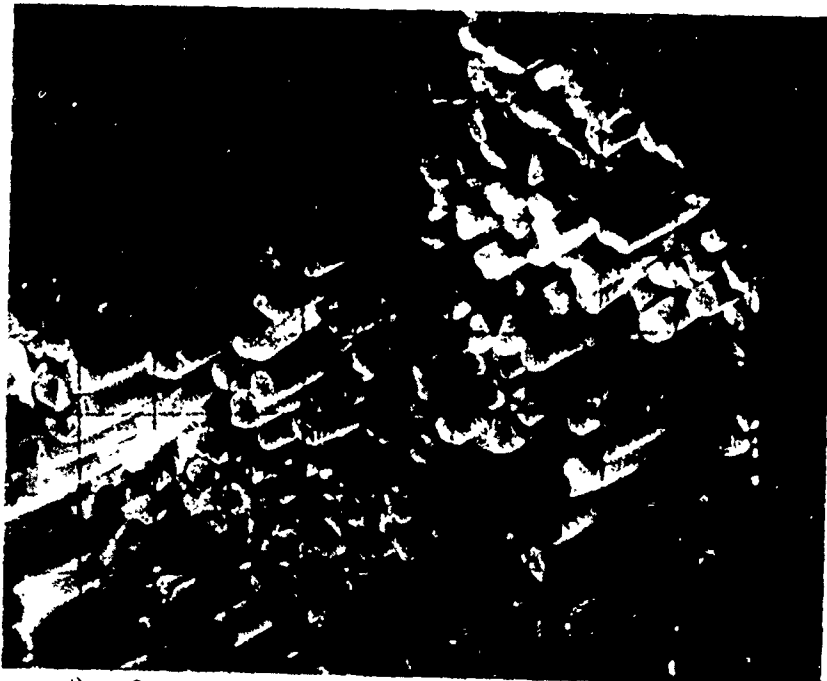
SEM DATA

REQUEST # 7215  
SPECIMEN EP-9A

DATE 28 Mar  
OPERATOR JRL



Magnification 1000  
Angle of View 45°  
Det. Mode sec  
Coating An  
  
Operating Conditions:  
Accel. Potent. 25 kv  
Condenser Lens \_\_\_\_\_  
Obj. Lens \_\_\_\_\_  
Detector Type \_\_\_\_\_  
Settings \_\_\_\_\_  
  
Erosion in pit



NEG IDENT A5  
Magnification 500  
Angle of View 45°  
Det. Mode Sec  
Coating An  
  
Operating Conditions:  
Accel. Potent. 25 kv  
Condenser Lens \_\_\_\_\_  
Obj. Lens \_\_\_\_\_  
Detector Type \_\_\_\_\_  
Settings \_\_\_\_\_  
  
Erosion in pit

Figure 8. Scanning electron Micrographs of specimen EP-9A  
(cont) (ECG-Epon 825/Versamid 140, 55/45, end-oriented)

Neg Ident A15

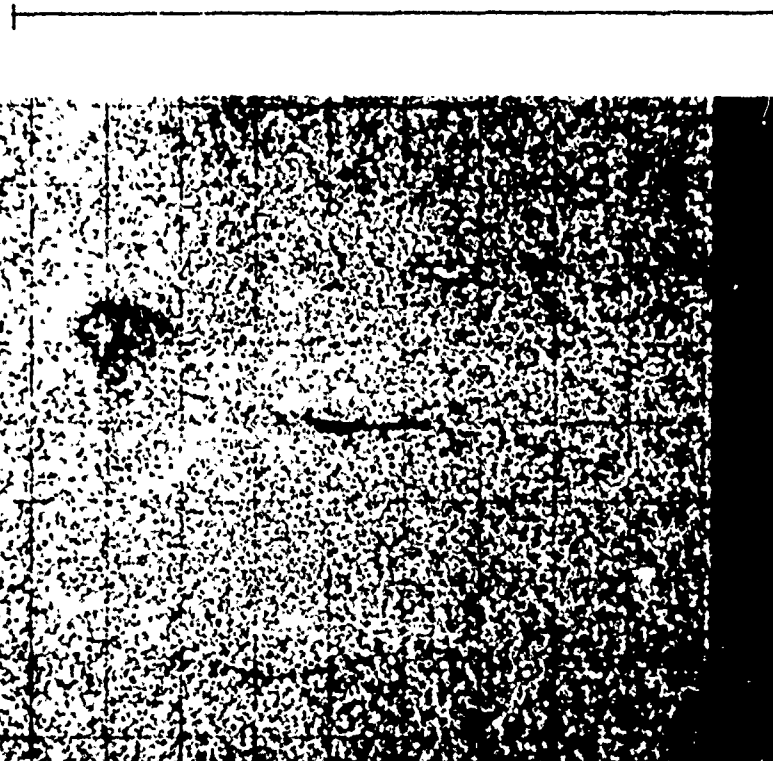
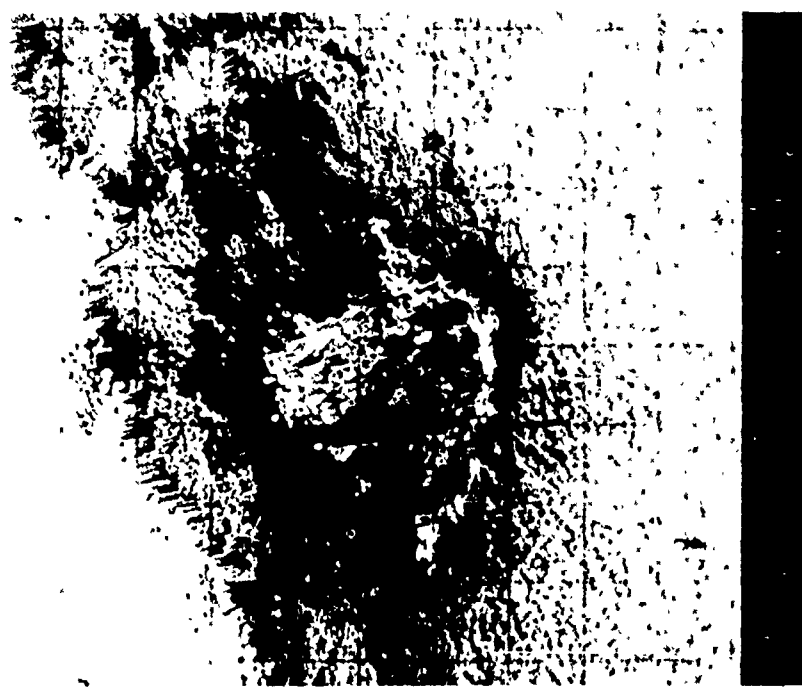
SEI DATA

REQUEST # 7215

SPECIMEN EP-9A

DATE 28 Mar

OPERATOR JRL



Magnification 100

Angle of View 45°

Det. Mode sc

Coating An

Operating Conditions:

Accel. Potent. 25 kv

Condenser Lens

Obj. Lens

Detector Type

Settings

Erosion in pit

NEG IDENT A6

Magnification 100

Angle of View 0°

Det. Mode sc

Coating An

Operating Conditions:

Accel. Potent. 25 kv

Condenser Lens

Obj. Lens

Detector Type

Settings

'Rill' on surface of specimen

NEG IDENT A9

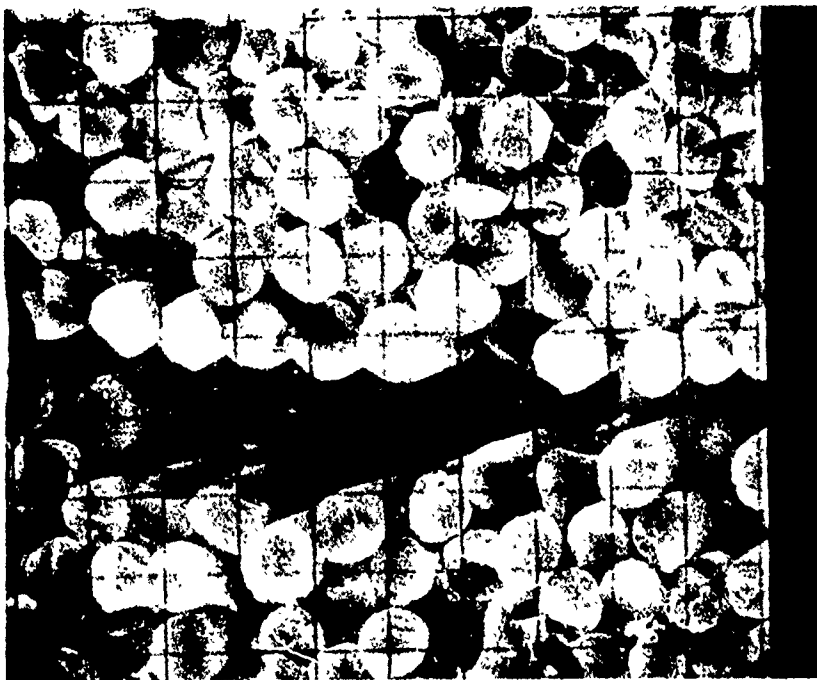
Figure 3. Scanning electron Micrographs of specimen EP-9A  
(Cont.) (ECG-Epon 825/Versamid 140, 55/45, end-oriented)

SEM DATA

REQUEST # 7215  
SPECIMEN EP-9A

DATE 28 Mar

OPERATOR JRL



Magnification 1000

Angle of View 20°

Det. Mode rec

Coating An

Operating Conditions:

Accel. Potent. 25 kv

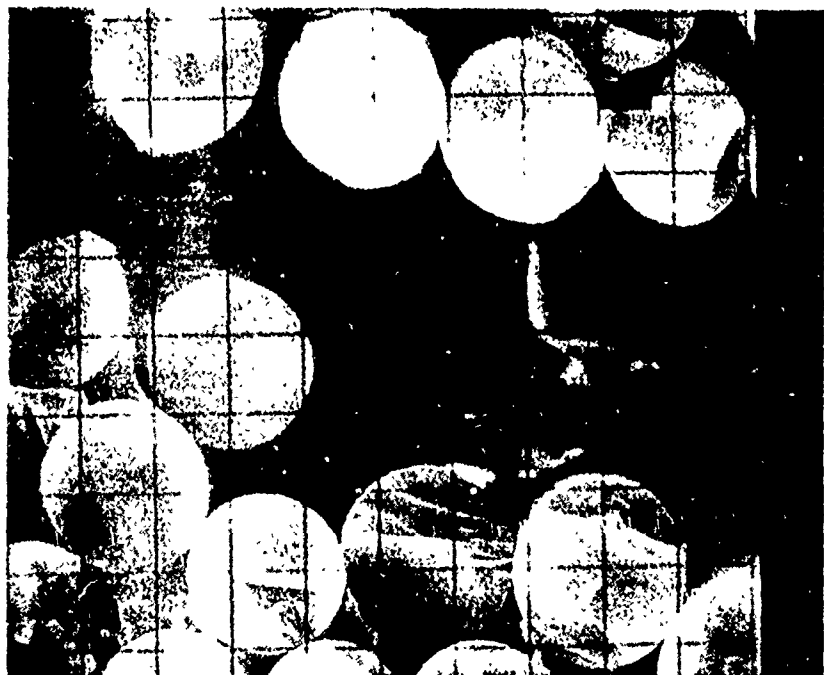
Condenser Lens

Obj. Lens

Detector Type

Settings

View into Rill (so A7)



NEG IDENT A7

Magnification 2500

Angle of View 0°

Det. Mode rec

Coating An

Operating Conditions:

Accel. Potent. 25 kv

Condenser Lens

Obj. Lens

Detector Type

Settings

View into Rill

Figure 8. Scanning electron Micrographs of specimen EP-9A  
(Cont.) (ECG-Epon 825/Versamid 140, 55/45, end-oriented)

Neg Ident A8

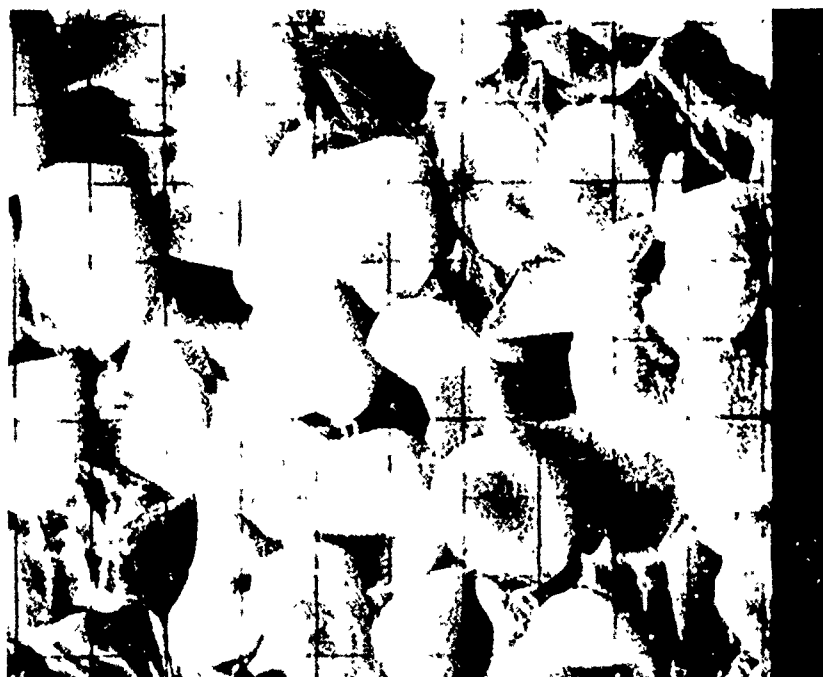
SEM DATA

REQUEST # 7215  
SPECIMEN EP-9A

DATE 28 May  
OPERATOR JRF



Magnification 5000  
Angle of View 45°  
Det. Mode sec  
Coating An  
  
Operating Conditions:  
Accel. Potent. 25 kv  
Condenser Lens \_\_\_\_\_  
Obj. Lens \_\_\_\_\_  
Detector Type \_\_\_\_\_  
Settings \_\_\_\_\_  
Eroded Area



NEG IDENT A10  
Magnification 2500  
Angle of View 45°  
Det. Mode Sec  
Coating An  
  
Operating Conditions:  
Accel. Potent. 25 kv  
Condenser Lens \_\_\_\_\_  
Obj. Lens \_\_\_\_\_  
Detector Type \_\_\_\_\_  
Settings \_\_\_\_\_  
Eroded area

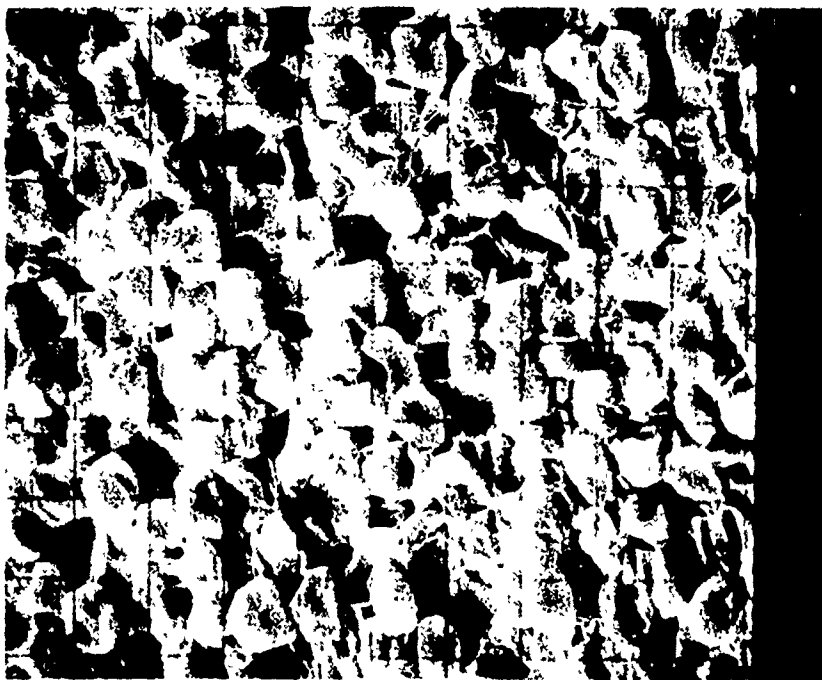
Figure 6. Scanning electron Micrographs of specimen EP-9A  
(Cont.) (ECG-Epon 825/Versamid 140, 55/45, end-oriented)

NEG IDENT A12

SEM DATA

REQUEST # 7215  
SPECIMEN EP-9A

DATE 28 Mar  
OPERATOR JRD



1

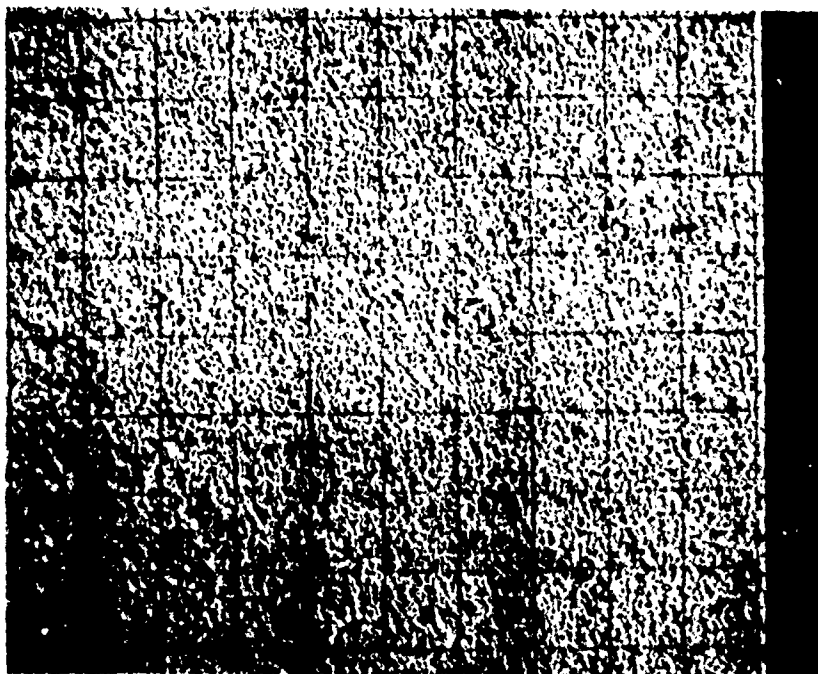
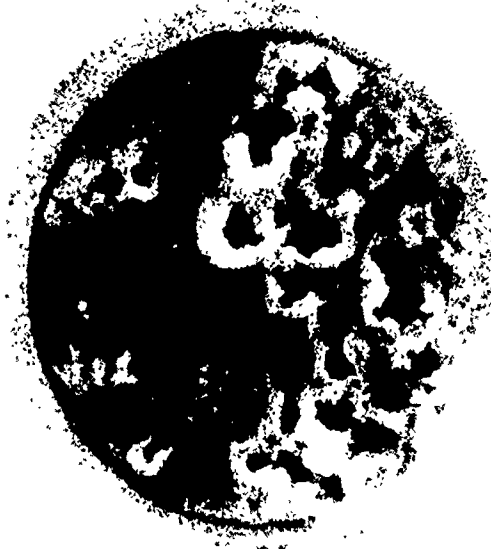


Figure 8. Scanning electron Micrographs of specimen EP-9A  
(cont) (ECG-Epon 825/Versamid 140, 55/45, end-oriented)

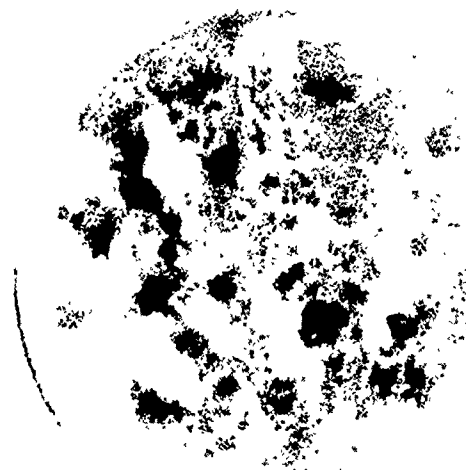
Magnification 1000  
Angle of View 45°  
Det. Mode Sec  
Coating An  
  
Operating Conditions:  
Accel. Potent. 25 kv  
Condenser Lens \_\_\_\_\_  
Obj. Lens \_\_\_\_\_  
Detector Type \_\_\_\_\_  
Settings \_\_\_\_\_  
  
Eroded area

NEG IDENT A13  
Magnification 100  
Angle of View 45°  
Det. Mode Sec  
Coating An  
  
Operating Conditions:  
Accel. Potent. 25 kv  
Condenser Lens \_\_\_\_\_  
Obj. Lens \_\_\_\_\_  
Detector Type \_\_\_\_\_  
Settings \_\_\_\_\_  
  
Eroded area

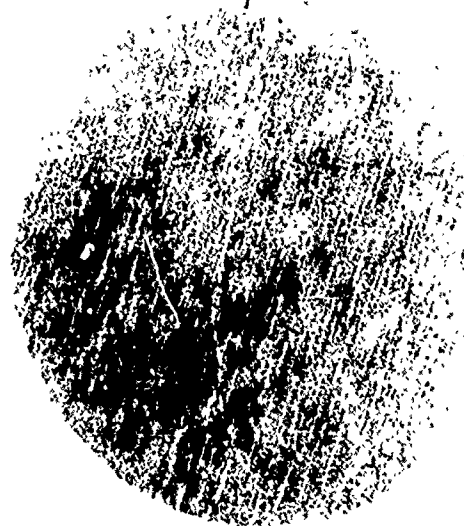
NEG IDENT A14



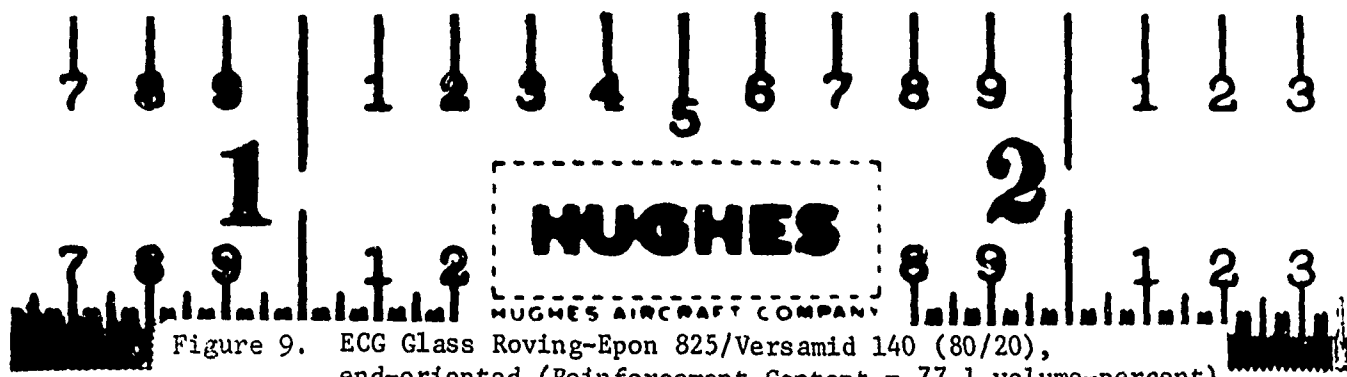
a. Specimen No. EP-11A, 30 seconds  
at 333 meters/second



b. Specimen No. EP-11B, 60 seconds  
at 333 meters/second



c. Unexposed Control





a. Specimen No. U-2A, 30 seconds  
at 333 meters/second



b. Specimen No. U-2B, 60 seconds  
at 333 meters/second



c. Unexposed Control

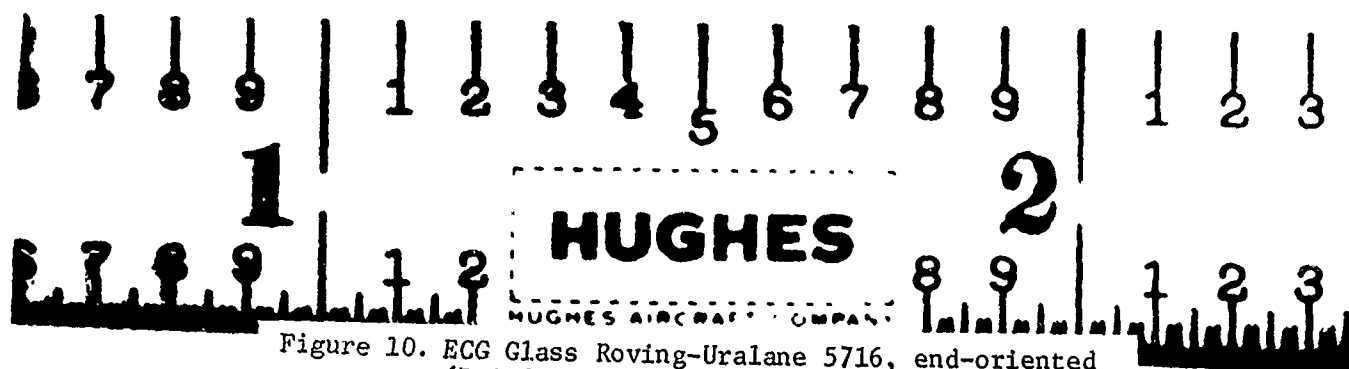


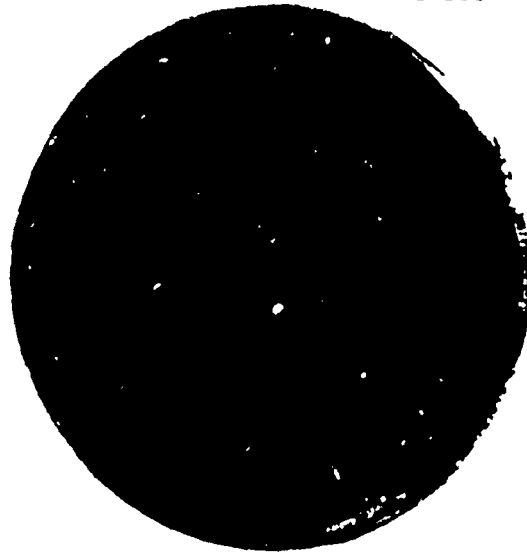
Figure 10. ECG Glass Roving-Uralane 5716, end-oriented  
(Reinforcement Content = 73.3 volume-percent)



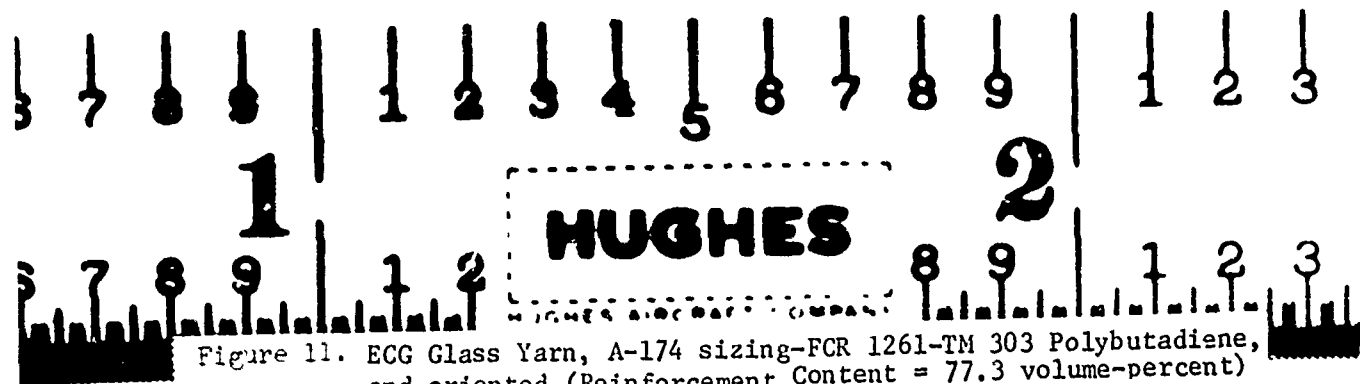
a. Specimen No. PB-1A, 30 seconds  
at 333 meters/second



b. Specimen No. PB-1B, 30 seconds  
at 333 meters/second



c. Unexposed Control

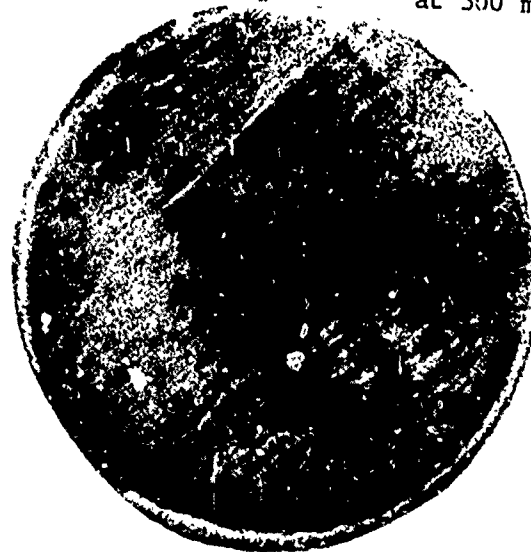




a. Specimen No. PB-2A, 30 seconds  
at 300 meters/second



b. Specimen No. PB-2B, 15 seconds  
at 300 meters/second



c. Unexposed Control

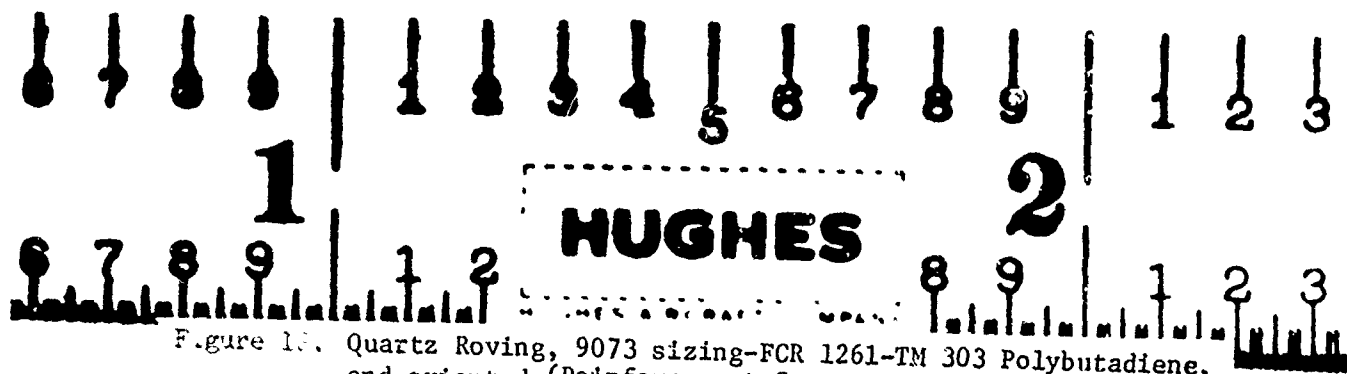


Figure 18. Quartz Roving, 9073 sizing-FCR 1261-TM 303 Polybutadiene,  
end-oriented (Reinforcement Content = 75.1 volume-percent)



a. Specimen No. P0-1A, 30 seconds  
at 333 meters/second



b. Specimen No. P0-1B, 10 seconds  
at 333 meters/second



c. Unexposed Control

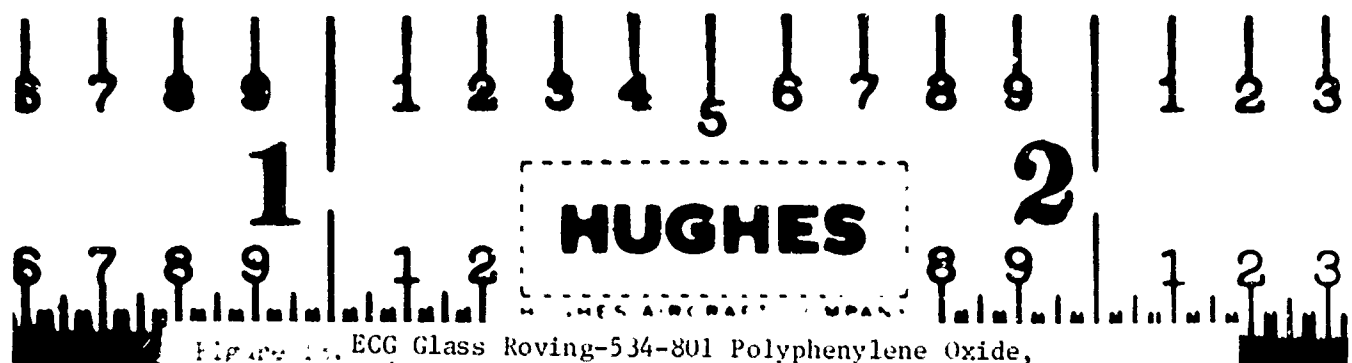
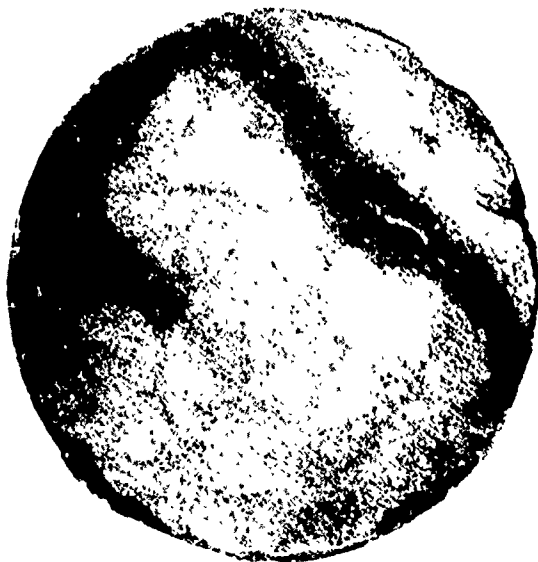


Figure 1. ECG Glass Roving-534-801 Polyphenylene Oxide,  
end-oriented (Reinforcement Content = 74.2 volume-percent)



a. Specimen No. P0-2B, 10 seconds  
at 333 meters/second



b. Unexposed Control

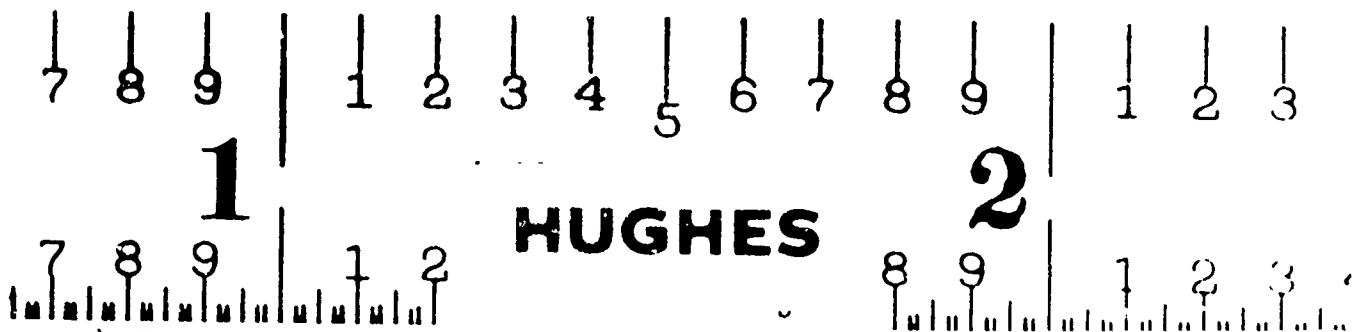


Figure 14. ECG Glass Roving-534-801 Polyphenylene Oxide Cross-Lined with Benzenetrifluoromethyl Chloride, end-oriented (Reinforcement Content = 79.1 volume-percent)



a. Specimen No. EP-10A, 30 seconds  
at 333 meters/second



b. Specimen No. EP-10B, 30 seconds  
at 333 meters/second



c. Unexposed Control

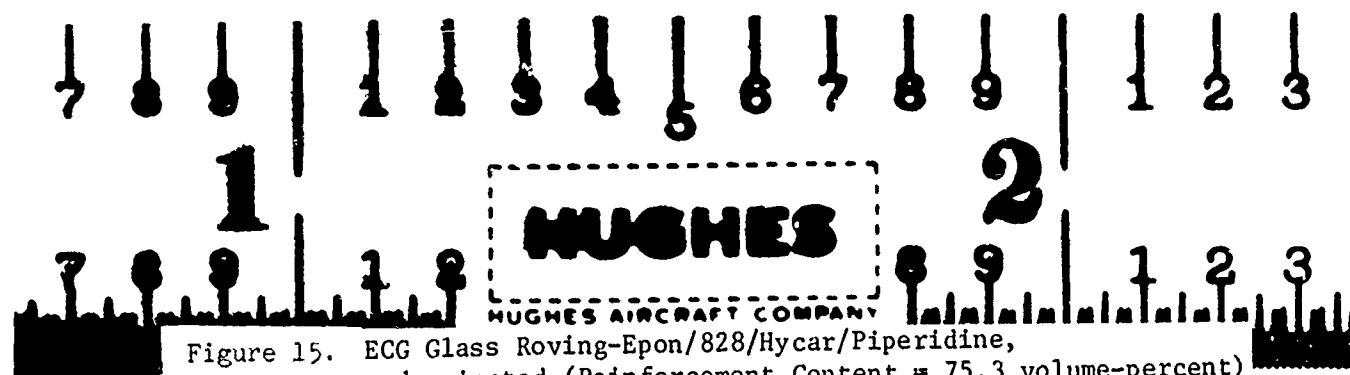


TABLE 2. RELATIVE RAIN EROSION RESISTANCE OF VARIOUS MATRICES  
(UNIDIRECTIONAL, END-ORIENTED NOMEX YARN)

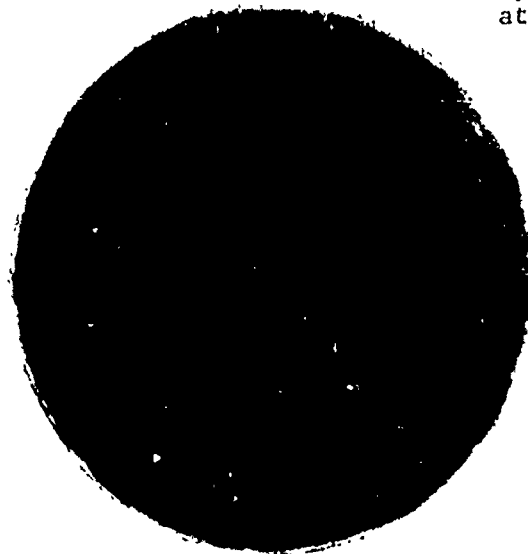
Specimen Code	Matrix	Reinforcement Content, volume-percent	Void Content, percent	Velocity, meters/sec	Exposure Time, sec	Weight Loss, mg	Erosion Depth, mils	Appearance	Figure Refs.
N-2A	Epon 828/MPDA (Standard)	78.6	3.6	333	30	1.6	-0.4	Broken around edge*	16
N-2B				333	60	1.0	-1.3	Local erosion next to retaining ring	
N-3A	Epon 825/ Versamid 140 (Flexibilized)	78.5	3.5	333	30	0.2	-0.4	Local erosion near retaining ring	17,18
N-3B				333	60	0.3	-0.4	Local erosion near retaining ring	
N-6A	Epon 328/ Menthane Dia- mine/MPDA BDMA (Brittle)	79.5	2.2	300	30	-	0.1	Very slightly eroded; No pitting	19,20
N-6B				300	60	-	0.6	Very slightly eroded; No pitting	
N-8A	Epon 828/ Hycar/Piper- idine	78.6	2.1	333	30	1.6	-0.2	Very slightly eroded; local erosion near retaining ring	21,22
N-8B				333	60	3.4	-0.3		

\*Specimen damaged or edge when removed from specimen holder.

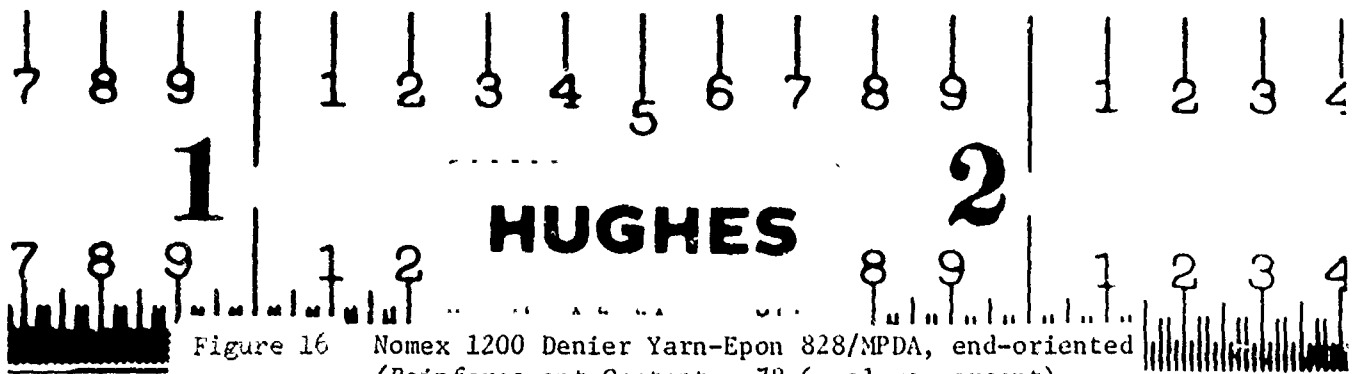


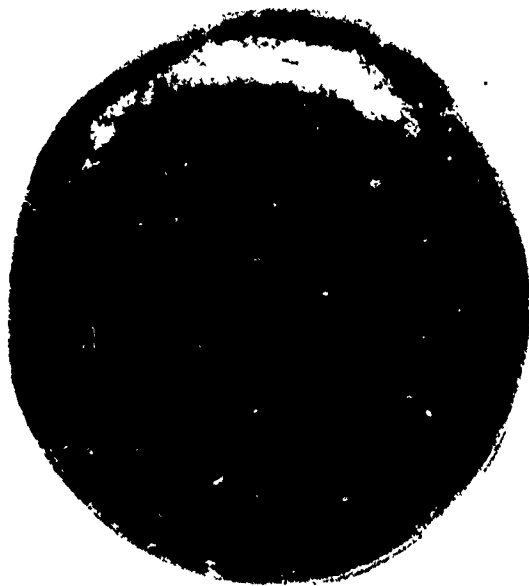
a. Specimen No. N-2A, 30 seconds  
at 333 meters/second

b. Specimen No. N-2B, 60 seconds  
at 333 meters/second



c. Unexposed Control

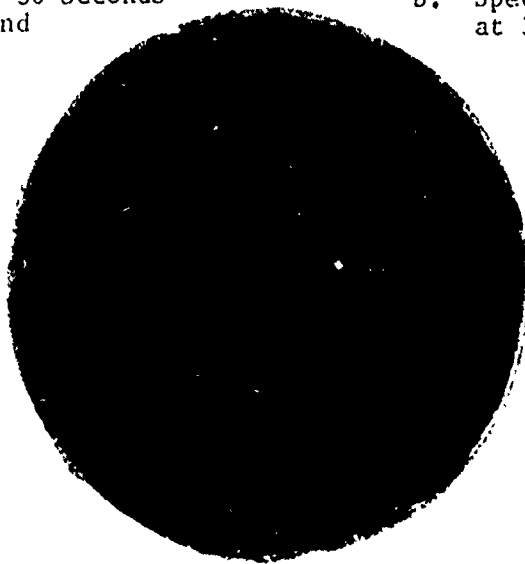




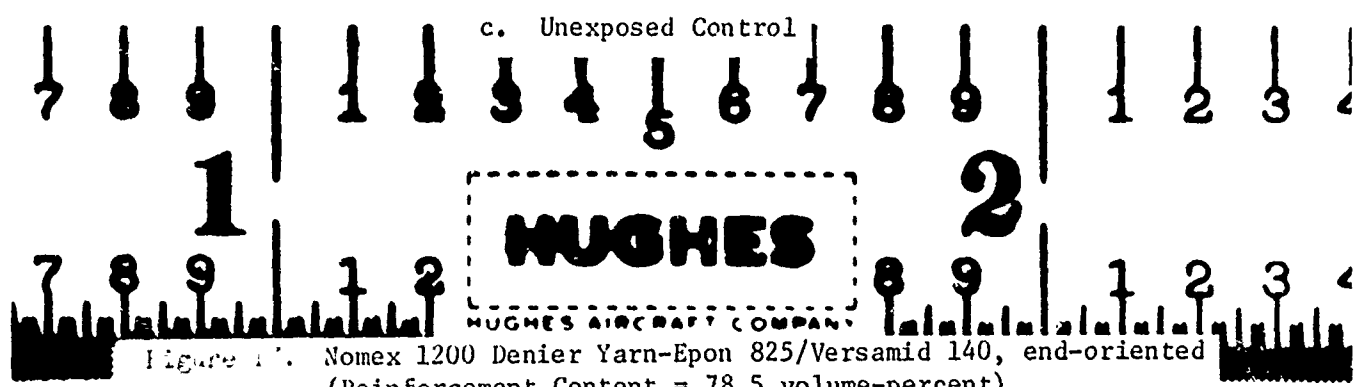
a. Specimen No. N-3A, 30 seconds  
at 333 meters/second



b. Specimen No. N-3B, 60 seconds  
at 333 meters/second



c. Unexposed Control



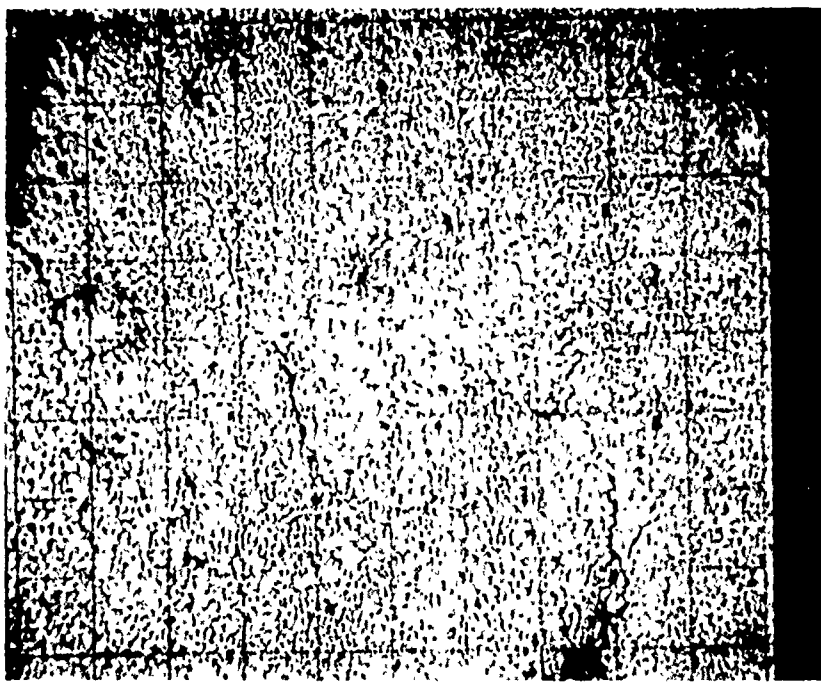
SEM DATA

REQUEST # 7215

SPECIMEN N-3A

DATE 27 May

OPERATOR JLP



Magnification 100 X

Angle of View 45

Det. Mode sec

Coating An

Operating Conditions:

Accel. Potent. 25 kv

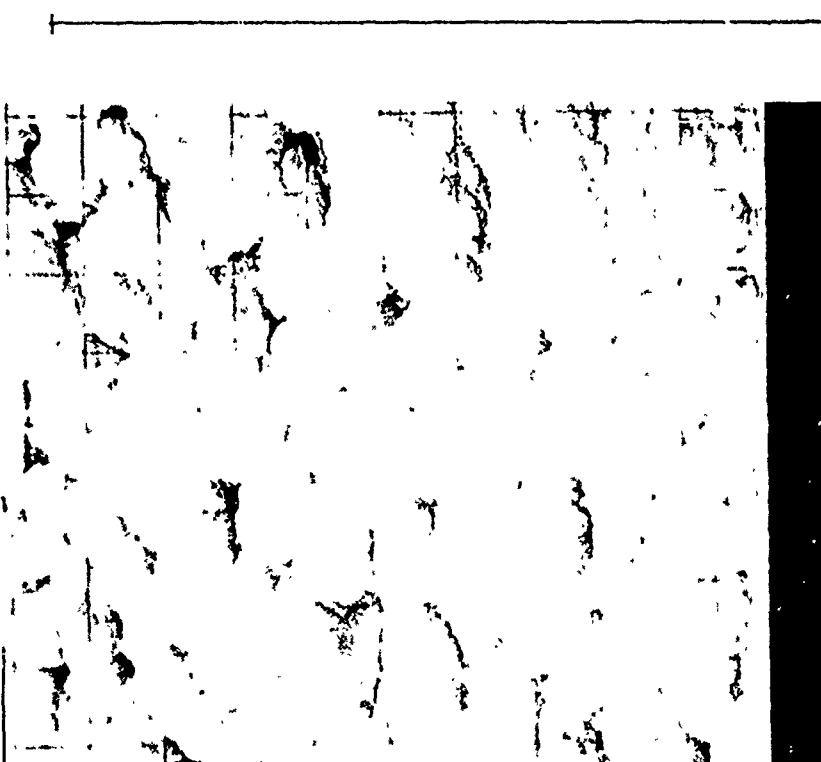
Condenser Lens \_\_\_\_\_

Obj. Lens \_\_\_\_\_

Detector Type \_\_\_\_\_

Settings \_\_\_\_\_

Eroded Area



NEG IDENT B5

Magnification 1000 X

Angle of View 450

Det. Mode Sec

Coating An

Operating Conditions:

Accel. Potent. 25 kv

Condenser Lens \_\_\_\_\_

Obj. Lens \_\_\_\_\_

Detector Type \_\_\_\_\_

Settings \_\_\_\_\_

Unersoded area

Neg Ident B6

Figure 18. Scanning electron micrographs of specimen N-3A  
(Nomex-Epon 825/Versamid 140, end-oriented)

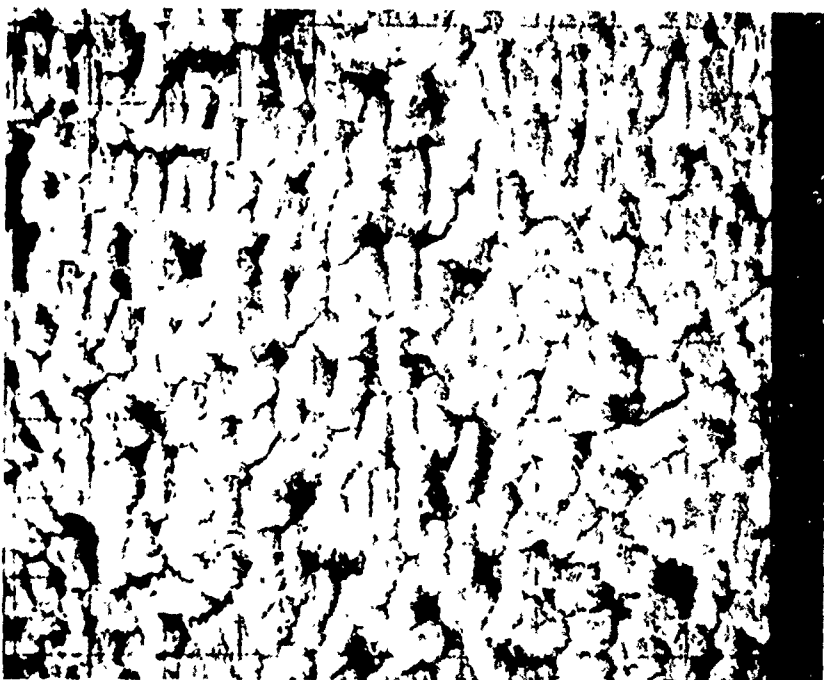
SEM DATA

REQUEST # 7215  
SPECIMEN N-3A

DATE 27 Mar  
OPERATOR JBD



Magnification 1000X  
Angle of View 45°  
Det. Mode sc  
Coating Ar  
  
Operating Conditions:  
Accel. Potent. 25 kv  
Condenser Lens \_\_\_\_\_  
Obj. Lens \_\_\_\_\_  
Detector Type \_\_\_\_\_  
Settings \_\_\_\_\_  
Eroded area



NEG IDENT B3  
Magnification 500 X  
Angle of View 45°  
Det. Mode sc  
Coating Ar  
  
Operating Conditions:  
Accel. Potent. 25 kv  
Condenser Lens \_\_\_\_\_  
Obj. Lens \_\_\_\_\_  
Detector Type \_\_\_\_\_  
Settings \_\_\_\_\_  
Eroded area

NEG IDENT B4

Figure 18. Scanning electron micrographs of specimen N-3A  
(Cont.) (Nomex-Epon 825/Versamid 140, end-oriented)

SEM DATA

REQUEST # 7215

SPECIMEN N-3A

DATE 27 May

OPERATOR JRL



Magnification 5000

Angle of View 45°

Det. Mode sec

Coating An

Operating Conditions:

Accel. Potent. 25 kv

Condenser Lens

Obj. Lens

Detector Type

Settings

Central Eroded Area



NEG IDENT B1

Magnification 2500

Angle of View 45°

Det. Mode sec

Coating An

Operating Conditions:

Accel. Potent. 25 kv

Condenser Lens

Obj. Lens

Detector Type

Settings

Crooked Area

NEG IDENT B2

Figure 18. Scanning electron micrographs of specimen N-3A  
(Cont.) (Nomex-Epon 825/Versamid 140, end-oriented)

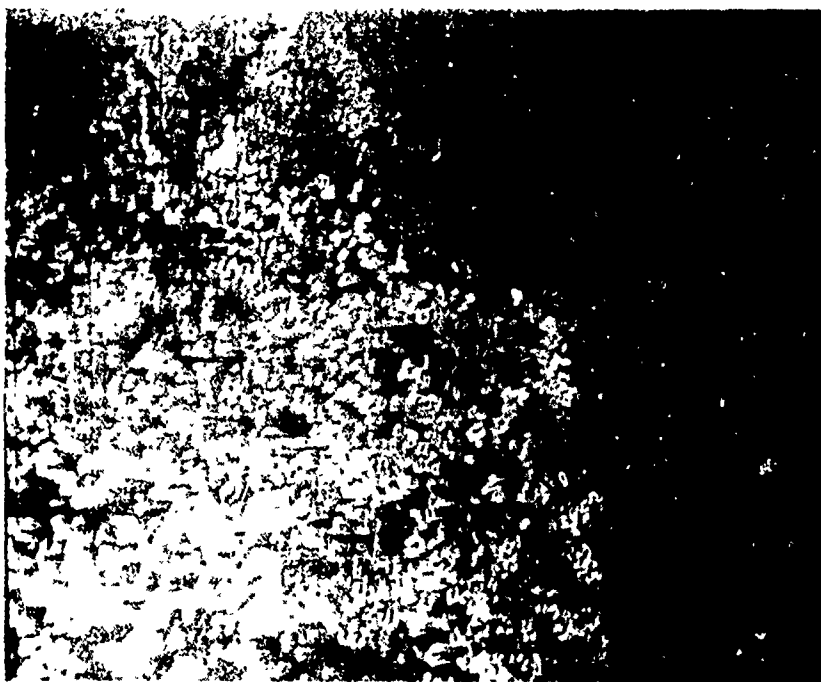
SEM DATA

REQUEST A-3A 7215

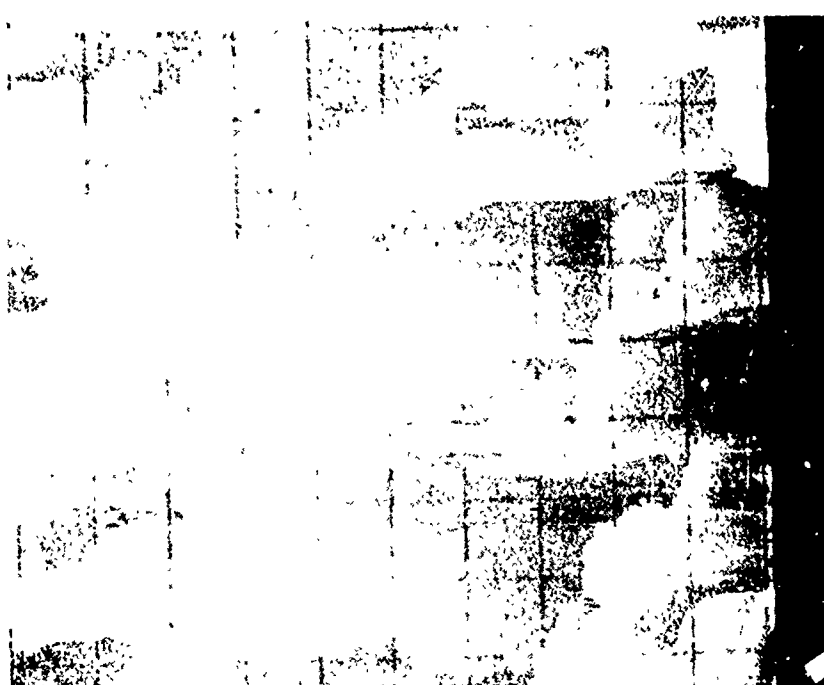
SPECIMEN A-3A

DATE 27 Mar

OPERATOR JAD



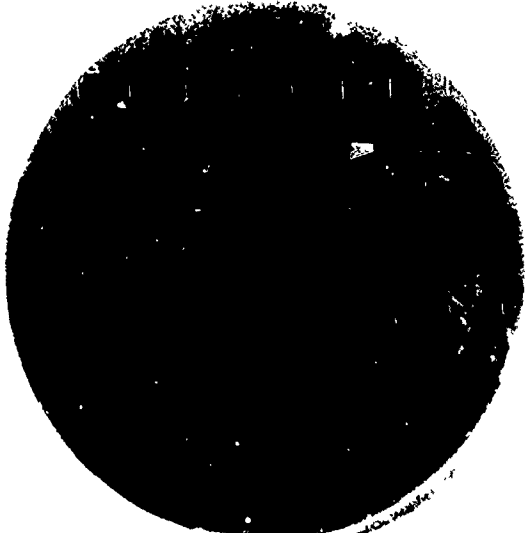
Magnification 100  
Angle of View 45°  
Det. Mode sec  
Coating An  
Operating Conditions:  
Accel. Potent. 25 kv  
Condenser Lens \_\_\_\_\_  
Obj. Lens \_\_\_\_\_  
Detector Type \_\_\_\_\_  
Settings \_\_\_\_\_  
Border of heavily eroded area



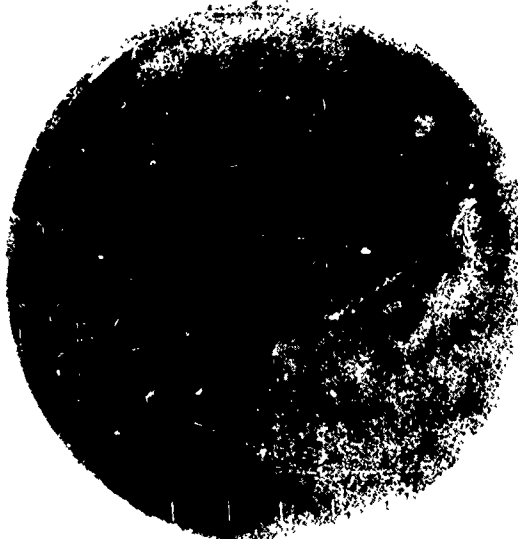
Neg Ident B7  
Magnification 1000  
Angle of View 45°  
Det. Mode Sec  
Coating An  
Operating Conditions:  
Accel. Potent. 25 kv  
Condenser Lens \_\_\_\_\_  
Obj. Lens \_\_\_\_\_  
Detector Type \_\_\_\_\_  
Settings \_\_\_\_\_  
Detail of center of B7.

Neg Ident B8

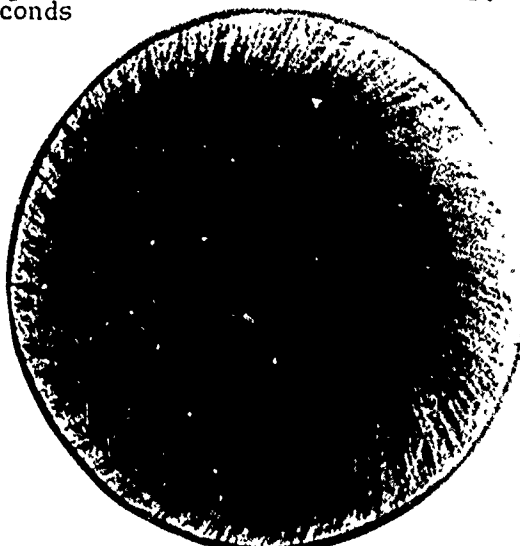
Fig. 2 Scanning electron micrographs of specimen A-3A  
(Glass fiber of Versamid 140, end-oriented)



a. Specimen No. N-6A, 30 seconds  
at 300 meters/second



b. Specimen No. N-6B, 60 seconds  
at 300 meters/second



c. Unexposed Control

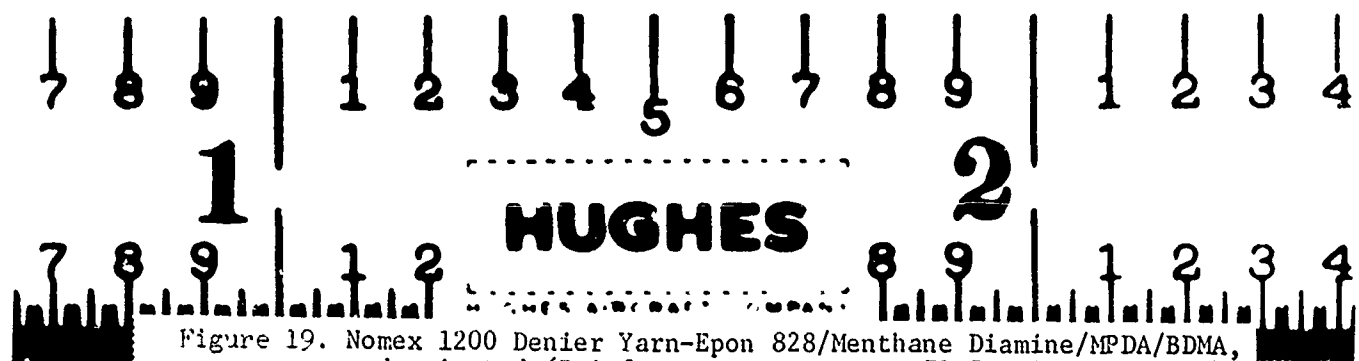


Figure 19. Nomex 1200 Denier Yarn-Epon 828/Menthane Diamine/MPDA/BDMA,  
end-oriented (Reinforcement Content = 79.5 volume-percent)

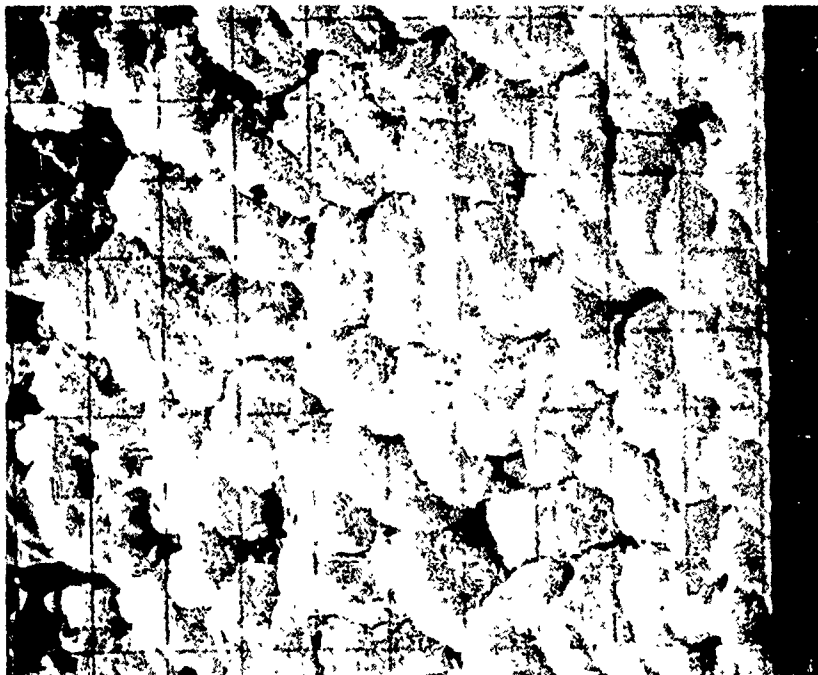
SEM DATA

REQUEST # 7215

SPECIMEN N-6B

DATE \_\_\_\_\_

OPERATOR JRC



Magnification 1000

Angle of View 45°

Det. Mode Se

Coating An

Operating Conditions:

Accel. Potent. 25 kv

Condenser Lens \_\_\_\_\_

Obj. Lens \_\_\_\_\_

Detector Type \_\_\_\_\_

Settings \_\_\_\_\_

Neg Ident C3

Magnification 500

Angle of View 45°

Det. Mode Se

Coating An

Operating Conditions:

Accel. Potent. 25 kv

Condenser Lens \_\_\_\_\_

Obj. Lens \_\_\_\_\_

Detector Type \_\_\_\_\_

Settings \_\_\_\_\_

Neg Ident C4

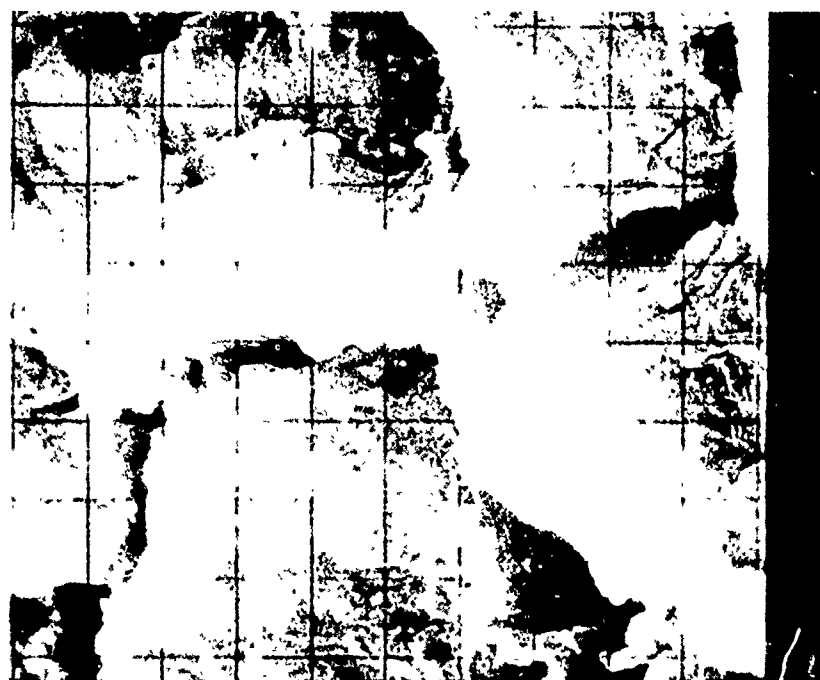
Figure 20. Scanning electron micrographs of specimen N-6B  
(Nomex-Epon 828/menthane diamine/MPDA/BDMA,  
end-oriented)

SEM DATA

REQUEST # 7215

SPECIMEN N-6B

DATE 27 Mar  
OPERATOR JPS



Magnification 5000

Angle of View 45°

Det. Mode sec

Coating An

Operating Conditions:

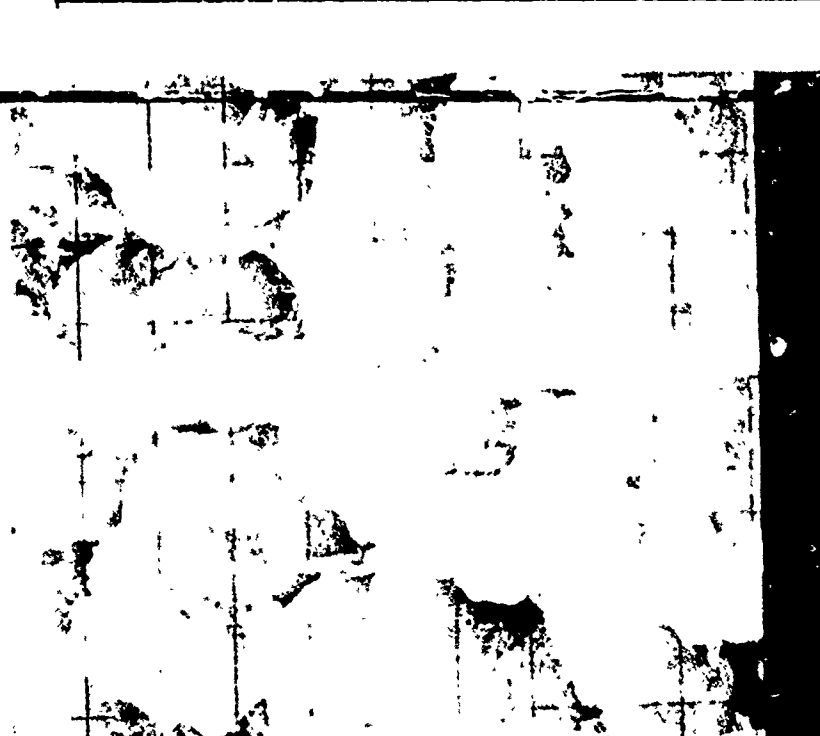
Accel. Potent. 25 kv

Condenser Lens

Obj. Lens

Detector Type

Settings



Neg Ident C1

Magnification 2500

Angle of View 45°

Det. Mode sec

Coating An

Operating Conditions:

Accel. Potent. 25 kv

Condenser Lens

Obj. Lens

Detector Type

Settings

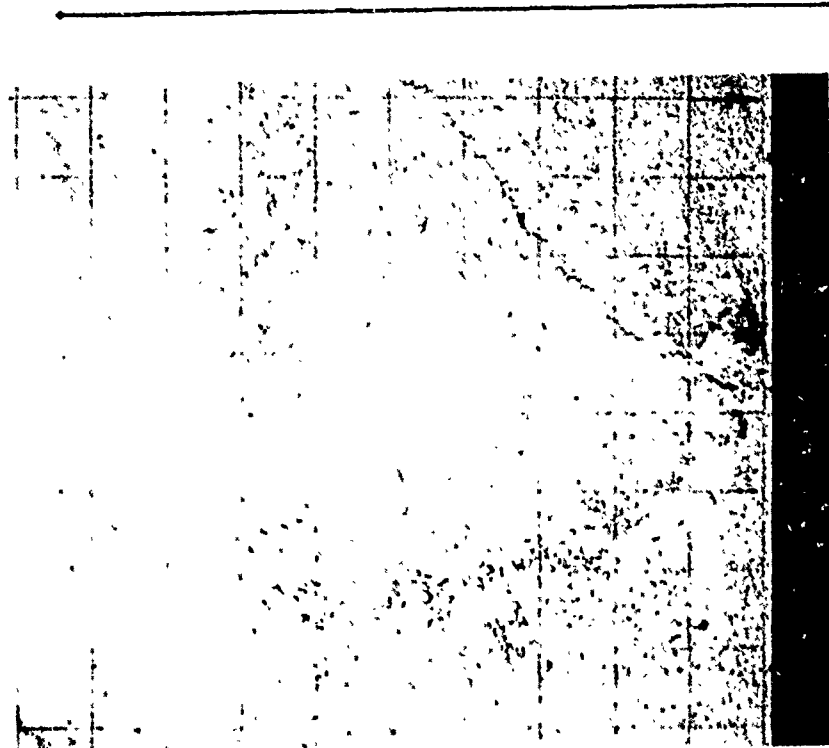
Neg Ident C2

Figure 20. Scanning electron micrographs of specimen N-6B  
(Cont.) (Nomex-Epon 828/menthane diamine/MPDA/BDMA,  
end-oriented)

SEM DATA

REQUEST # 7215  
SPECIMEN N-6B

DATE 27 Mar  
OPERATOR JPL



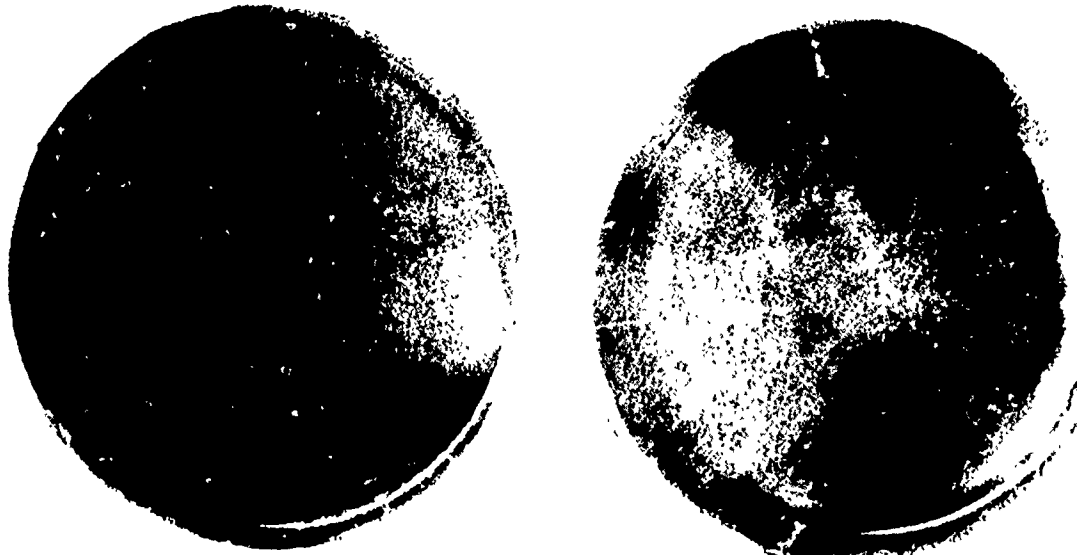
Magnification 100  
Angle of View 45°  
Det. Mode Sec  
Coating An

Operating Conditions:

Accel. Potent. 25 KV  
Condenser Lens \_\_\_\_\_  
Obj. Lens \_\_\_\_\_  
Detector Type \_\_\_\_\_  
Settings \_\_\_\_\_  
\_\_\_\_\_  
\_\_\_\_\_

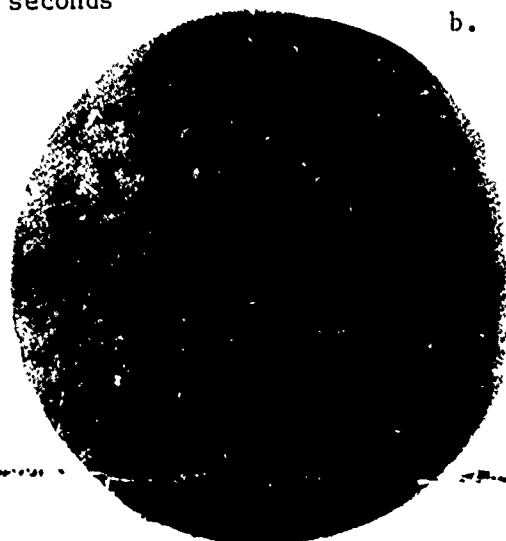
NEG IDENT CS

Figure 20. Scanning electron micrographs of specimen N-6B  
(Cont.) (Nomex-Epon 828/menthane diamine/MPDA/BDMA,  
end-oriented).

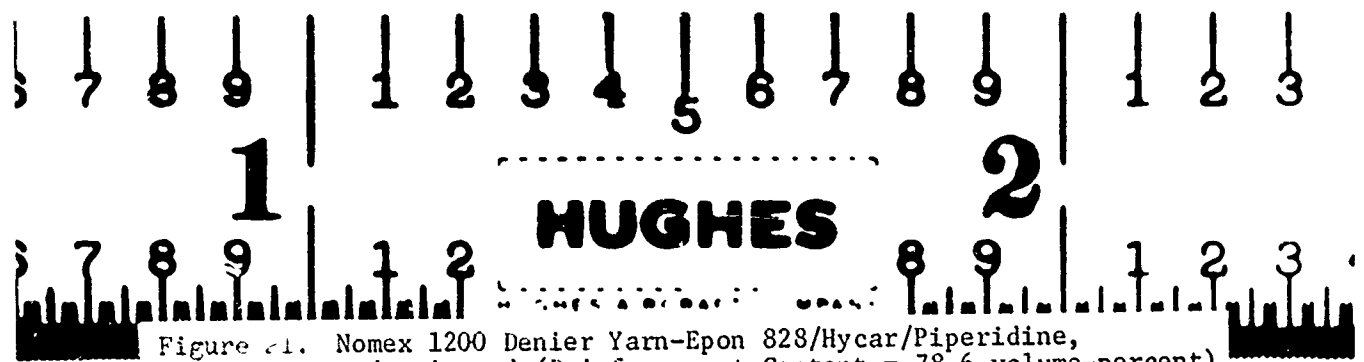


a. Specimen No. N-8A, 30 seconds  
at 333 meters/second

b. Specimen No. N-8B, 60 seconds  
at 333 meters/second



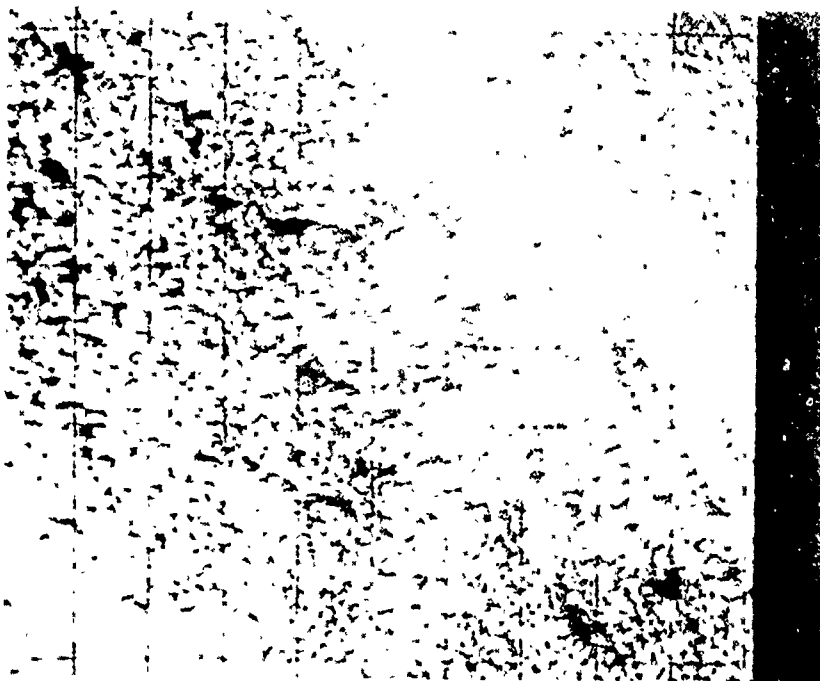
c. Unexposed Control



SEM DATA

REQUEST # 7215  
SPECIMEN N-8B

DATE 28 Mar  
OPERATOR JRL



Magnification 100  
Angle of View 45°  
Det. Mode Sec  
Coating An  
  
Operating Conditions:  
Accel. Potent. 25 KV  
Condenser Lens \_\_\_\_\_  
Obj. Lens \_\_\_\_\_  
Detector Type \_\_\_\_\_  
Settings \_\_\_\_\_  
Area of heavy erosion  
\_\_\_\_\_  
\_\_\_\_\_



NEG IDENT F7  
Magnification 500  
Angle of View 45°  
Det. Mode sec  
Coating An  
  
Operating Conditions:  
Accel. Potent. 25 KV  
Condenser Lens \_\_\_\_\_  
Obj. Lens \_\_\_\_\_  
Detector Type \_\_\_\_\_  
Settings \_\_\_\_\_  
Area of heavy erosion  
\_\_\_\_\_  
\_\_\_\_\_

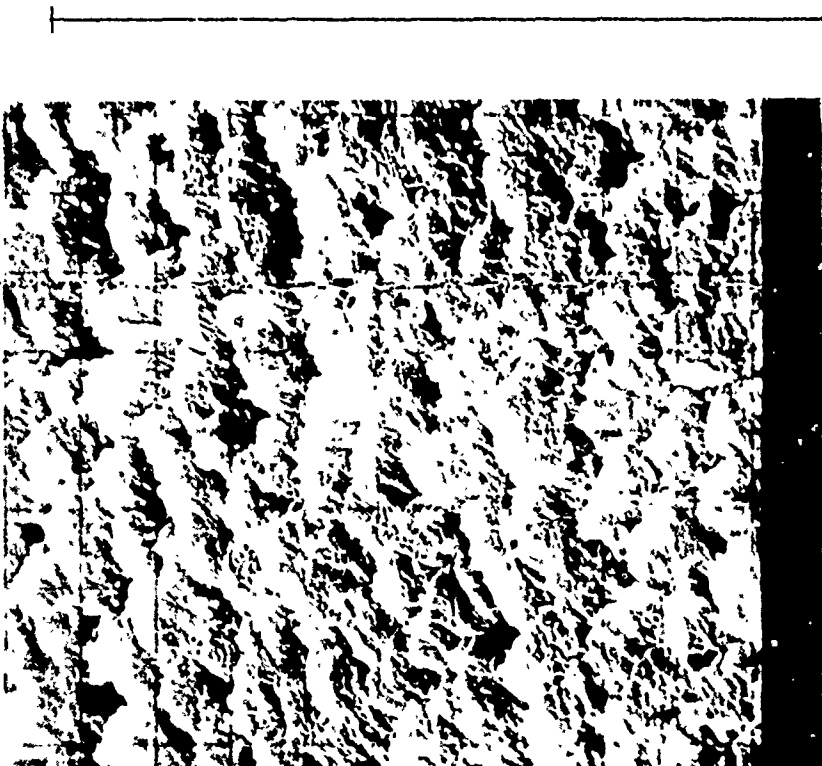
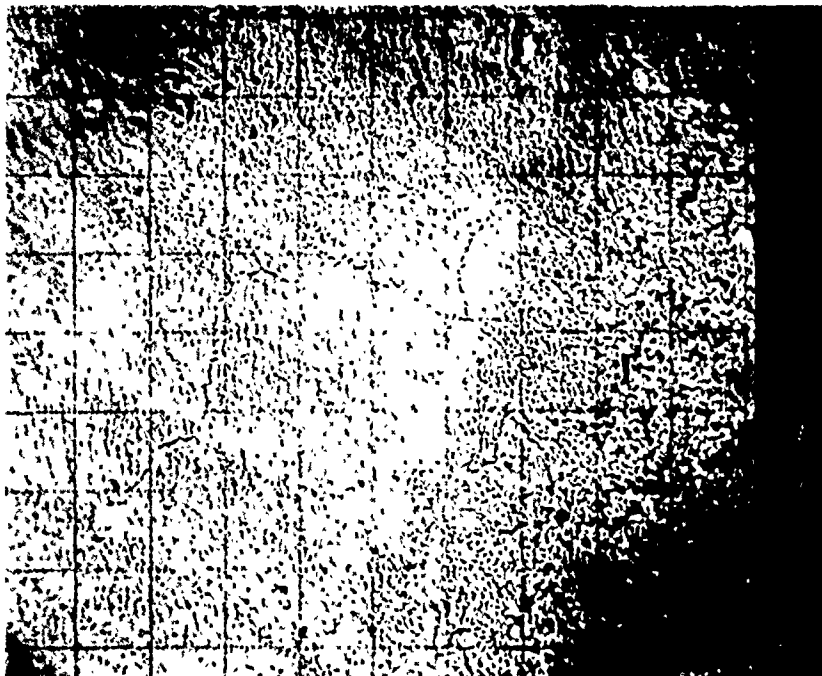
Figure 22. Scanning electron micrographs of specimen N-8B  
(Nomex-Epon 828/Hycar/piperidine, end-oriented)

SEM DATA

REQUEST # 7215

SPECIMEN N-8B

DATE 28 May  
OPERATOR JPS



Magnification 100

Angle of View 45°

Det. Mode sec

Coating Ar

Operating Conditions:

Accel. Potent. 25 KV

Condenser Lens \_\_\_\_\_

Obj. Lens \_\_\_\_\_

Detector Type \_\_\_\_\_

Settings \_\_\_\_\_

Uneroded area

NEG IDENT F8

Magnification 1000

Angle of View 45°

Det. Mode sec

Coating Ar

Operating Conditions:

Accel. Potent. 25 KV

Condenser Lens \_\_\_\_\_

Obj. Lens \_\_\_\_\_

Detector Type \_\_\_\_\_

Settings \_\_\_\_\_

Uneroded area

NEG IDENT F9

Figure 22. Scanning electron micrographs of specimen N-8B  
(cont) (Nomex-Epon 828/Hycar/piperidine, end-oriented)

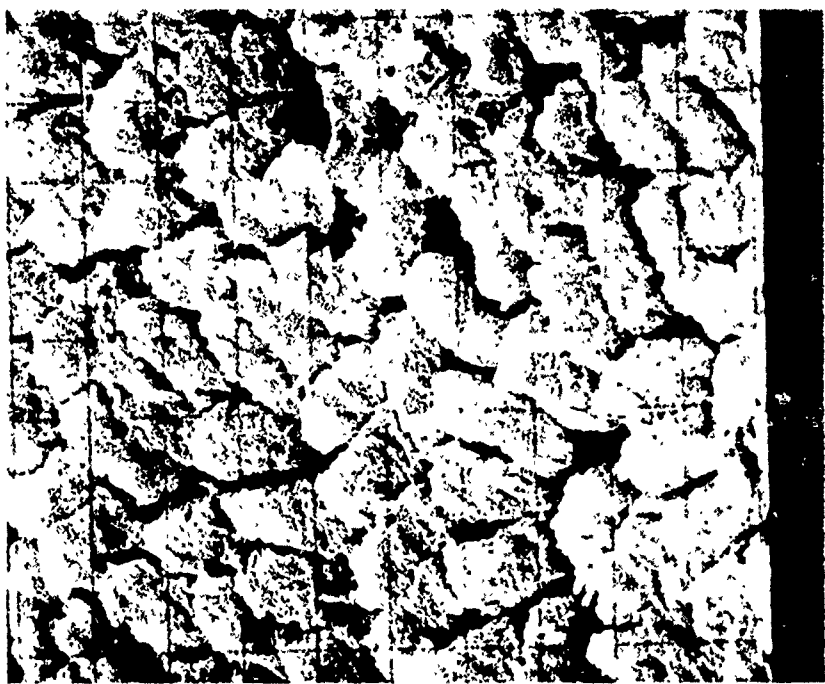
SEM DATA

REQUEST # 7215

SPECIMEN N-8B

DATE 28 May

OPERATOR JR



Magnification 1000

Angle of View 45°

Det. Mode Sec

Coating Au

Operating Conditions:

Accel. Potent. 25 kV

Condenser Lens

Obj. Lens

Detector Type

Settings

NEG IDENT F3

Magnification 500

Angle of View 45°

Det. Mode Sec

Coating Au

Operating Conditions:

Accel. Potent. 25 kV

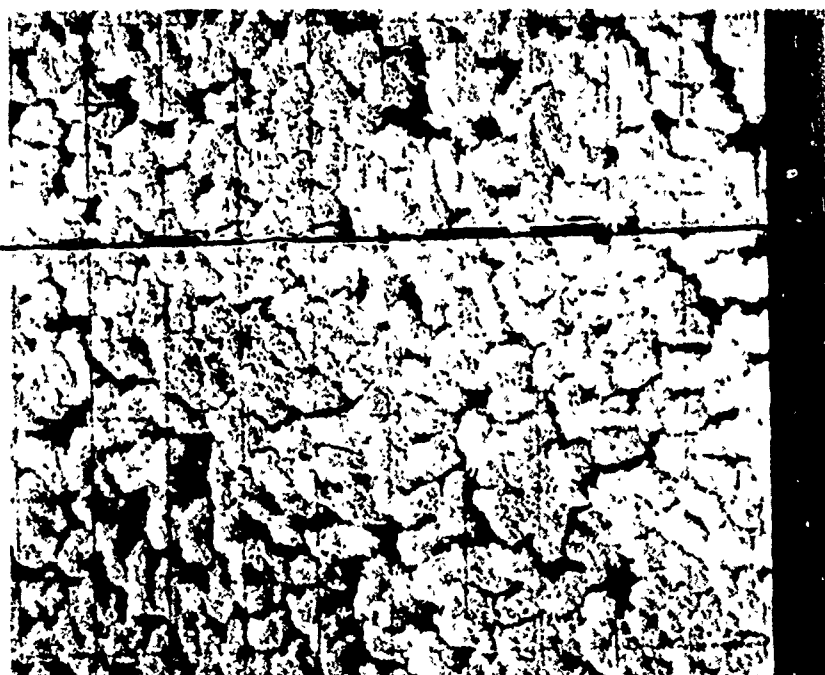
Condenser Lens

Obj. Lens

Detector Type

Settings

Eroded Au



NEG IDENT F4

Figure 22. Scanning electron micrographs of specimen N-8B  
(Cont.) (Nomex-Epon 828/Hycar/piperidine, end-oriented)

SEM DATA

REQUEST # 7215

SPECIMEN N-8B

DATE 28 Mar

OPERATOR JPL



Magnification 5000

Angle of View 45°

Det. Mode See

Coating Au

Operating Conditions:

Accel. Potent. 25 kv

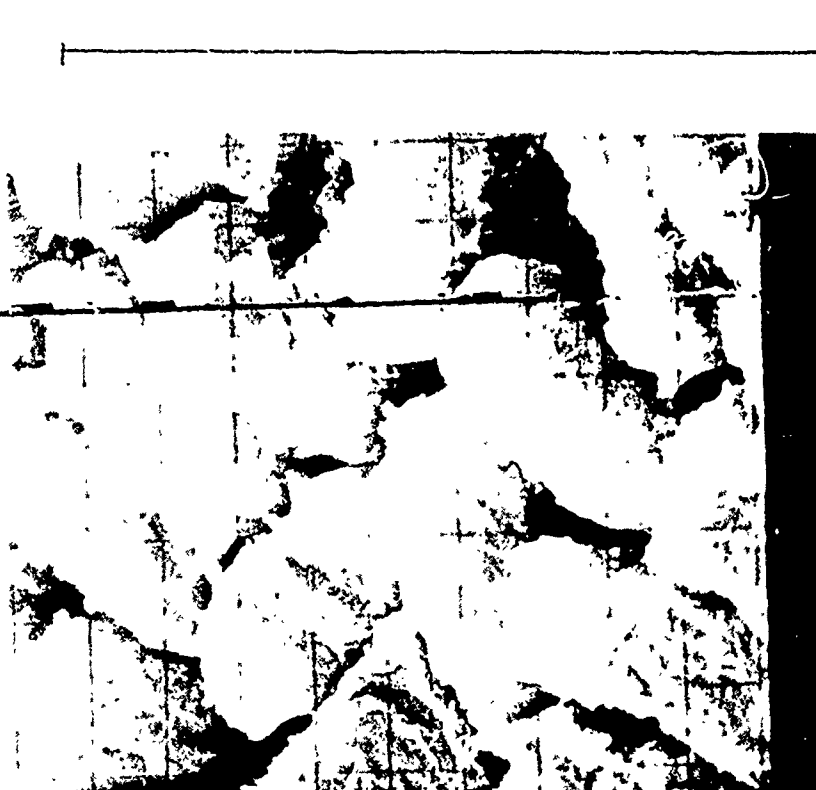
Condenser Lens \_\_\_\_\_

Obj. Lens \_\_\_\_\_

Detector Type \_\_\_\_\_

Settings \_\_\_\_\_

Eroded Area



Neg Ident F1

Magnification 2500

Angle of View 45

Det. Mode See

Coating Au

Operating Conditions:

Accel. Potent. 25 kv

Condenser Lens \_\_\_\_\_

Obj. Lens \_\_\_\_\_

Detector Type \_\_\_\_\_

Settings \_\_\_\_\_

Eroded Area

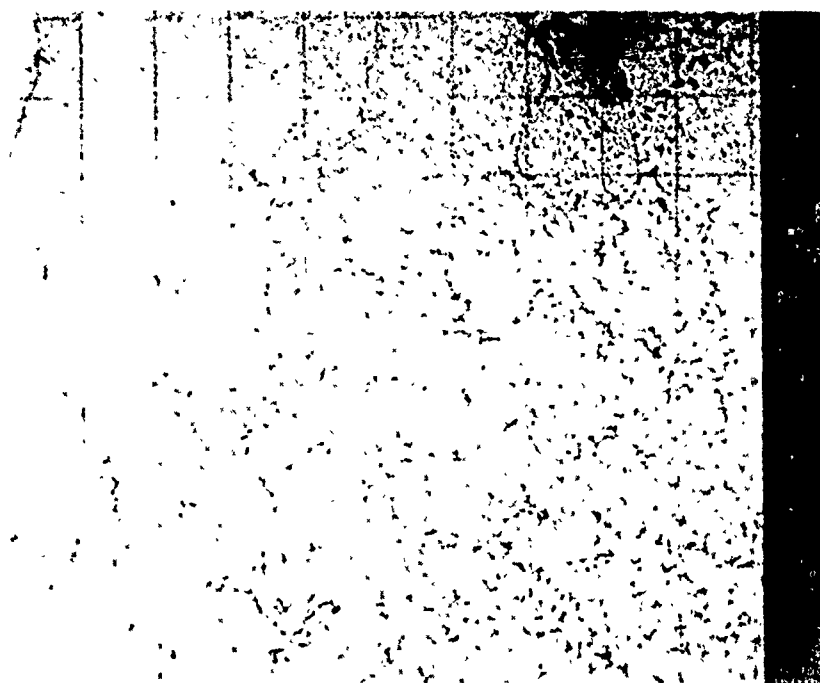
Neg Ident F2

Figure 22. Scanning electron micrographs of specimen N-8B  
(cont) (Nomex-Epon 828/Hycar/piperidine, end-oriented)

SEM DATA

REQUEST # 7215  
SPECIMEN N-8B

DATE 28 Mar  
OPERATOR JRL



Magnification 100  
Angle of View 45°  
Det. Mode Se  
Coating An  
  
Operating Conditions:  
Accel. Potent. 25 KV  
Condenser Lens \_\_\_\_\_  
Obj. Lens \_\_\_\_\_  
Detector Type \_\_\_\_\_  
Settings \_\_\_\_\_  
Eroded Area

NEG IDENT F5

Magnification \_\_\_\_\_  
Angle of View \_\_\_\_\_  
Det. Mode \_\_\_\_\_  
Coating \_\_\_\_\_  
Operating Conditions:

Accel. Potent. \_\_\_\_\_ KV  
Condenser Lens \_\_\_\_\_  
Obj. Lens \_\_\_\_\_  
Detector Type \_\_\_\_\_  
Settings \_\_\_\_\_

NEG IDENT

Figure 22. Scanning electron micrographs of specimen N-8B  
(Cont.) (Nomex-Epon 828/Hycar/piperidine, end-oriented)

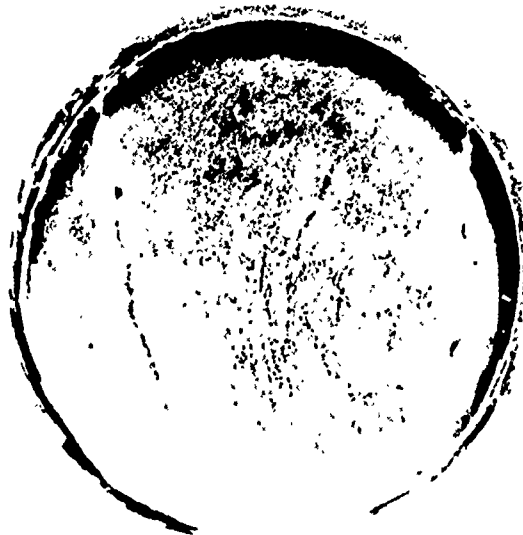
TABLE 3. RELATIVE RAIN EROSION RESISTANCE OF VARIOUS REINFORCEMENTS  
(EPON 328/MPDA, UNIDIRECTIONAL, END-ORIENTED)

Specimen Code	Reinforcement	Reinforcement Content, one-percent	Void Content, percent	Velocity meters/sec	Exposure time, sec	Weight loss, mg	Erosion Depth, mils	Appearance	Figure Refs.
Q-1A	Astroquartz			333	30	1206	—	Eroded through	
Q-1B	52/9073	71.8	2.1	333	15	354	0.4	Extremely eroded	6*
Q-1C				466	5	622	11.6	Extremely eroded	
Q-1D				466	5	357	7.1	Extremely eroded	
N-2A	Nomex 1200 denier yarn			333	30	1.6	-0.4	Broken around edge	
N-2B		78.6	3.0	333	60	1.0	-1.3	Local erosion next to retaining ring	16
PR-1A	PRD-49			05.6	0.6	333	30	17.0	
PR-1B						23.3	0.1	Eroded slightly except near fracture in surface	23
PR-2A	PRD-49 Type I					30	46		
PR-2B	400 denier yarn (plasma-treated)	76.8	3.1	333	30	20	-0.2	Deeply eroded locally; cracked	24
PR-2C	Epox 825/					60	30		
PR-2D	Versamid 140					60	10		
DA-1A	Dacron 1100 denier yarn		75.3	0	300	30	0.9	Very slightly eroded	25, 26
DA-1B						60	2.0		
DA-2A	Dacron 1160 denier yarn					30	51		
DA-2B						30	53		
DA-2C						30	41		
DA-2D						60	71		
DA-2F						60	100		
DA-2F						60	79		
DA-2G						120	134		
DA-2H						120	175		
DA-2I						120	118		
DA-3A	Dacron 1160 denier yarn, plasma-etched					30	5	-0.1	
DA-3B						30	4	0.7	Deeply eroded locally
DA-3C						30	6	0.4	
DA-3D						60	71	0.7	
DA-3E						60	100	1.0	
DA-3F						60	79	3.0	
DA-3G						120	134	9.3	
DA-3H						120	175	7.8	
DA-3I						120	118	5.9	

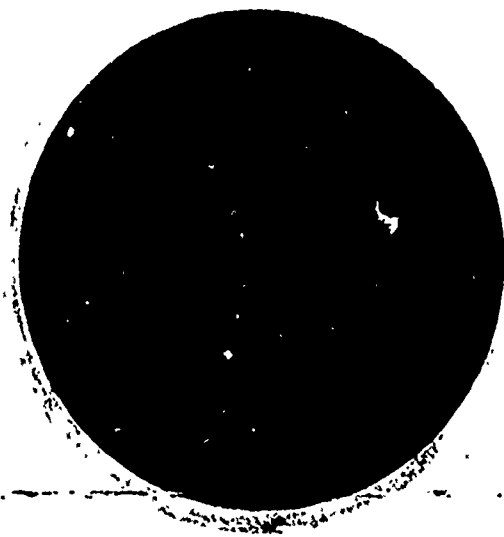
Figure 6 in Final Summary Report dated December 1971 (N00019-71-C-0167)



a. Specimen No. PR-1A, 30 seconds  
at 333 meters/second



b. Specimen No. PR-1B, 30 seconds  
at 333 meters/second



c. Unexposed Control



Figure 23. PRD 49 Type 1, 400 Denier Yarn-Epon 828/MPDA,  
end-oriented (Reinforcement Content = 65.6 volume-percent)

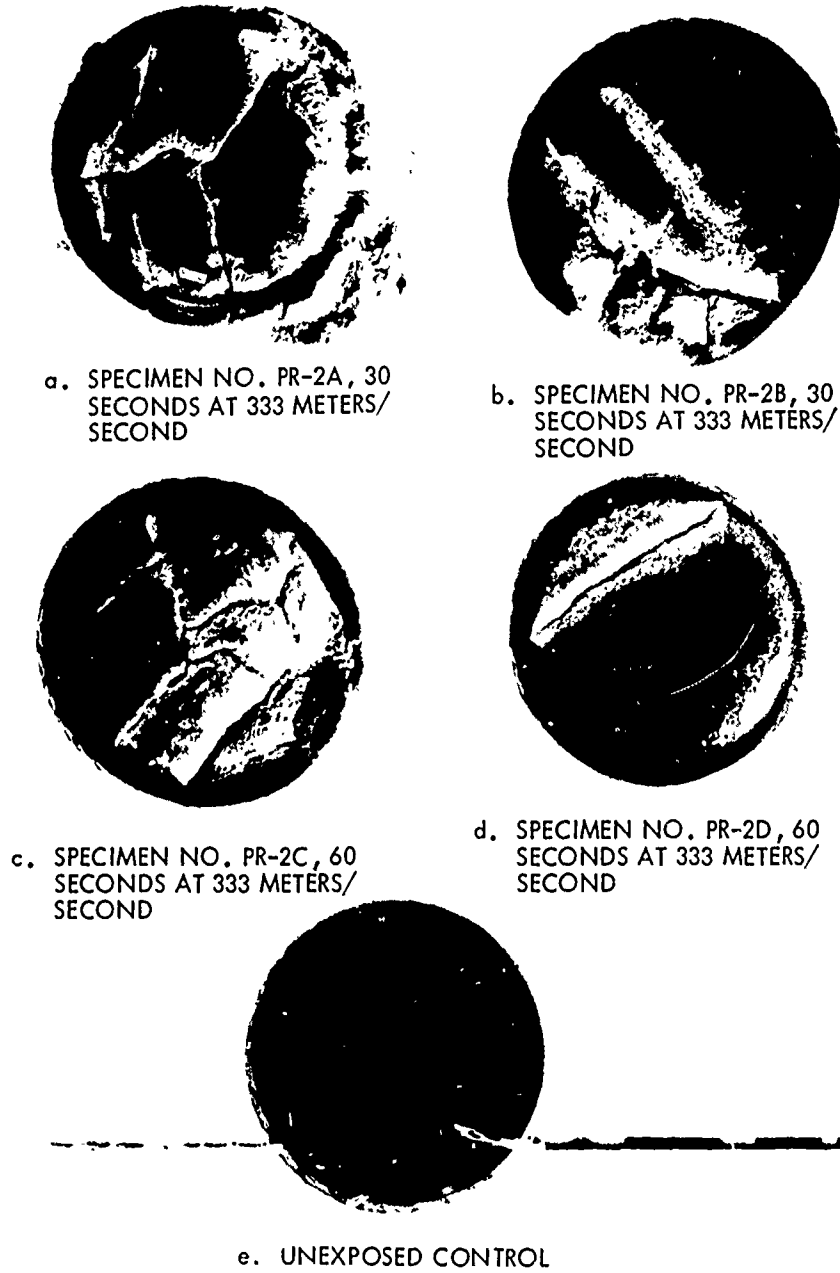
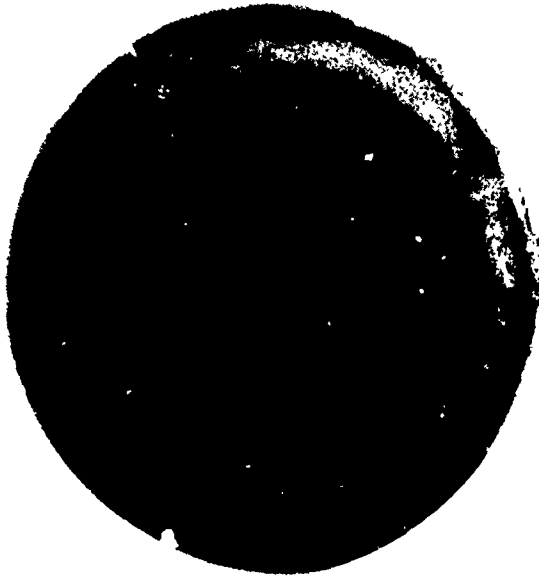


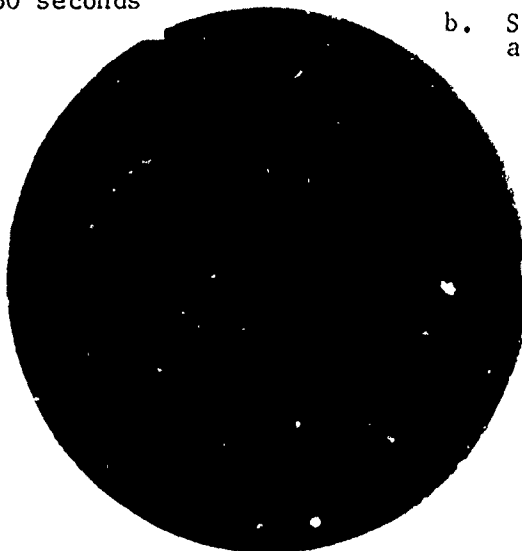
Figure 24. PRD-49, Type I, 400 denier yarn (plasma-treated)-  
Epon 825/Versamid 140, end-oriented (reinforcement  
content = 76.8 volume-percent).



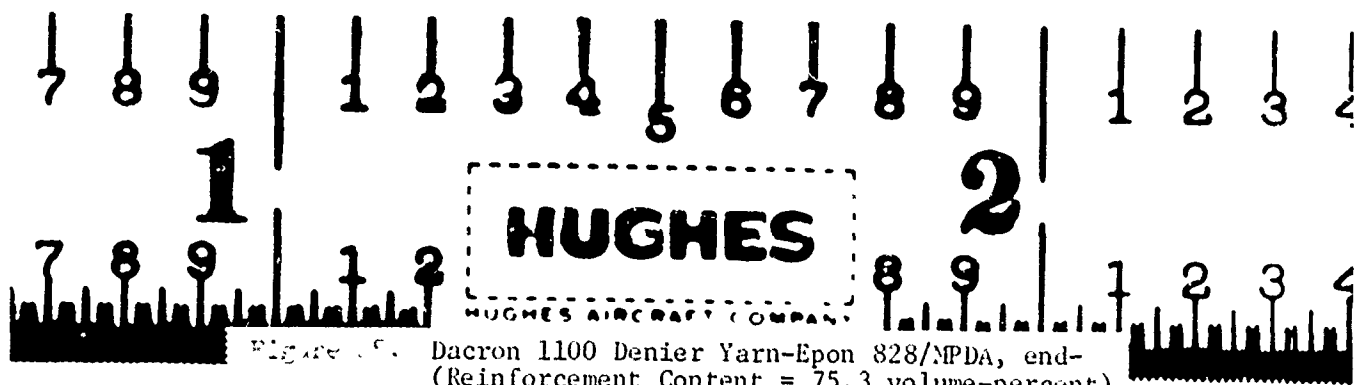
a. Specimen No. DA-1A, 30 seconds  
at 300 meters/second



b. Specimen No. DA-1B, 60 seconds  
at 300 meters/second



c. Unexposed Control

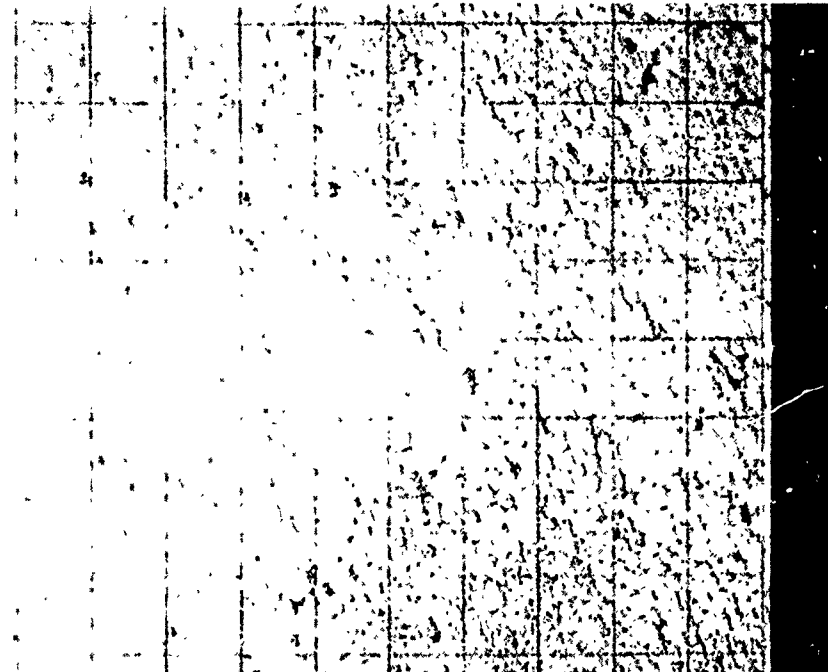


SEM DATA

REQUEST # 7215

SPECIMEN DA-1B

DATE 27 Mar  
OPERATOR Rf



Magnification 100  
Angle of View 45°  
Det. Mode sec  
Coating An

Operating Conditions:  
Accel. Potent. 25 kv  
Condenser Lens  
Obj. Lens  
Detector Type  
Settings

NEG IDENT E5  
Magnification 2000  
Angle of View 45°  
Det. Mode sec  
Coating An

Operating Conditions:  
Accel. Potent. 25 kv  
Condenser Lens  
Obj. Lens  
Detector Type  
Settings

Detail of Fiber Ends

NEG IDENT F6

Figure 26. Scanning electron micrographs of specimen DA-1B  
(Dacron-Epon 828/MPDA, end-oriented)

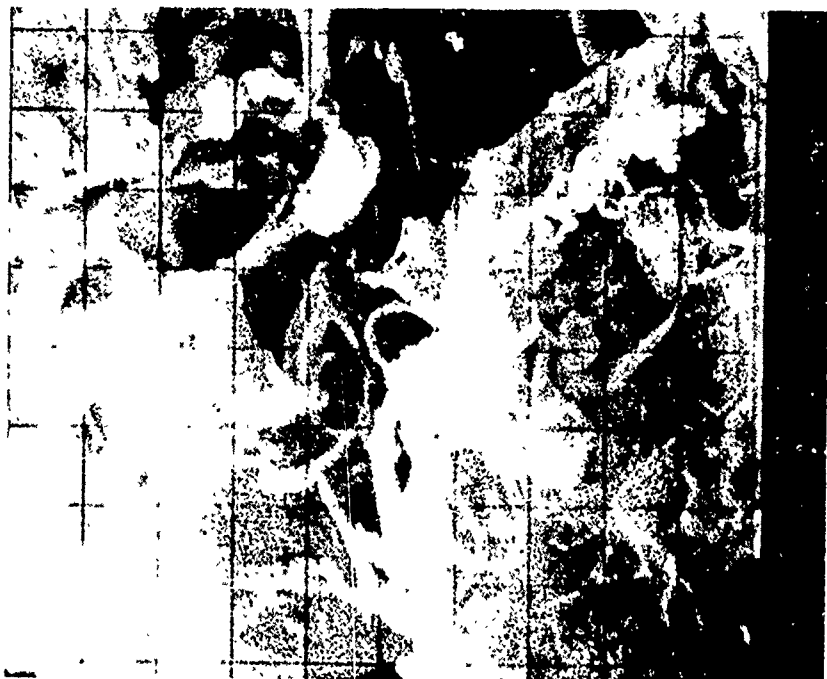
SEM DATA

REQUEST # 7815

SPECIMEN DA-1B

DATE 27 Mar

OPERATOR JPL



Magnification 5000

Angle of View 45°

Det. Mode Se

Coating An

Operating Conditions:

Accel. Potent. 25 kv

Condenser Lens \_\_\_\_\_

Obj. Lens \_\_\_\_\_

Detector Type \_\_\_\_\_

Settings \_\_\_\_\_

NEG IDENT E 1

Magnification 2500

Angle of View 45°

Det. Mode Se

Coating An

Operating Conditions:

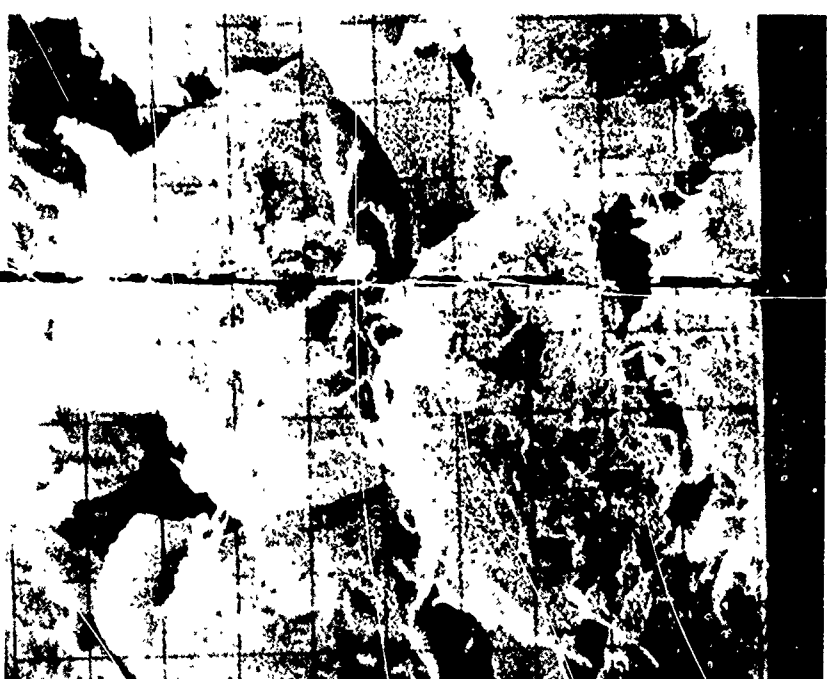
Accel. Potent. 25 kv

Condenser Lens \_\_\_\_\_

Obj. Lens \_\_\_\_\_

Detector Type \_\_\_\_\_

Settings \_\_\_\_\_



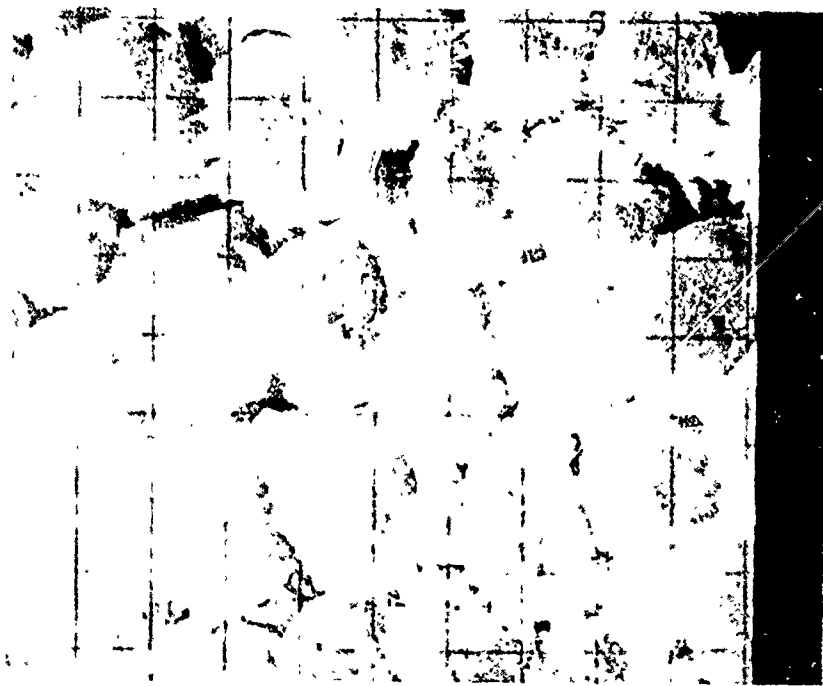
Neg Ident E 2

Figure 26. Scanning electron micrographs of specimen DA-1B  
(cont) (Dacron-Epon 828/MPDA, end-oriented)

SEM DATA

REQUEST # 7215  
SPECIMEN DA-1B

DATE 27 Ma  
OPERATOR JLH

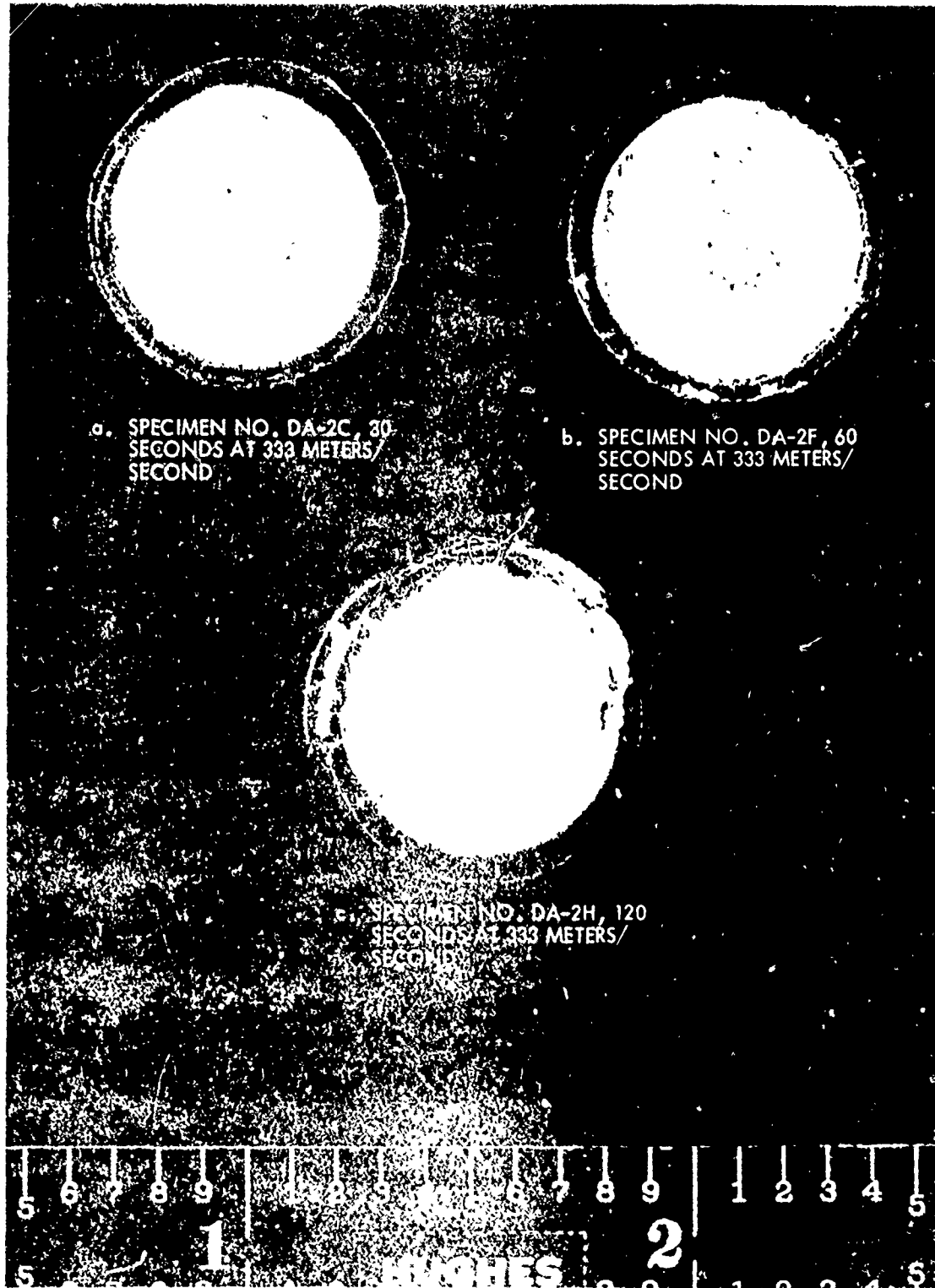


Magnification 1000  
Angle of View 45  
Det. Mode sc  
Coating Ar  
Operating Conditions:  
Accel. Potent. 25 KV  
Condenser Lens \_\_\_\_\_  
Obj. Lens \_\_\_\_\_  
Detector Type \_\_\_\_\_  
Settings \_\_\_\_\_  
\_\_\_\_\_  
\_\_\_\_\_

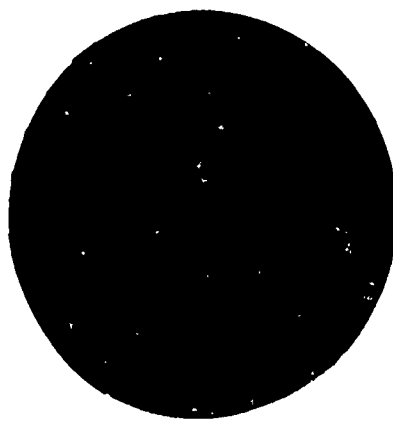
Neg Ident E3  
Magnification 500  
Angle of View 45°  
Det. Mode Se  
Coating Ar  
Operating Conditions:  
Accel. Potent. 25 KV  
Condenser Lens \_\_\_\_\_  
Obj. Lens \_\_\_\_\_  
Detector Type \_\_\_\_\_  
Settings \_\_\_\_\_  
\_\_\_\_\_  
\_\_\_\_\_

Neg Ident E4

Figure 26. Scanning electron micrographs of specimen DA-1B  
(cont) (Dacron-Epon 828/MPDA, end-oriented)



b. SPECIMEN NO. DA-2F, 60  
SECONDS AT 333 METERS/  
SECOND



a. SPECIMEN NO. DA-3A, 30  
SECONDS AT 333 METERS/  
SECOND



b. SPECIMEN NO. DA-3D, 60  
SECONDS AT 333 METERS/  
SECOND



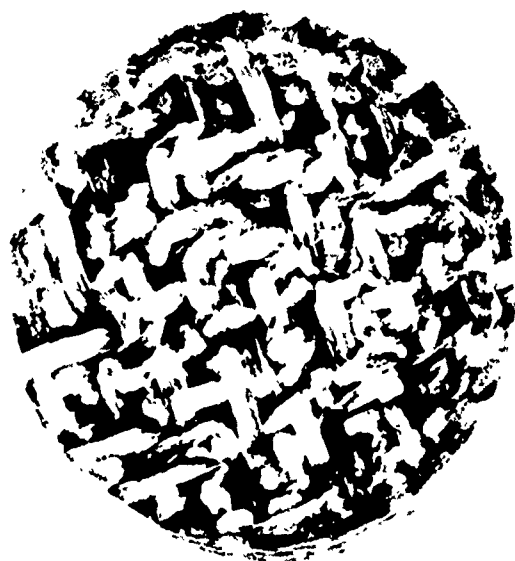
c. SPECIMEN NO. DA-3I, 120  
SECONDS AT 333 METERS/  
SECOND



Figure 28. Dacron 110c denier yarn (plasma-treated) - Ipon 828/  
MPDA, end-oriented reinforcement  
(content  $\approx$  73.9 volume-percent).

TABLE 4. RELATIVE RAIN EROSION RESISTANCE OF VARIOUS REINFORCEMENT CONFIGURATIONS (MATRIX: EPON 828/MPDA, EXCEPT AS NOTED; REINFORCEMENT: SCG GLASS, NOMEX OR PRD-49)

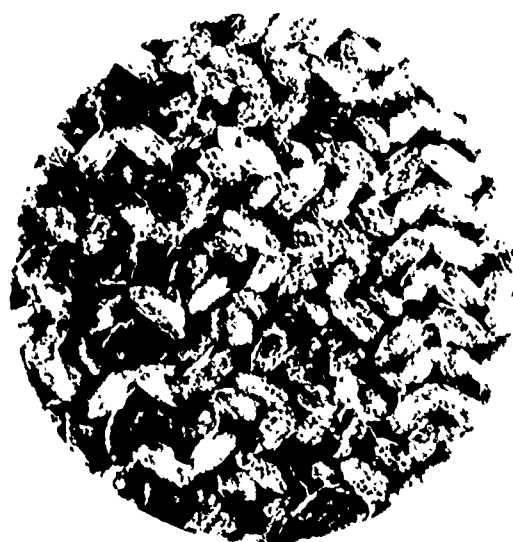
Specimen Code	Reinforcement Configuration	Reinforcement Content, volume-percent	Void Content, percent	Velocity, meters/sec	Exposure Time, sec	Weight Loss, mg	Erosion Depth, mils	Appearance	Figure Refs.
3D-5A 3D-5B	Omnaweave 337-04AA (Nomex 1014)	42.3	3.3	333	10	352	21.4	Extremely eroded	25
3D-6A 3D-6B	Omnaweave 337-04AA (Nomex 1200 denier yarn)	53.8	13.5	333	30	896	-	Eroded through	
L-2A L-2B L-2C L-2D	Nomex Fabric Style 3105 with Epon 825, 55 PBW and Versamid 140, 45 PBW	60.7	3.2	333	30	68	-3.4	Moderately eroded	30
L-2A L-2B L-2C L-2D	Nomex Fabric Style 3105 with Epon 825, 55 PBW and Versamid 140, 45 PBW	60.7	3.2	333	30	57	-5.1	Moderately eroded	31
3D-7A 3D-7B 3D-7C 3D-7D	Omnaweave 337-04AA (Nomex 1200 denier yarn) Epon 825/Versamid 140	49.6	10.8	333	30	336	77.6	Deeply eroded	
3D-7E 3D-7F					30	45	74.2	Deeply eroded	32
3D-7E 3D-7F					30	45	74.0	Deeply eroded	
3D-7E 3D-7F					30	285	74.4	Deeply eroded	
3D-8A 3D-8B 3D-8C 3D-8D	PRD-49 Type III, 3-D orthogonal construction, 0.090 inch centers (plasma treated)	-	-	333	60	95	15.8	Moderately eroded	
3D-8A 3D-8B 3D-8C 3D-8D	PRD-49 Type III, 3-D layer-to-layer lock fabric (0.060 inch/ply) Epon 828/methane diamine 57.3	3.4	333	60	66	15.6	13.7	Moderately eroded	33
3D-9A 3D-9B 3D-9C 3D-9D 3D-9E 3D-9F	PRD-49 Type III, 3-D layer-to-layer lock fabric (0.060 inch/ply) Epon 828/methane diamine 57.3	3.4	333	60	117	129	16.3	Moderately eroded	
3D-9A 3D-9B 3D-9C 3D-9D 3D-9E 3D-9F	PRD-49 Type III, 3-D layer-to-layer lock fabric (0.060 inch/ply) Epon 828/methane diamine 57.3	3.4	333	60	200	200	26	Extremely eroded	
3D-9G 3D-9H 3D-9I					60	317	37	Extremely eroded	
3D-9G 3D-9H 3D-9I					60	381	36	Extremely eroded	
3D-9A 3D-9B 3D-9C 3D-9D 3D-9E 3D-9F	PRD-49 Type III, 3-D layer-to-layer lock fabric (0.060 inch/ply) Epon 828/methane diamine 57.3	3.4	333	60	30	346	73	Extremely eroded	34
3D-9A 3D-9B 3D-9C 3D-9D 3D-9E 3D-9F	PRD-49 Type III, 3-D layer-to-layer lock fabric (0.060 inch/ply) Epon 828/methane diamine 57.3	3.4	333	60	60	444	101	Extremely eroded	
3D-9A 3D-9B 3D-9C 3D-9D 3D-9E 3D-9F	PRD-49 Type III, 3-D layer-to-layer lock fabric (0.060 inch/ply) Epon 828/methane diamine 57.3	3.4	333	60	60	502	104	Extremely eroded	
3D-9A 3D-9B 3D-9C 3D-9D 3D-9E 3D-9F	PRD-49 Type III, 3-D layer-to-layer lock fabric (0.060 inch/ply) Epon 828/methane diamine 57.3	3.4	333	60	120	462	103	Eroded through	
3D-9A 3D-9B 3D-9C 3D-9D 3D-9E 3D-9F	PRD-49 Type III, 3-D layer-to-layer lock fabric (0.060 inch/ply) Epon 828/methane diamine 57.3	3.4	333	60	120	686	197	Eroded through	



a. Specimen No. 3D-5A, 10 seconds  
at 333 meters/second



b. Specimen No. 3D-5B, 30 seconds  
at 333 meters/second



c. Unexposed Control

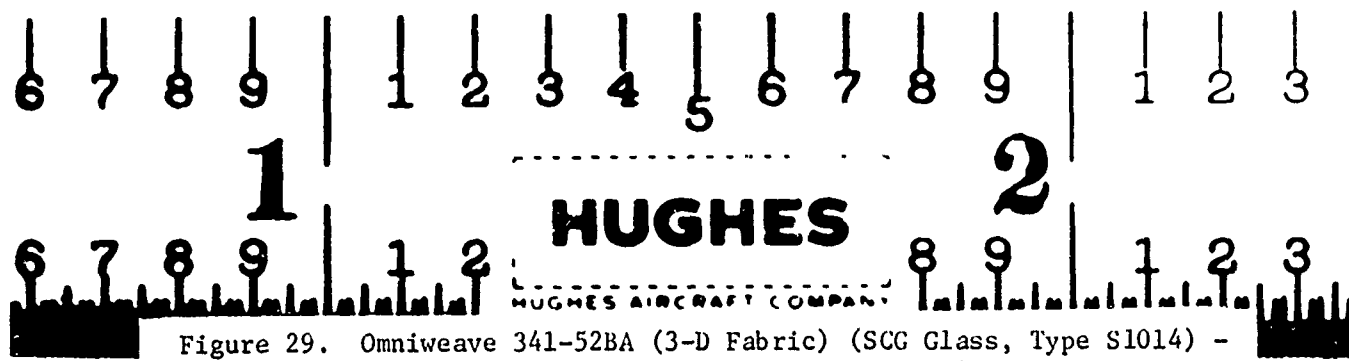
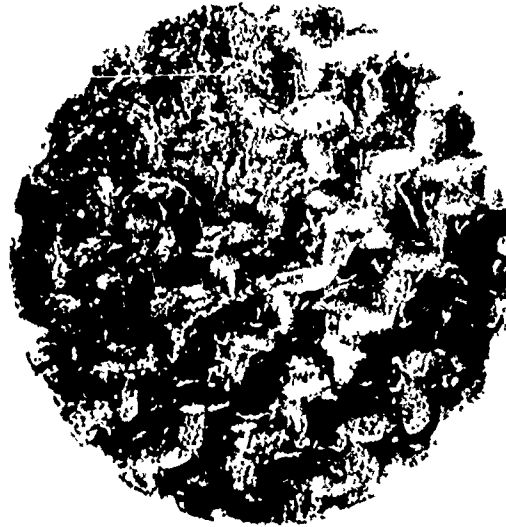


Figure 29. Omniweave 341-52BA (3-D Fabric) (SCG Glass, Type S1014) -  
Epon 828/MPDA (Reinforcement Content = 42.3 volume-  
percent)



a. Specimen No. 3D-6A, 30 seconds  
at 333 meters/second

b. Specimen No. 3D-6B, 30 seconds  
at 333 meters/second



c. Unexposed Control

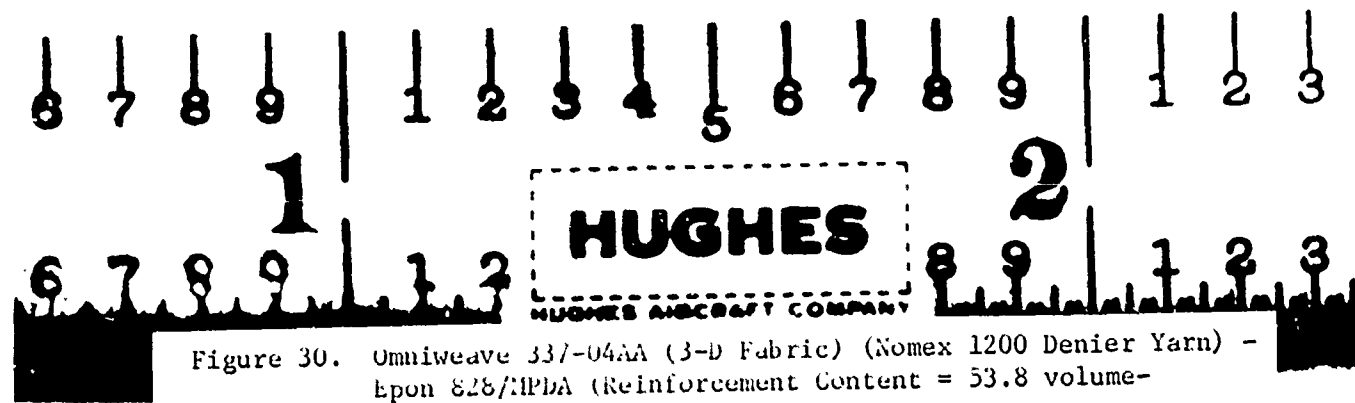
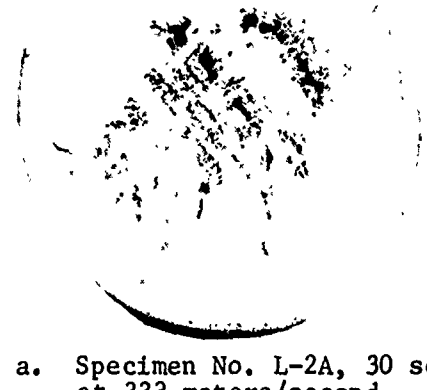


Figure 30. Omniweave 337-04AA (3-D Fabric) (Nomex 1200 Denier Yarn) -  
Epon 828/TPDA (Reinforcement Content = 53.8 volume-  
percent)



a. Specimen No. L-2A, 30 seconds  
at 333 meters/second



b. Specimen No. L-2B, 30 seconds  
at 333 meters/second



c. Specimen No. L-2C, 30 seconds  
at 333 meters/second



d. Specimen No. L-2D, 30 seconds  
at 333 meters/second

e. Unexposed Control

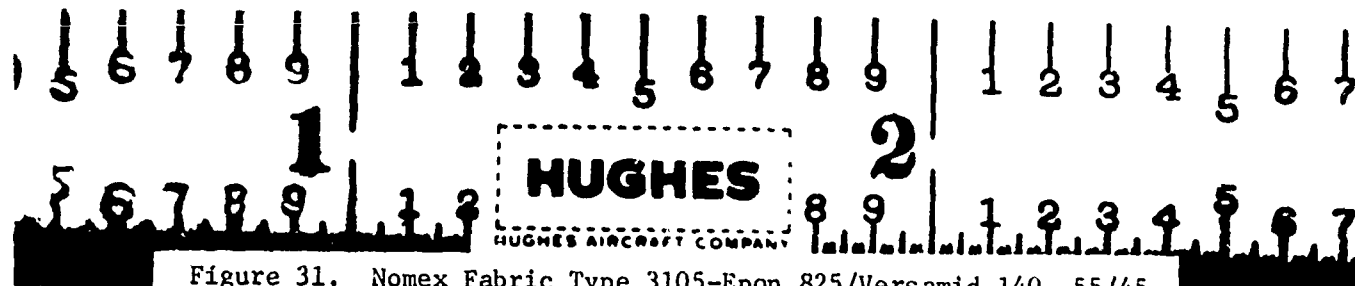


Figure 31. Nomex Fabric Type 3105-Epon 825/Versamid 140, 55/45  
(Reinforcement Content = 60.7 volume-percent, not  
end-oriented)

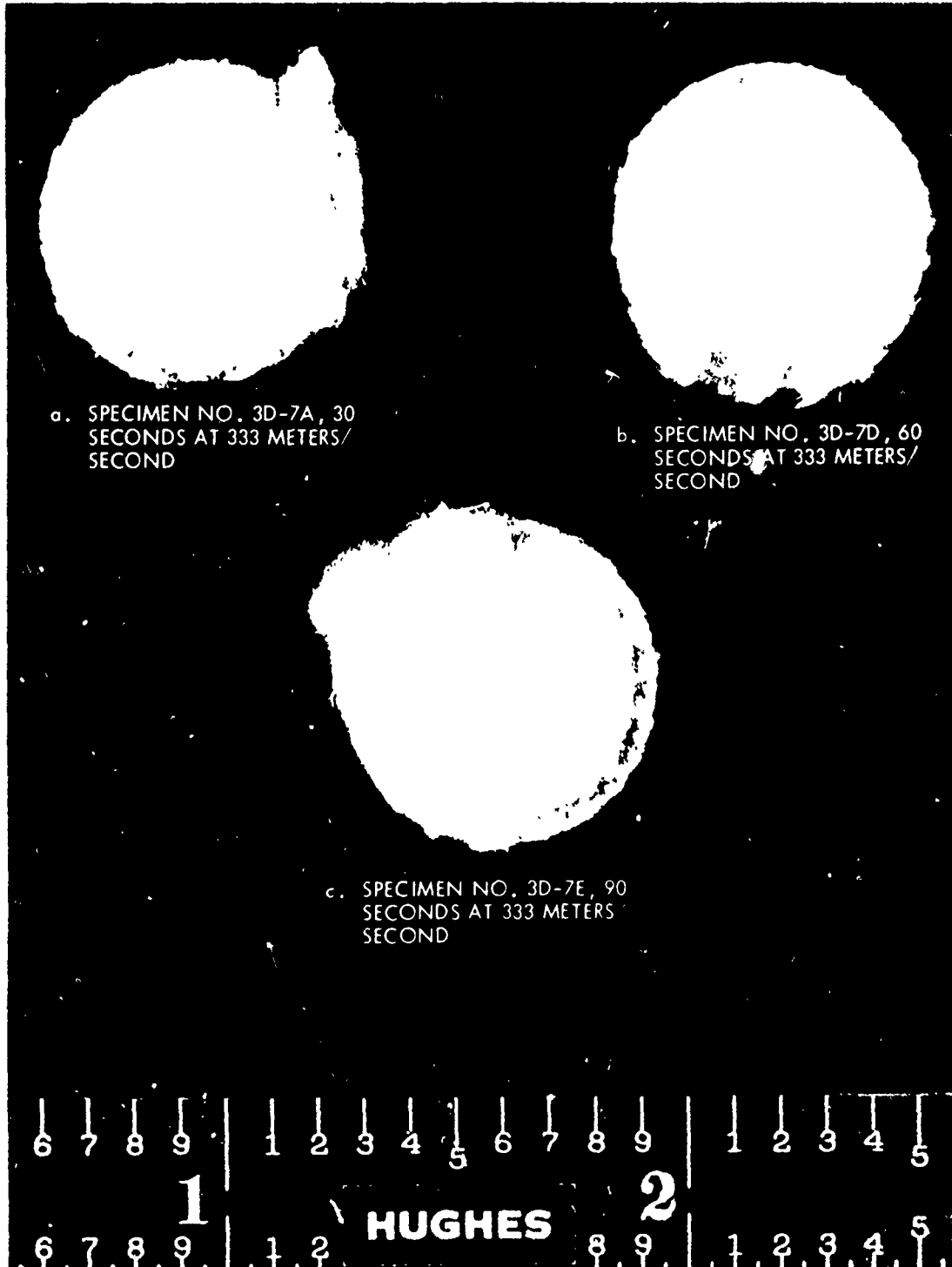


Figure 12. Orientation of 3D-7A (3-D Fabric) (Nomex 120 g/m<sup>2</sup>)  
on 120 g/m<sup>2</sup> Versamid 410 (reinforcement  
content = 19.6 g/m<sup>2</sup> per cent).



a. SPECIMEN NO. 3D-8A, 30  
SECONDS AT 333 METERS/  
SECOND



b. SPECIMEN NO. 3D-8C, 60  
SECONDS AT 333 METERS/  
SECOND



c. UNEXPOSED CONTROL



Figure 33. PRD-4<sup>c</sup> Type III 3-D orthogonal construction  
(plasma-treated) - Epon 828/MPDA.



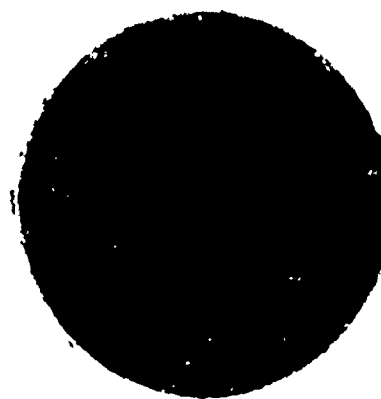
a. SPECIMEN NO. 3D-9B, 30  
SECONDS AT 333 METERS/  
SECOND



b. SPECIMEN NO. 3D-9F, 60  
SECONDS AT 333 METERS/  
SECOND



c. SPECIMEN NO. 3D-9G, 120  
SECONDS AT 333 METERS/  
SECOND



d. UNEXPOSED CONTROL



Figure 34. PRD-49 Type III 3-D fabric-Epon 828/menthane  
diamine (reinforcement content = 57.3 volume-percent).

TABLE 5. RELATIVE RAIN EROSION RESISTANCE OF EPON 828/MPDA-ECG GLASS ROVING, END-ORIENTED COMPOSITES WITH VARIOUS HARDENER CONTENTS (ALL SPECIMENS EXPOSED 30 SECONDS AT 333 METERS/SECOND)

Specimen Code	Reinforcement Content, volume-percent	Void Content, percent	Weight Loss, mg	Erosion Depth, mils	Appearance	Figure Refs.
UD-12A	75.0 (FRESH MPDA, 1.4X STOI.)	0	12.3	0.1	Deeply eroded locally	35
UD-12B			216	0.3	Deeply eroded	
UD-13A	73.1 (FRESH MPDA, STOI.)	0	62	0.3	Deeply eroded locally	36
UD-13B			237		Deeply eroded	
UD-14A	75.0 (FRESH MPDA, 1.6X STOI.)	0	147	0.1	Deeply eroded locally	37
UD-14B			13	0.1	Scattered pitting	
UD-15A	75.7 (FRESH MPDA, 1.2X STOI.)	0	165	0.1	Deeply eroded	38
UD-15B			41	0.2	Deeply eroded locally	
UD-16A	74.8 (OLD MDPA, 1.4X STOI.)	0	154	0.2	Deeply eroded	39
UD-16B			114	0.5	Deeply eroded	
UD-17A	69.6 (OLD MDPA, STOI.)	0	375	5.0	Deeply eroded	40
UD-17B			349	13.0	Deeply eroded	
UD-18A	75.8 (FRESH MDPA, STOI.)	0	119	0.3	Deeply eroded locally	41
UD-18B			18	0.2	Scattered deep pits	



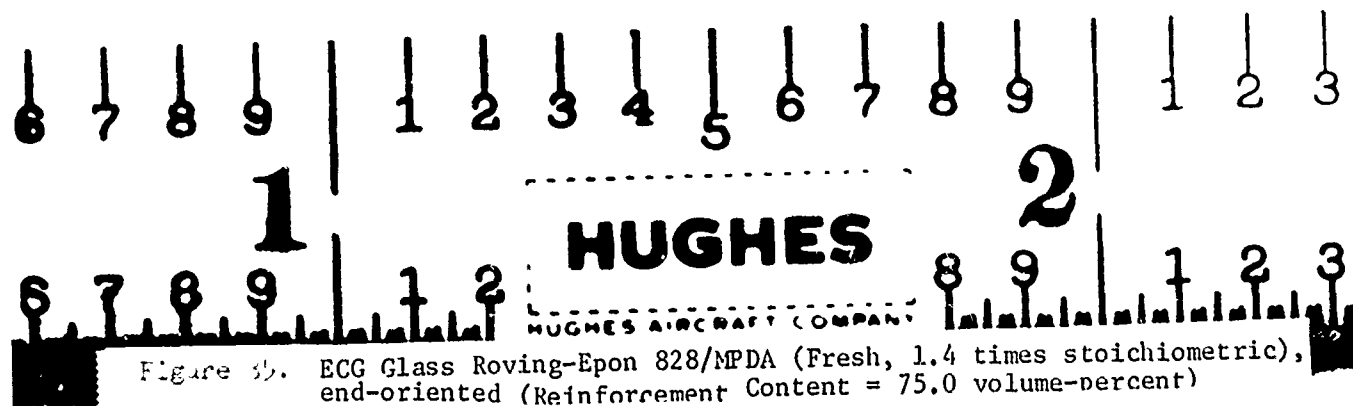
a. Specimen No. UD-12A, 30 seconds  
at 333 meters/second

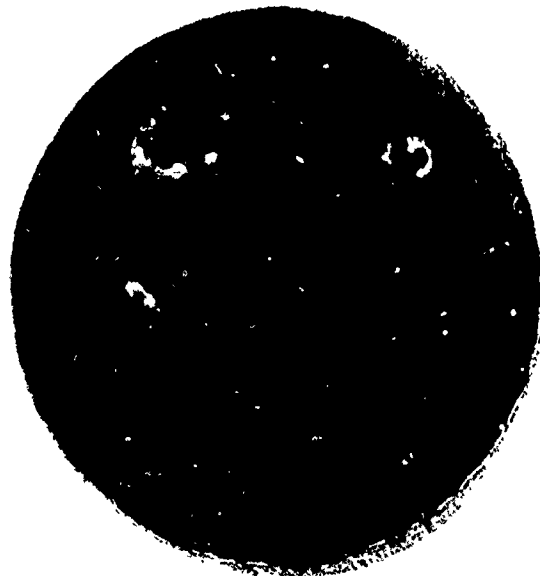


b. Specimen No. UD-12B, 30 seconds  
at 333 meters/second



c. Unexposed Control

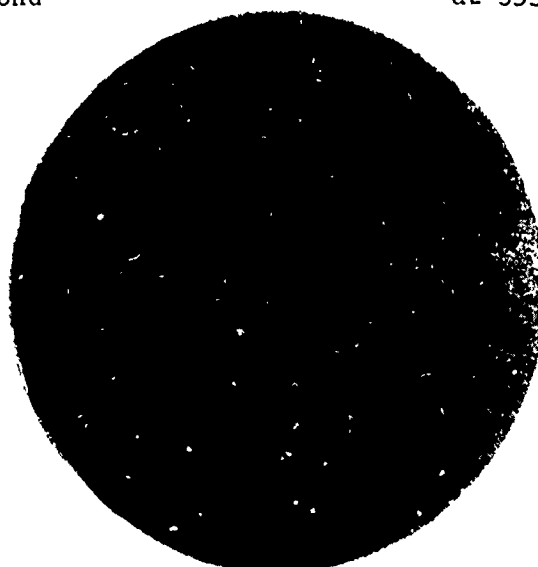




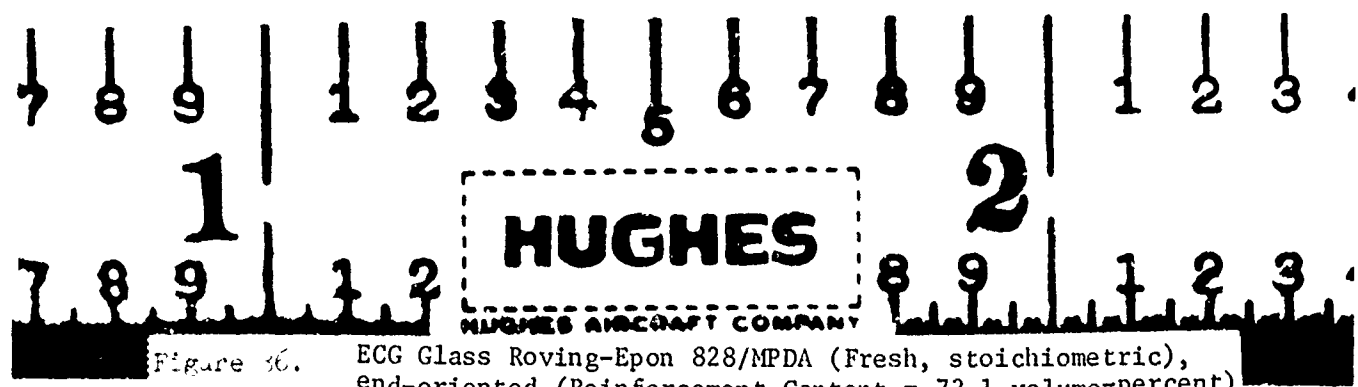
a. Specimen No. UD-13A, 30 seconds  
at 333 meters/second

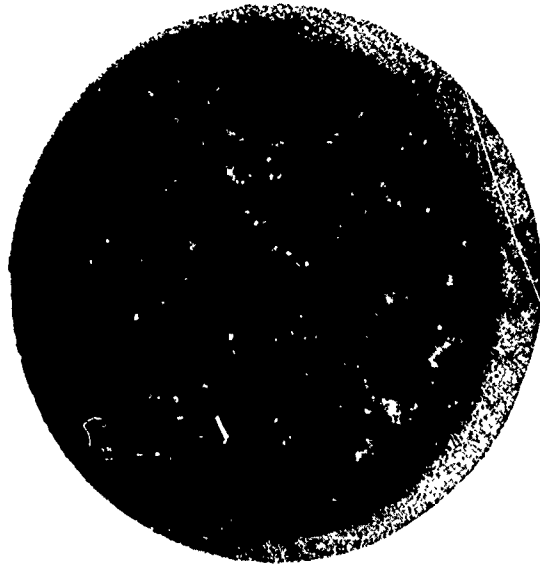


b. Specimen No. UD-13B, 30 seconds  
at 333 meters/second

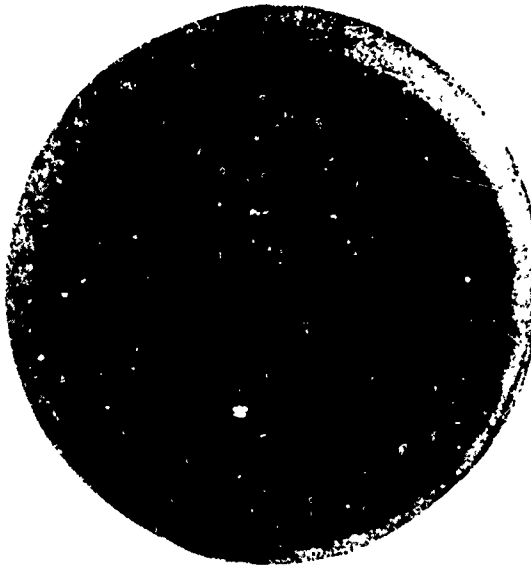


c. Unexposed Control

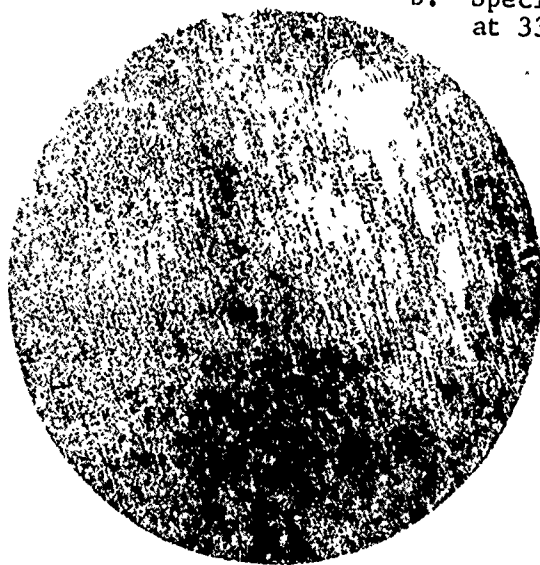




a. Specimen No. UD-14A, 30 seconds  
at 333 meters/second



b. Specimen No. UD-14B, 30 seconds  
at 333 meters/second



c. Unexposed Control

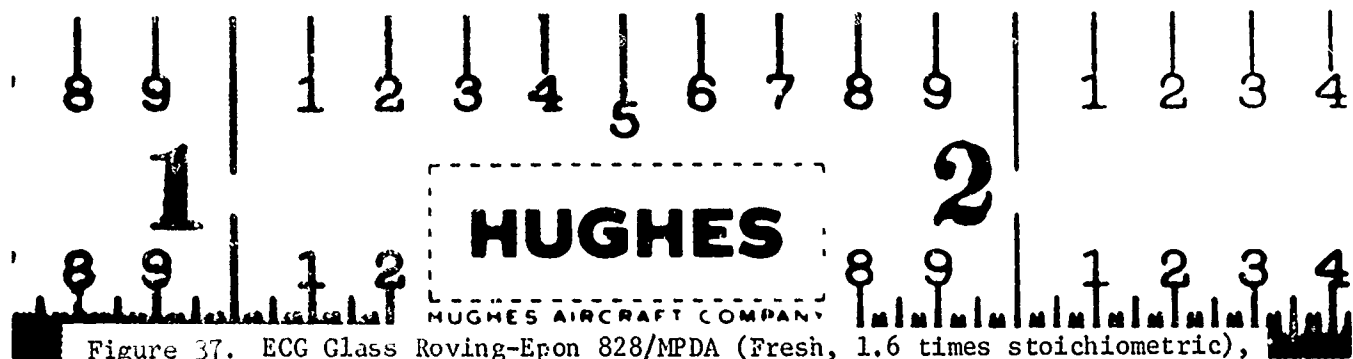


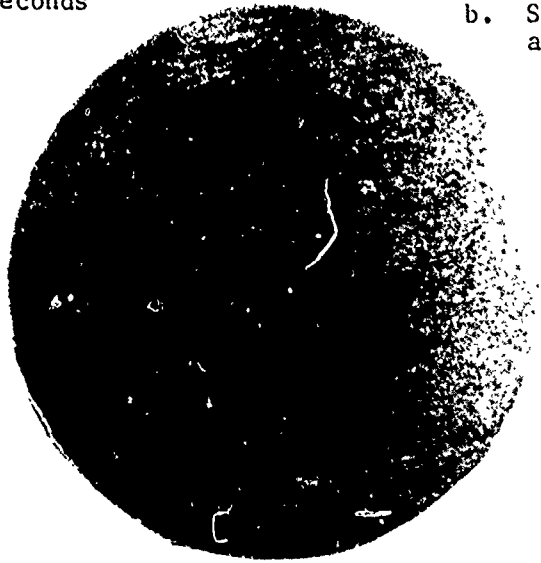
Figure 37. ECG Glass Roving-Epon 828/MPDA (Fresh, 1.6 times stoichiometric),  
end-oriented (Reinforcement Content = 75.0 volume-percent)



a. Specimen No. UD-15A, 30 seconds  
at 333 meters/second



b. Specimen No. UD-15B, 30 seconds  
at 333 meters/second



c. Unexposed Control

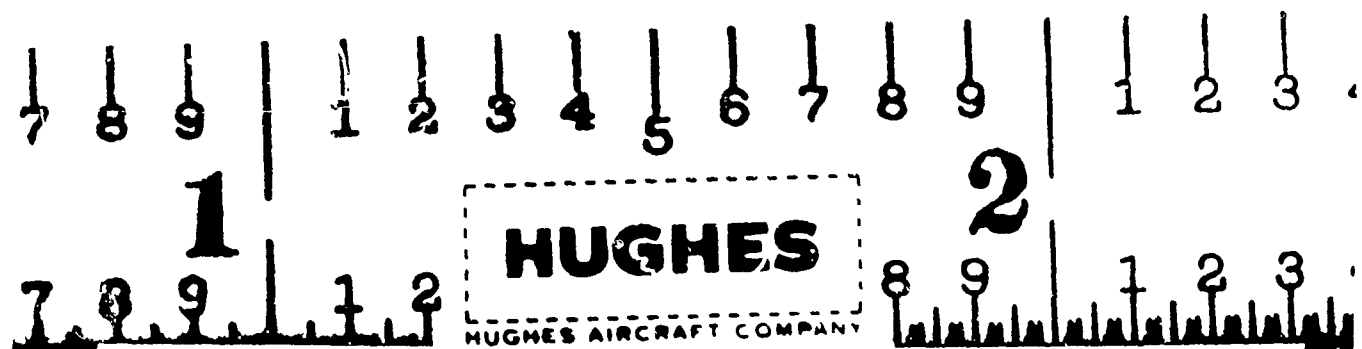
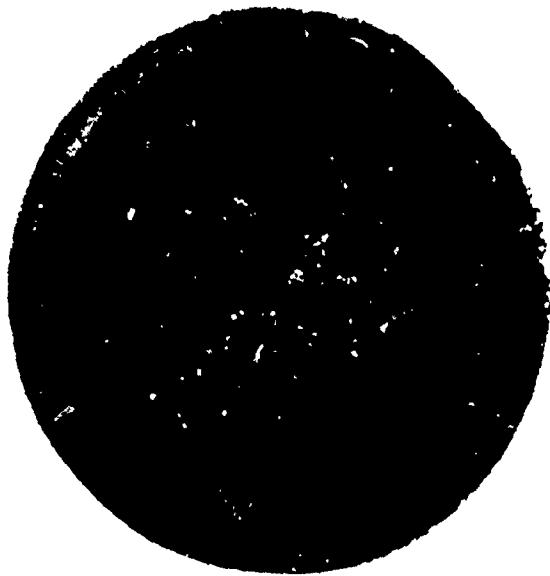


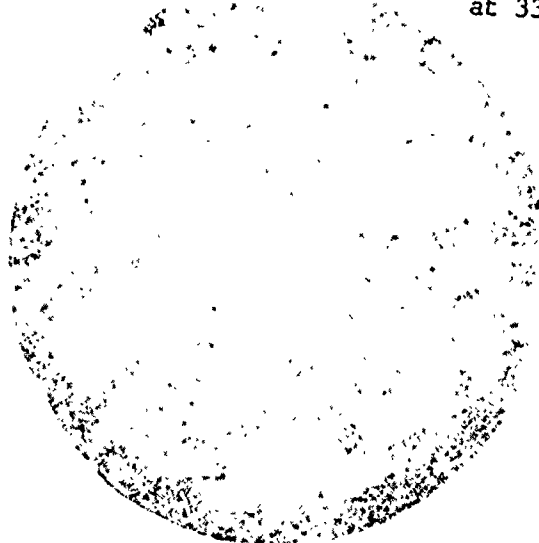
Figure 7. ECG Glass Roving-Epon 828/MPDA (Fresh, 1.2 times stoichiometric),  
end-oriented (Reinforcement Content = 75.7 volume-percent)



a. Specimen No. UD-16A, 30 seconds  
at 333 meters/second



b. Specimen No. UD-16B, 30 seconds  
at 333 meters/second



c. Unexposed Control

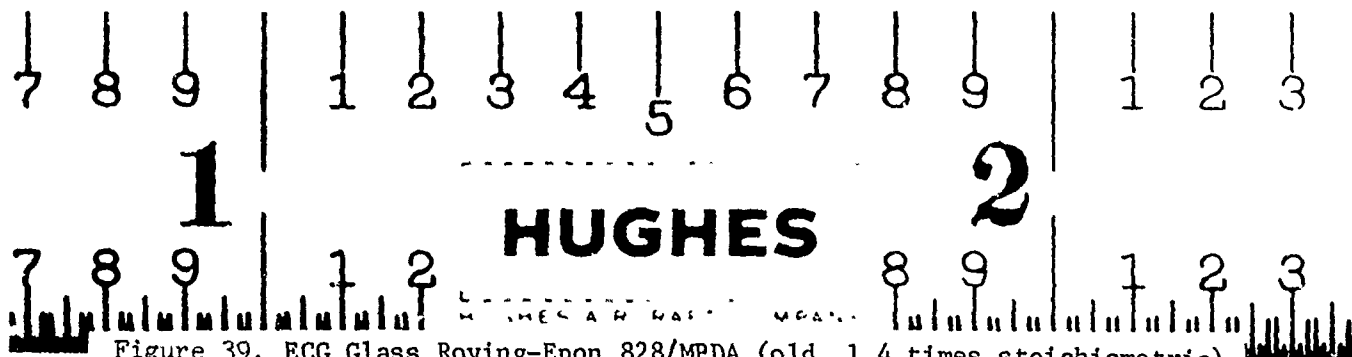
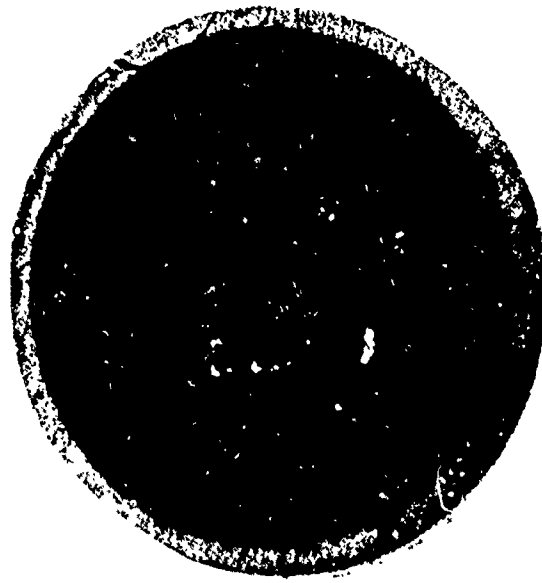


Figure 39. ECG Glass Roving-Epon 828/MPDA (old, 1.4 times stoichiometric),  
end-oriented (Reinforcement Content = 74.8 volume-percent)



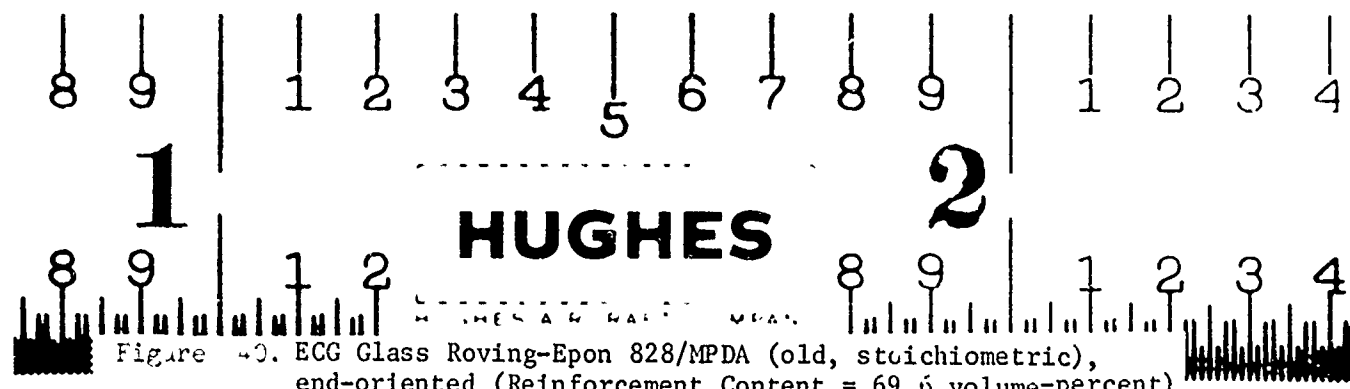
a. Specimen No. UD-17A, 30 seconds  
at 333 meters/second

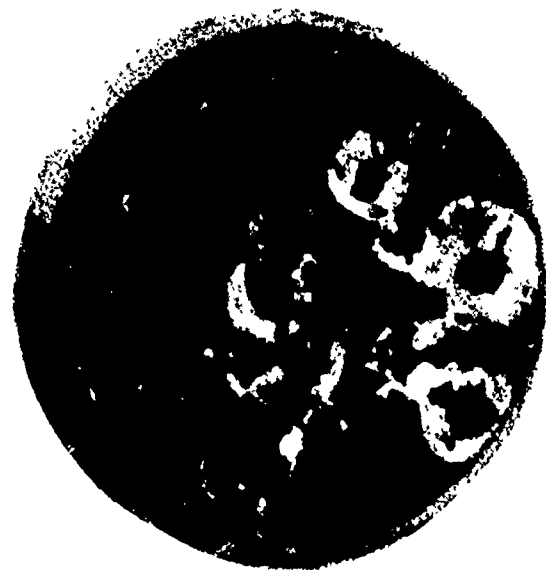


b. Specimen No. UD-17B, 30 seconds  
at 333 meters/second

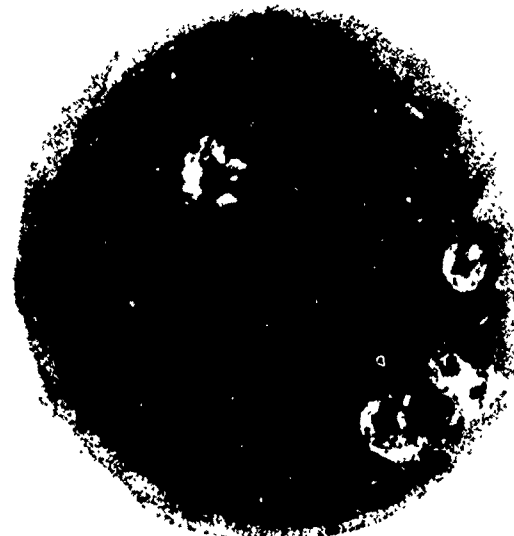


c. Unexposed Control

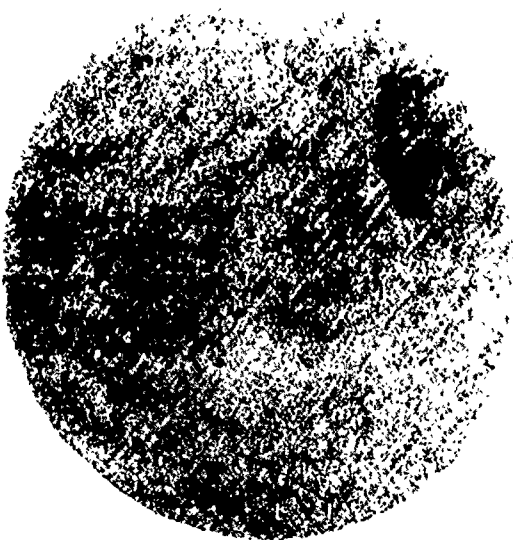




a. Specimen No. UD-18A, 30 seconds  
at 333 meters/second



b. Specimen No. UD-18B, 30 seconds  
at 333 meters/second



c. Unexposed Control

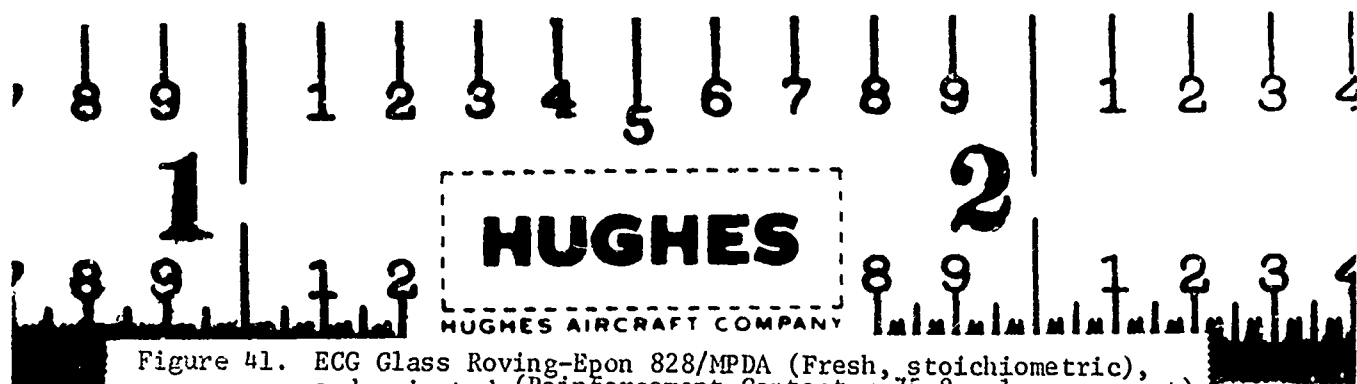


Figure 41. ECG Glass Roving-Epon 828/MPDA (Fresh, stoichiometric),  
end-oriented (Reinforcement Content = 75.8 volume-percent)

TABLE 6. RELATIVE RAIN EROSION RESISTANCE OF EPON 828/MPDA-NOMEX,  
END-ORIENTED COMPOSITES WITH VARIOUS FIBER LOADINGS  
(ALL SPECIMENS TESTED AT 333 METERS/SECOND)

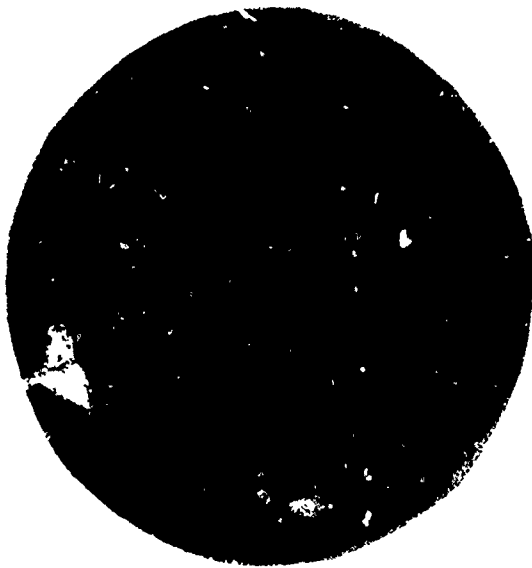
Specimen Code	Reinforcement Content, volume-percent	Void Content, percent	Exposure Time, sec	Weight Loss, mg	Erosion Depth, mils	Appearance	Figure Refs.
N-2A N-2B	78.6	3.6	30 60	1.6 1.0	-0.4 -1.3	Broken around edge Local erosion next to retaining ring	16
N-4A N-4B	64.0	2.4	30 60	0.4 4.4	-0.1 -0.1	Very slightly eroded; large radial crack Very slight erosion except next to retaining ring	42, 43
N-5A N-5B	52.4	2.0	30 60	4.1 9.1	-0.4 -0.4	Slightly eroded Slightly eroded	44
N-7A N-7B	80.3	2.3	30 60	1.0 3.6	-	Broken into many pieces Broken into three pieces	45
N-9A N-9B N-9C			30 30 30	2.3 3.1 2.7	1.5 -0.2 -0.4		
N-9D N-9E N-9F	35.3	2.2	60 60 60	57 75 86	0 0.3 0.7	Deeply eroded locally	46
N-9G N-9H N-9I			120 120 120	209 168 161	7.2 7.4 5.0		
N-10A N-10B N-10C			30 30 30	2.5 2.3 2.7	-0.2 1.5 -0.4	Slightly eroded except near retaining ring	
N-10D N-10E N-10F	41.2	3.1	60 60	4.4 4.3 4.1	-0.4 -0.3 -0.7	Moderately eroded with scattered pitting	47
N-10G N-10H N-10I			120 120 120	89 78 84	0.9 0.9 1.8	Deeply eroded locally	

(continued)

Table 6. (Concluded)

Specimen Code	Reinforcement Content, volume-percent	Void Content, percent	Exposure Time, sec	Weight Loss, mg	Erosion Depth, mils	Appearance	Figure Refs.
N-11A N-11B N-11C			30 30 30	22 22 22	-0.1 -0.2 -0.8	Slightly eroded except near retaining ring	
N-11D N-11E N-11F	45.4	2.6	60 60 60	34 31 29	-0.1 -0.1 -0.7	Moderately eroded locally	*48
N-11G N-11H N-11I			120 120 120	58 65 58	0.5 -0.7 -0.3	Deeply eroded locally	
N-15A N-15B N-15C			30 30 30	16 36 14	-0.1 -0.3 -0.2	Lightly eroded	
N-15D N-15E N-15F	41.2 <sup>a</sup>	2.1	60 60 60	20 29 23	-0.2 -0.3 -0.4	Moderately eroded, deep pitting	49
N-15G N-15H N-15I			120 120 120	50 42 59	0.1 -0.3 0	Deeply eroded locally	
N-16A N-16B N-16C			30 30 30	11 15 14	-0.2 -0.1 -0.3	Lightly eroded	
N-16D N-16E N-16F	76.8 <sup>b</sup>	5.9	60 60	26 22 16	-0.6 -0.4 0.1	Deeply eroded locally	50
N-16G N-16H N-16I			120 120 120	41 25 24	0.1 -0.4 0	Deeply eroded; cracked	

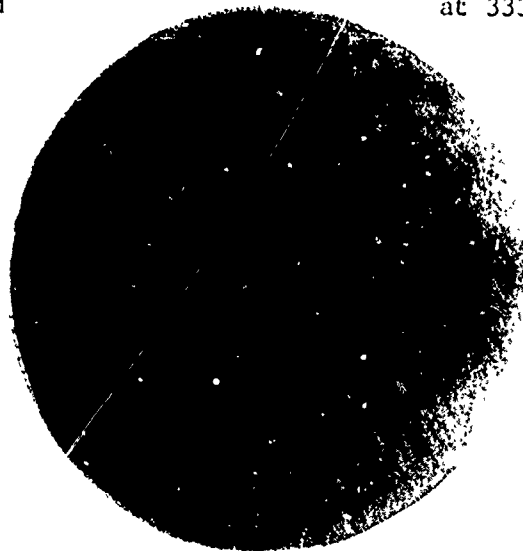
<sup>a</sup> Nomex yarn treated with a low pressure plasma prior to impregnation with resin system.



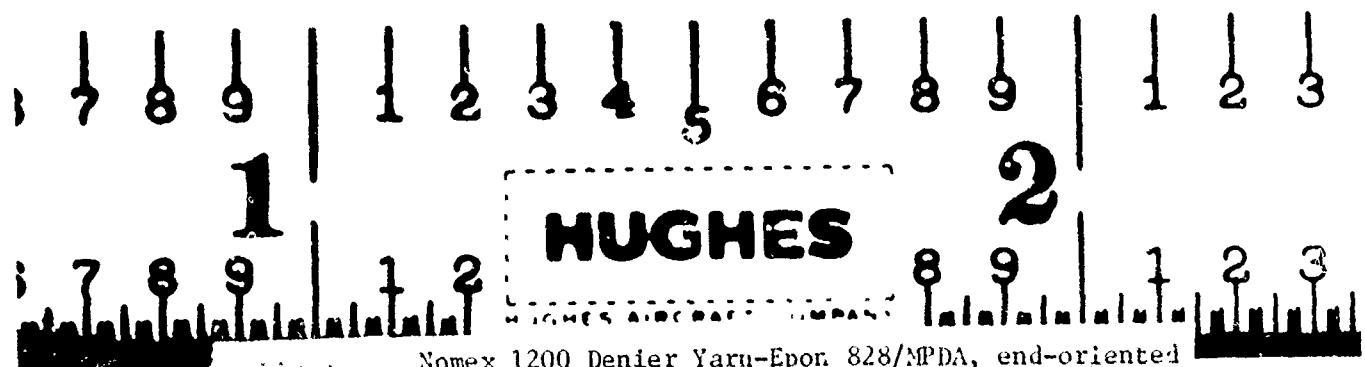
a. Specimen No. N-4A, 30 seconds  
at 333 meters/second



b. Specimen No. N-4B, 60 seconds  
at 333 meters/second



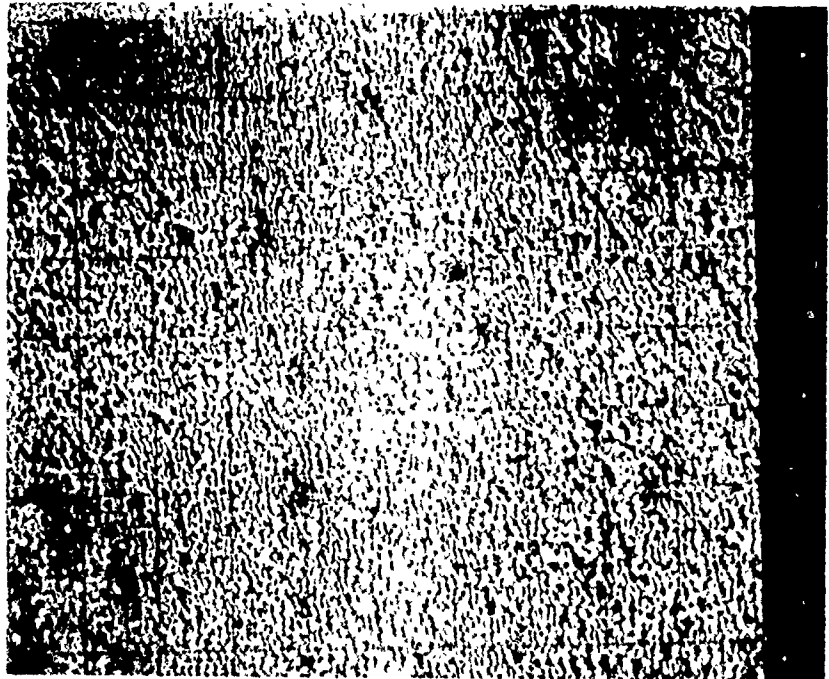
c. Unexposed Control



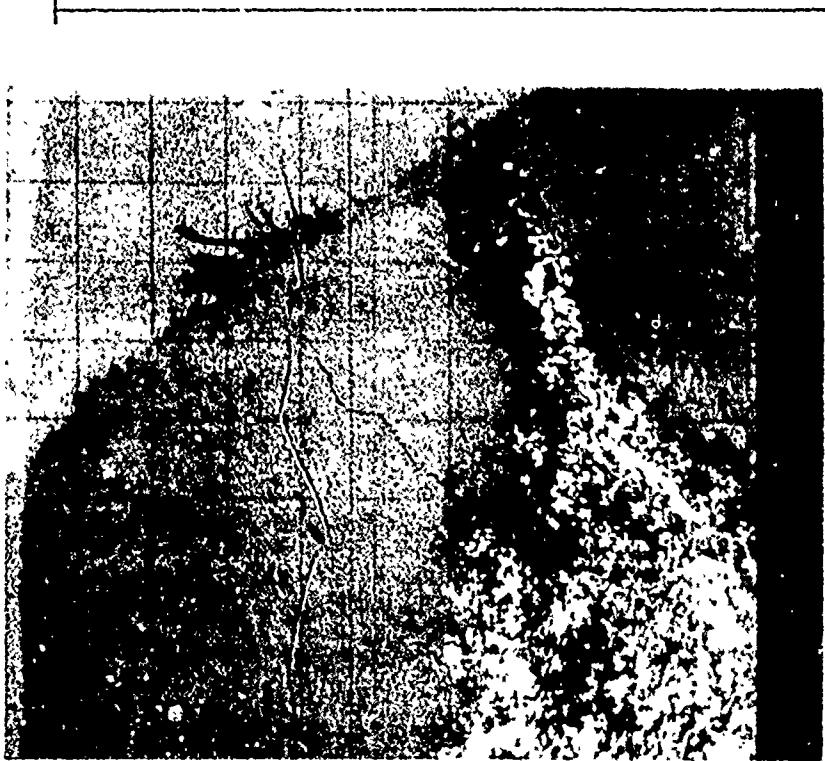
## SEM DATA

REQUEST # 7215  
 SPECIMEN N-4A

DATE 27 Mar  
 OPERATOR JL



Magnification 100X  
 Angle of View 45°  
 Det. Mode Sec  
 Coating An  
 Operating Conditions:  
 Accel. Potent. 25 KV  
 Condenser Lens \_\_\_\_\_  
 Obj. Lens \_\_\_\_\_  
 Detector Type \_\_\_\_\_  
 Settings \_\_\_\_\_  
Eroded Area



Neg Id# D5  
 Magnification 50X  
 Angle of View 45°  
 Det. Mode Sec  
 Coating An  
 Operating Conditions:  
 Accel. Potent. 17 KV  
 Condenser Lens \_\_\_\_\_  
 Obj. Lens \_\_\_\_\_  
 Detector Type \_\_\_\_\_  
 Settings \_\_\_\_\_  
Area of crack

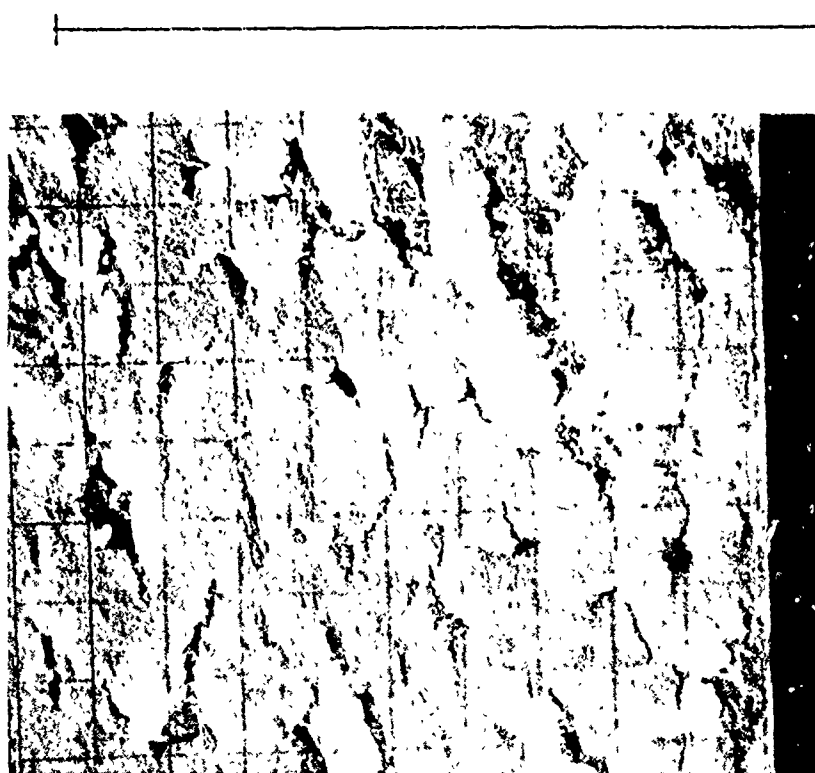
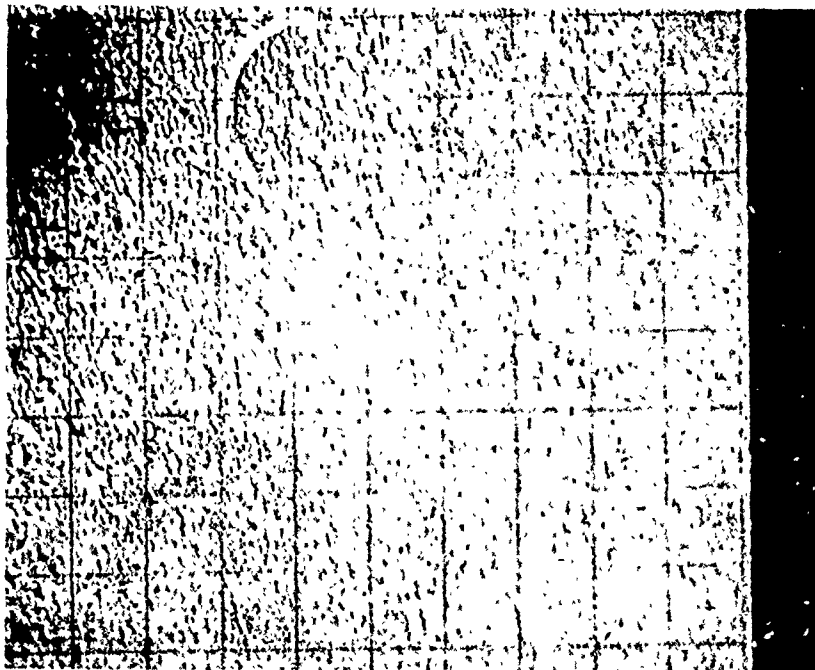
Neg Id# D8

Figure 43. Scanning electron micrographs of specimen N-4A (laminated upon 8-3/MPDA, end-oriented)

SEM DATA

REQUEST # 7215  
SPECIMEN N-4A

DATE 27 Mar  
OPERATOR JLD



Magnification 100  
Angle of View 45  
Det. Mode Rec  
Coating An  
Operating Conditions:  
Accel. Potent. 25 kv  
Condenser Lens \_\_\_\_\_  
Obj. lens \_\_\_\_\_  
Detector Type \_\_\_\_\_  
Settings \_\_\_\_\_  
Margins between eroded area (upper left) and uneroded area (lower right)

NEG IDENT D7  
Magnification 1000  
Angle of View 45°  
Det. Mode Rec  
Coating An  
Operating Conditions:  
Accel. Potent. 25 kv  
Condenser Lens \_\_\_\_\_  
Obj. lens \_\_\_\_\_  
Detector Type \_\_\_\_\_  
Settings \_\_\_\_\_  
Uneroded area

NEG IDENT D6

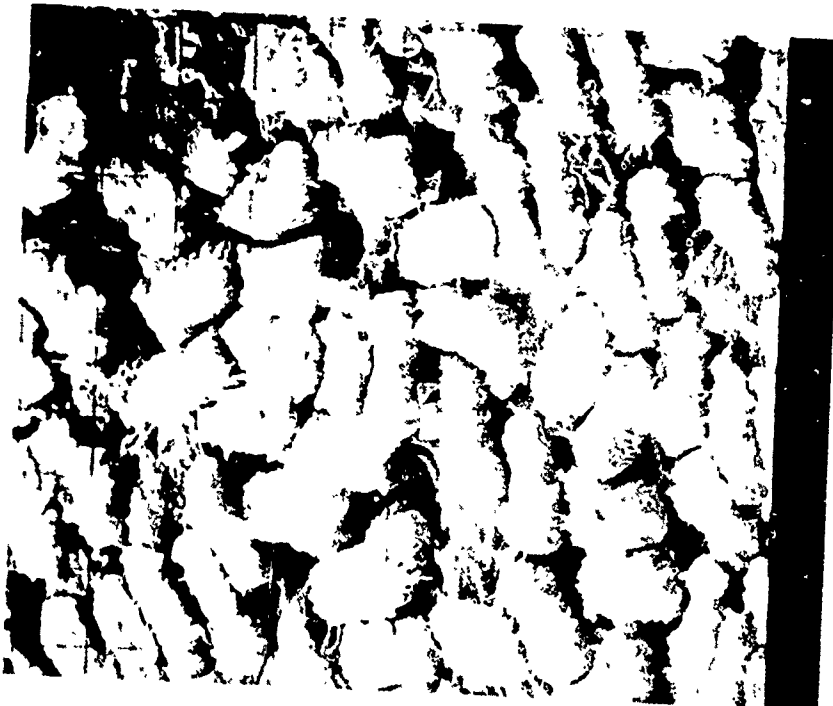
Figure 43. Scanning electron micrographs of specimen N-4A  
(cont) (Nomex-Epon 828/EPDA, end-oriented)

SEM DATA

REQUEST # 7215

SPECIMEN N-4A

DATE 27 Mar  
OPERATOR JRF



Magnification 1000

Angle of View 45°

Det. Mode sec

Coating An

Operating Conditions:

Accel. Potent. 25 kv

Condenser Lens

Obj. Lens

Detector Type

Settings

Eroded area

NEG IDENT D3

Magnification 500

Angle of View 45°

Det. Mode sec

Coating An

Operating Conditions:

Accel. Potent. 25 kv

Condenser Lens

Obj. Lens

Detector Type

Settings

Eroded area

NEG IDENT D4

Figure 43. Scanning electron micrographs of specimen N-4A  
(cont) (Nomex-Epon 828/MPDA, end-oriented)

SEM DATA

REQUEST # 7215

SPECIMEN N-4A (Nomex - 828/MPDA)

DATE 27 Mar

OPERATOR JCH



Magnification 5000

Angle of View 45°

Det. Mode See

Coating An

Operating Conditions:

Accel. Potent. 25 KV

Condenser Lens

Obj. Lens

Detector Type

Settings

Eroded Area



NEG IDENT D1

Magnification 2500X

Angle of View 45°

Det. Mode See

Coating An

Operating Conditions:

Accel. Potent. 25 KV

Condenser Lens

Obj. Lens

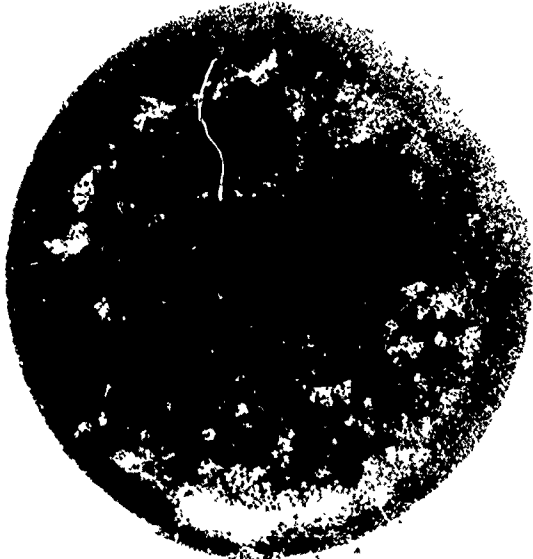
Detector Type

Settings

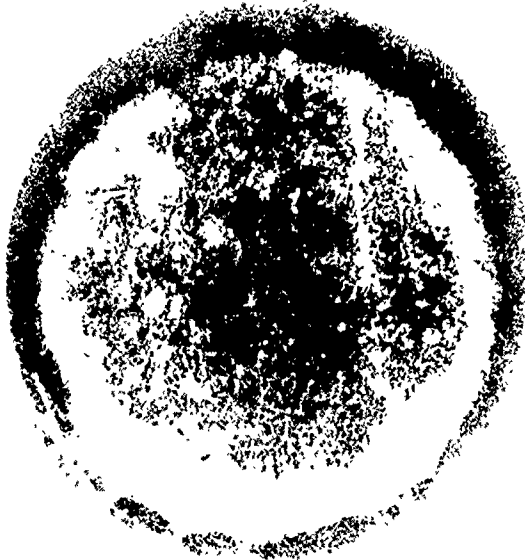
Eroded Area

NEG IDENT T

Figure 43. Scanning electron micrographs of specimen N-4A



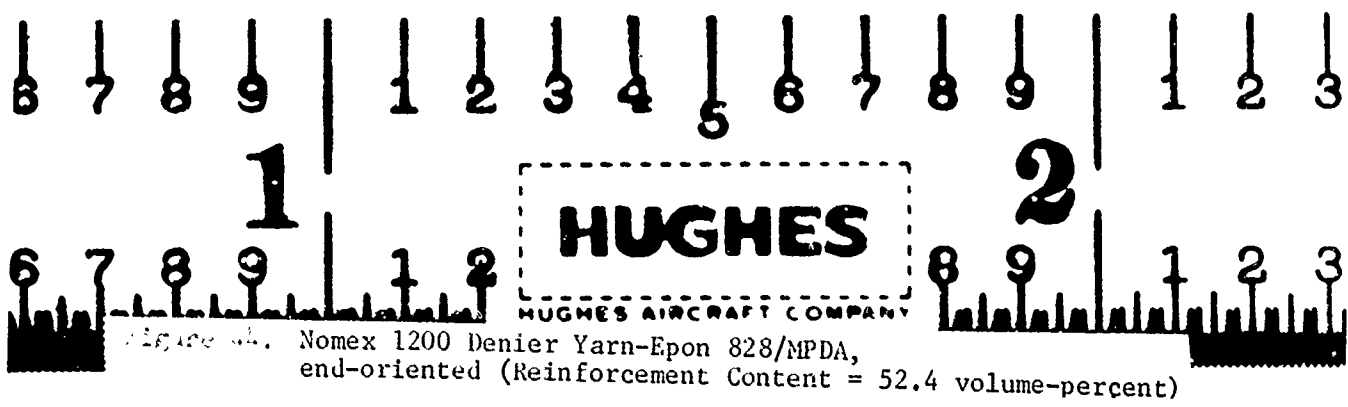
a. Specimen No. N-5A, 30 seconds  
at 333 meters/second

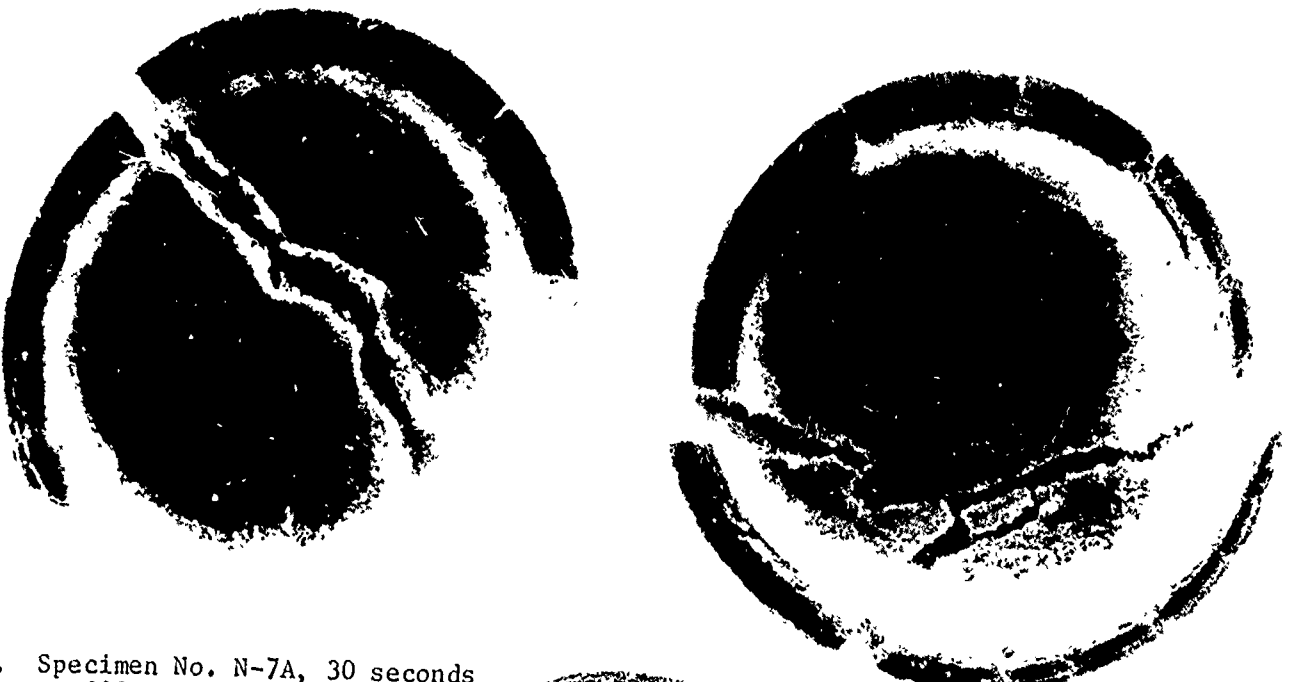


b. Specimen No. N-5B, 60 seconds  
at 333 meters/second



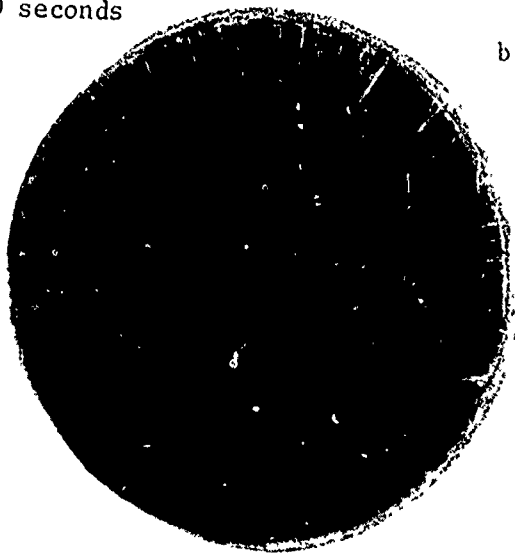
c. Unexposed Control



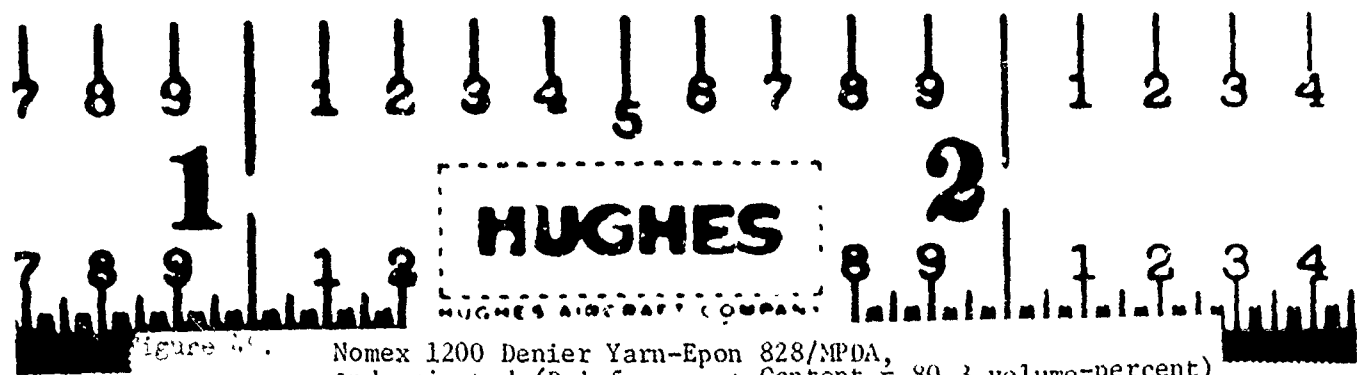


a. Specimen No. N-7A, 30 seconds  
at 333 meters/second

b. Specimen No. N-7B, 60 seconds  
at 333 meters/second



c. Unexposed Control



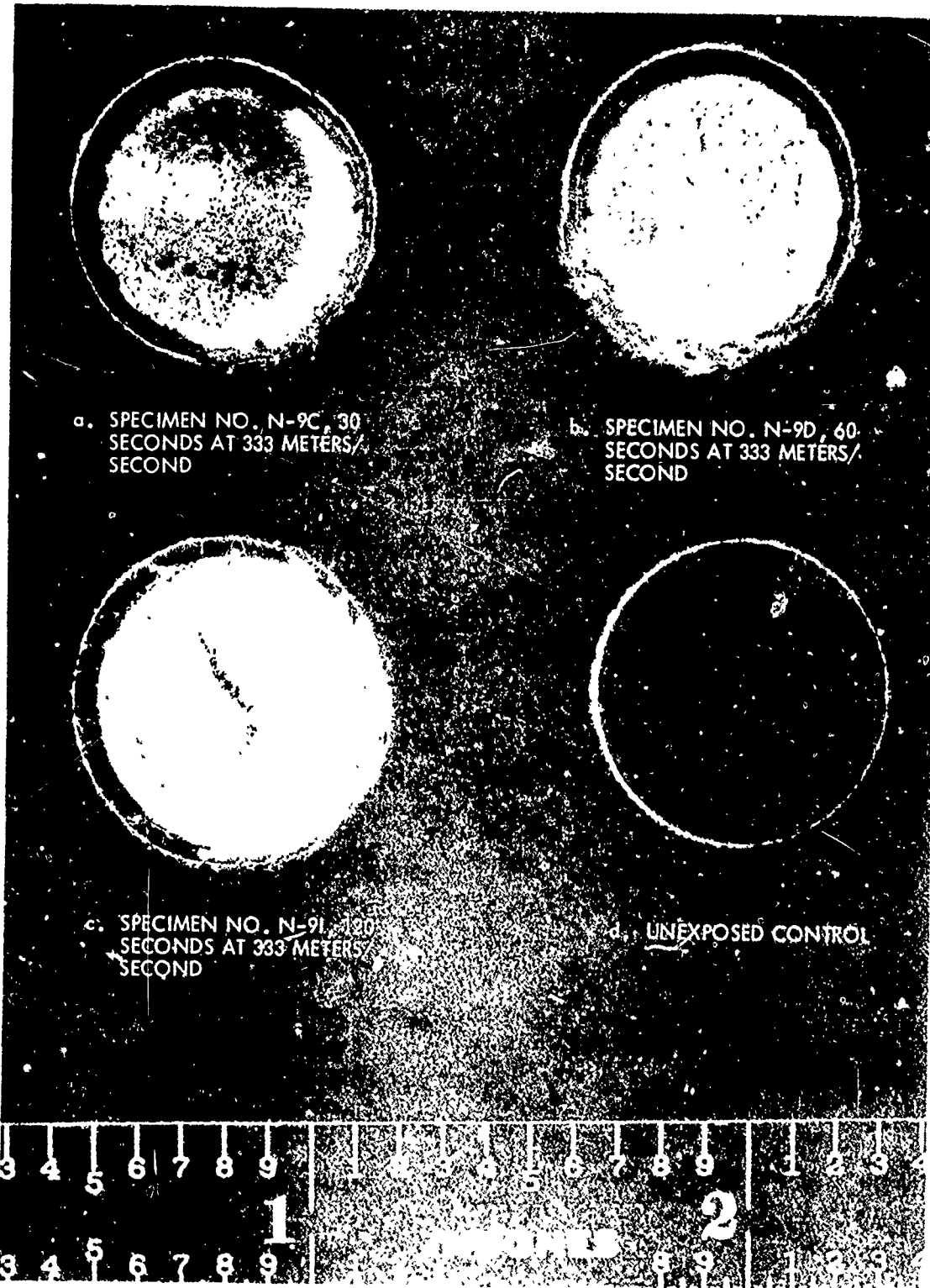
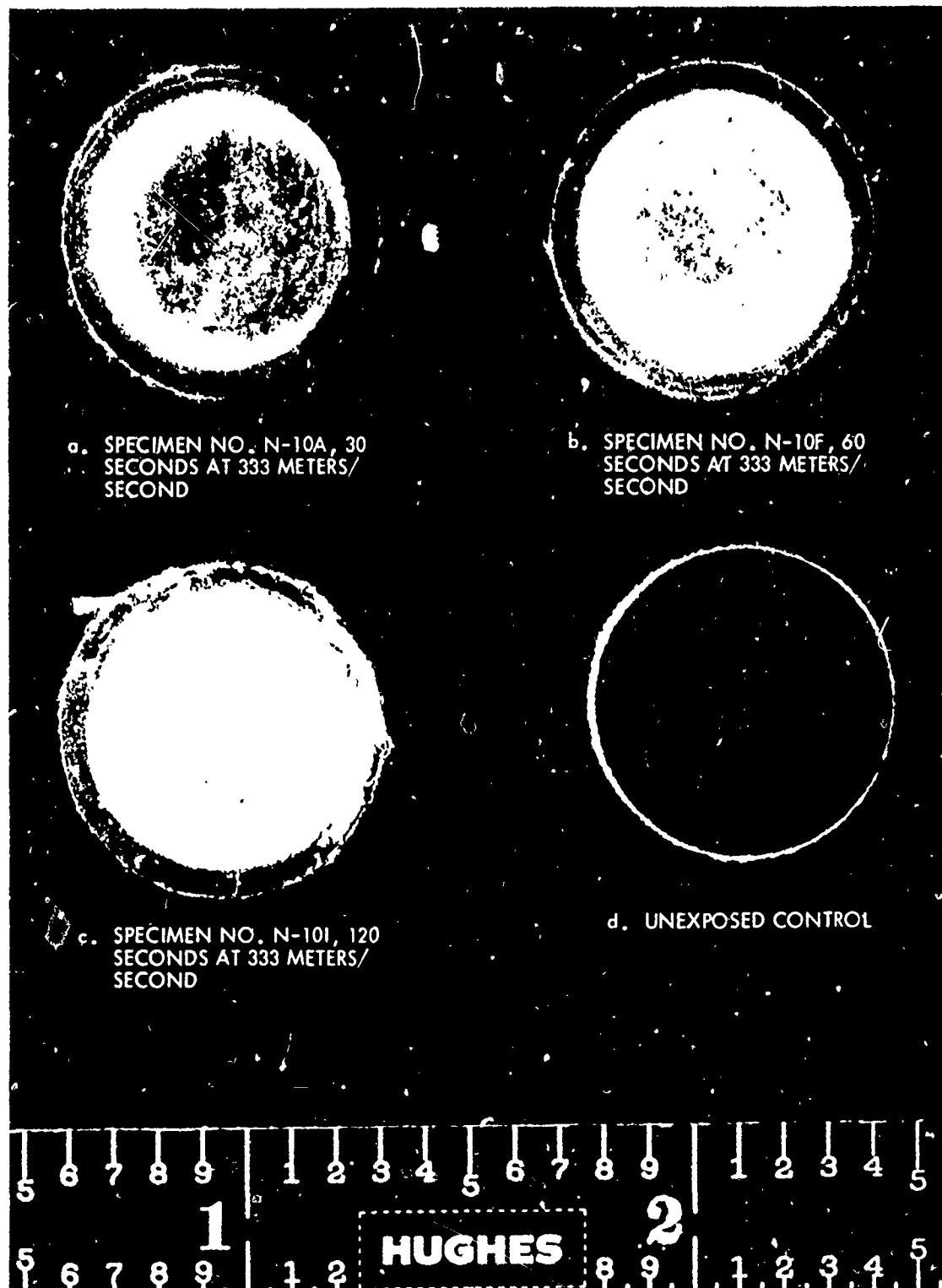
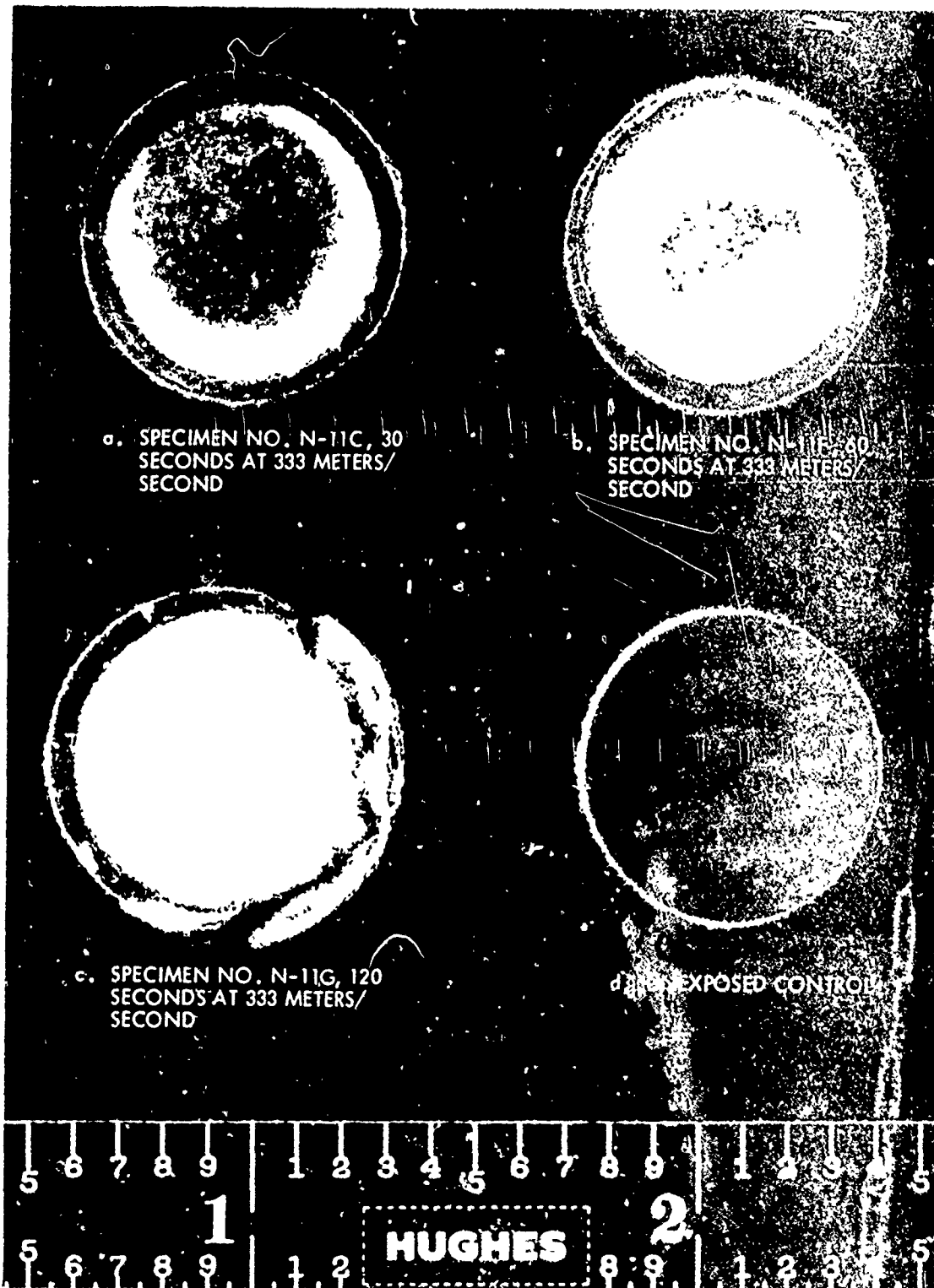


Figure 1  
Exposure Test



Specimen No. N-10A exposed 30 seconds at 333 Meters per second oriented  
Specimen No. N-10F exposed 60 seconds at 333 Meters per second oriented





a. SPECIMEN NO. N-16A, 30  
SECONDS AT 333 METERS/  
SECOND



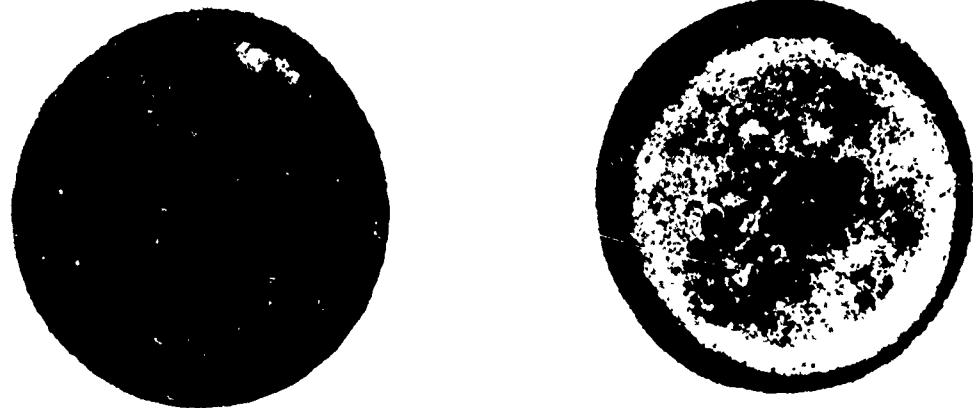
b. SPECIMEN NO. N-16E, 60  
SECONDS AT 333 METERS/  
SECOND



c. SPECIMEN NO. N-16H, 120 SECONDS  
AT 333 METERS/SECOND



Figure 49. Nomex 1200 denier yarn (plasma-treated) - Epon 828/  
MPDA, end-oriented (reinforcement content =  
41.2 volume-percent).



a. SPECIMEN NO. N-15B, 30  
SECONDS AT 333 METERS/  
SECOND

b. SPECIMEN NO. N-15D, 60  
SECONDS AT 333 METERS/  
SECOND



c. SPECIMEN NO. N-15H, 120  
SECONDS AT 333 METERS/  
SECOND

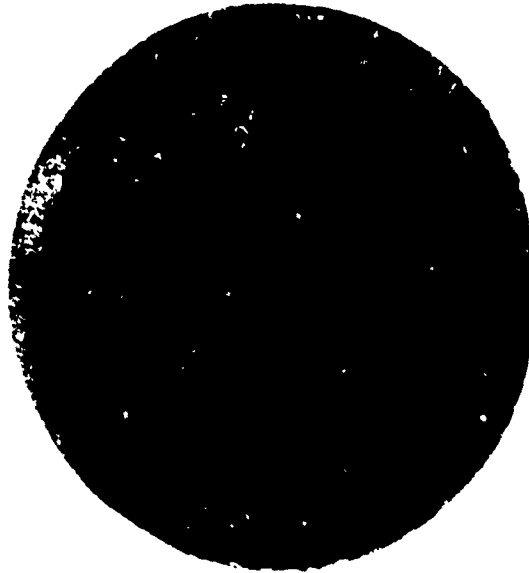


Figure 50. Nomex 1200 denier yarn (plasma-treated) - Epon 828/  
MPDA, end-oriented (reinforcement content =  
76.8 volume-percent).

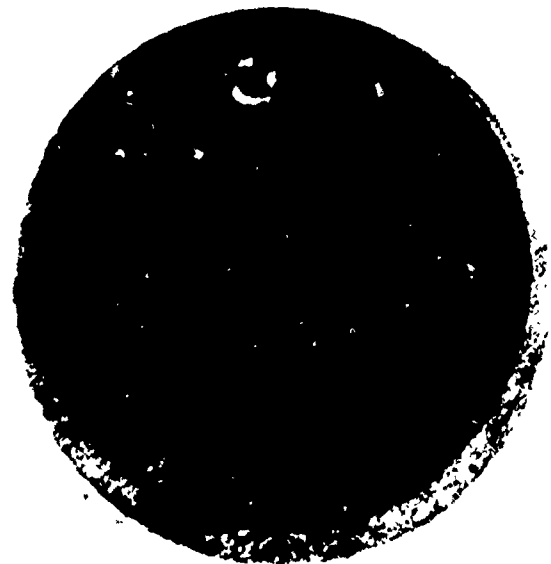
**TABLE 7. EFFECT OF FIBER ANGLE AND IMPACT ANGLE ON RELATIVE RAIN EROSION RESISTANCE OF EPON 828/MPDA-ECC GLASS, END-ORIENTED COMPOSITES (ALL SPECIMENS TESTED AT 300 METERS/SECOND)**

Specimen Code	Reinforcement Content, volume-percent	Void Content, percent	Fiber Angle, degrees	Exposure Time, sec	Impact Angle, degrees	Weight Loss, mg	Erosion Depth, mils	Appearance	Figure Refs.
UD-19A			90	30	90	7	0.5	Scattered moderate erosion	51
UD-19B			90	30	90	14	0.5	Scattered moderate erosion	51
UD-19C			90	53	90	20	0.4	Scattered moderate erosion	52
UD-19D			90	53	60	34	0.5	Scattered moderate erosion	52
UD-19E	76.1	0	90	120	45	32	0.5	Scattered light erosion	53
UD-19F			90	120	45	33	0.5	Scattered light erosion	53
UD-19G			90	480	30	53	0.7	Scattered moderate erosion	54
UD-19H			90	480	30	28	0.5	Scattered moderate erosion	54
UD-20A	76.7		90	30	90	3	0.6	Very lightly eroded	55
UD-20B	76.1		90	30	90	5	0.6	Very lightly eroded	55
UD-20C	76.7		60	53	60	255	0.4	Deeply eroded	56
UD-20D	76.1		60	53	60	134	0.4	Deeply eroded locally	56
UD-20E	76.7	0	45	120	45	62	0.1	Moderately eroded	57
UD-20F	76.1		45	120	45	72	0.5	Moderately eroded	57
UD-20G	76.7		30	480	30	546	0.2	Large section broken away	58
UD-20H	76.1		30	480	30	597	-0.3	Large section broken away	58

Specimen oriented in specimen holder at the specified impact angle so that rain drop velocity vector is parallel to the fiber direction.



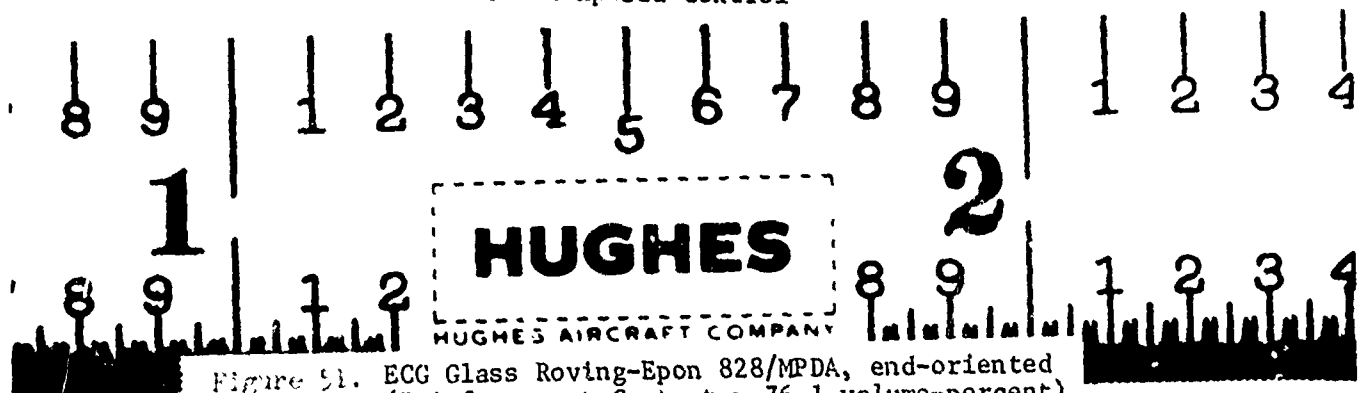
a. Specimen No. UD-19A, 30 seconds  
at 300 meters/second(impact angle, 90°)

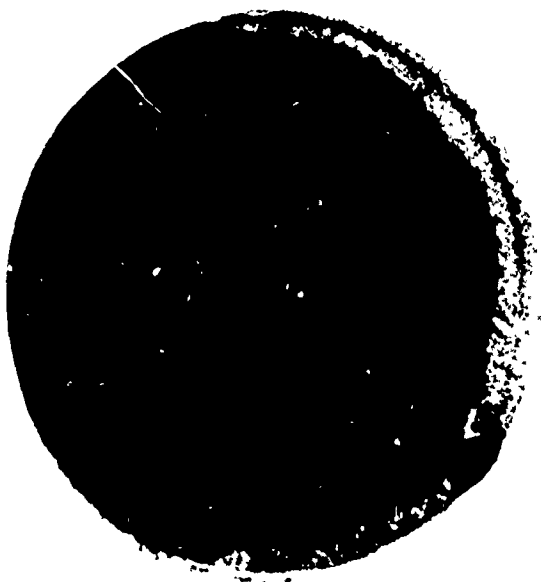


b. Specimen No. UD-19B, 30 seconds  
at 300 meters/second(impact angle, 90°)



c. Unexposed Control

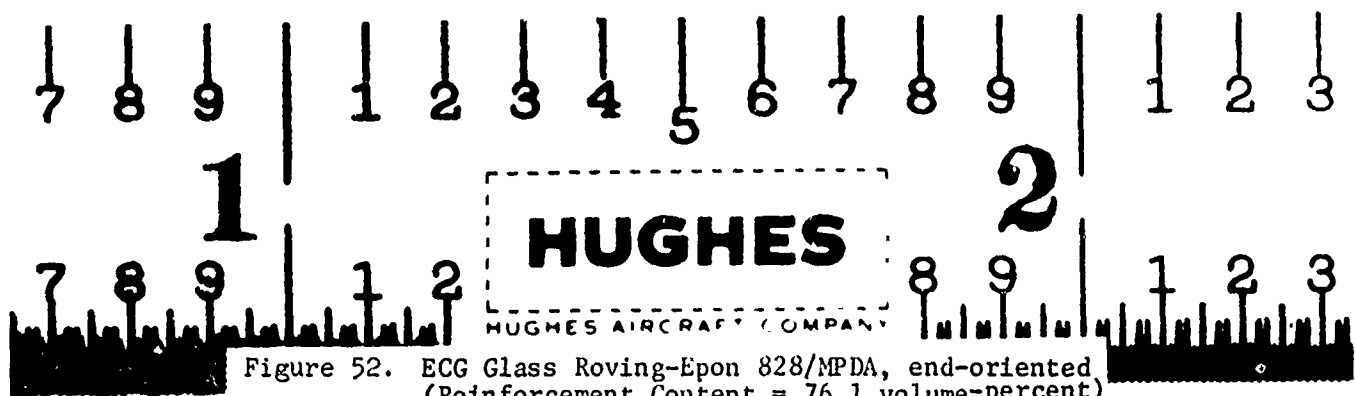


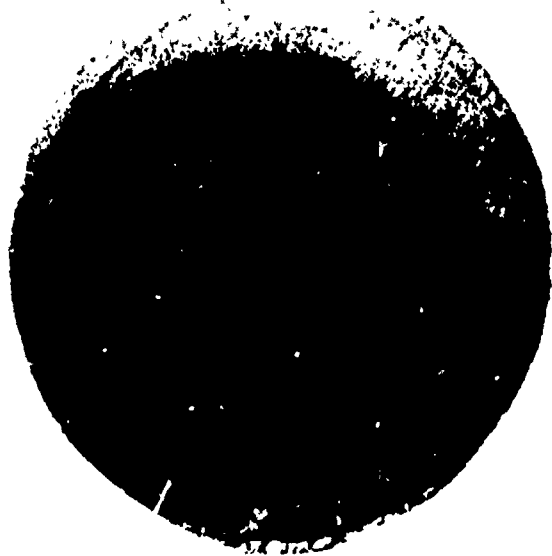


a. Specimen No. UD-19C, 53 seconds  
at 300 meters/second (impact angle, 60°)

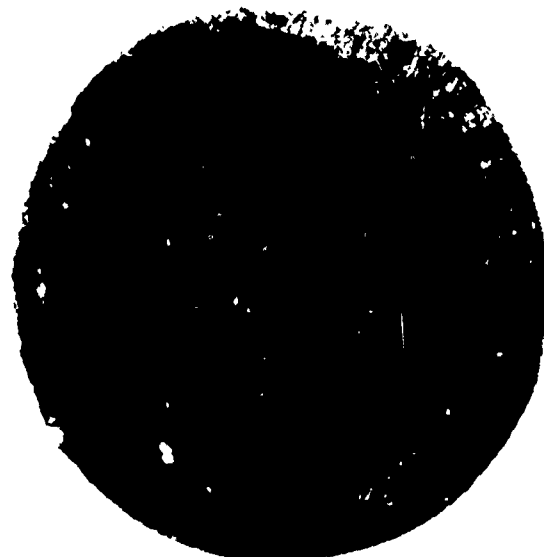


b. Specimen No. UD-19D, 53 seconds  
at 300 meters/second (impact angle, 60°)

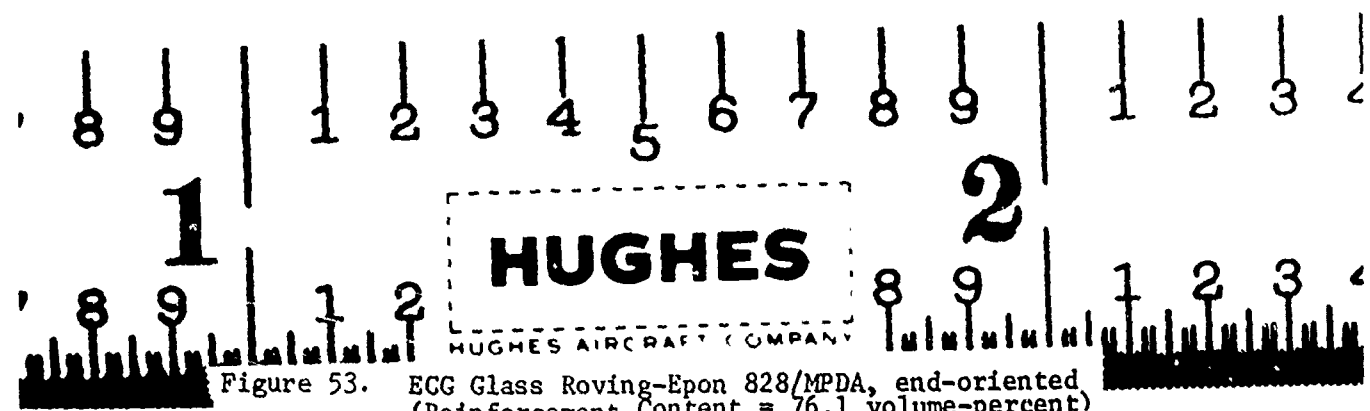


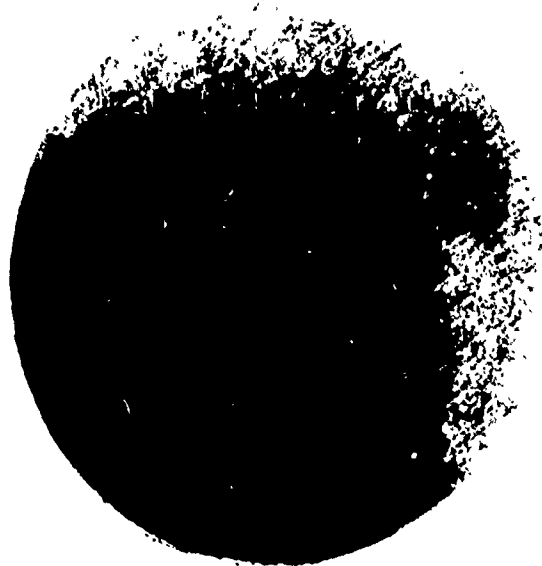


a. Specimen No. UD-19E, 120 seconds  
at 300 meters/second (impact angle.45°)



b. Specimen No. UD-19F, 120 seconds  
at 300 meters/second (impact angle.45°)





a. Specimen No. UD-19G, 480 seconds  
at 300 meters/second (impact angle, 30°)



b. Specimen No. UD-19H, 480 seconds  
at 300 meters/second (impact angle, 30°)

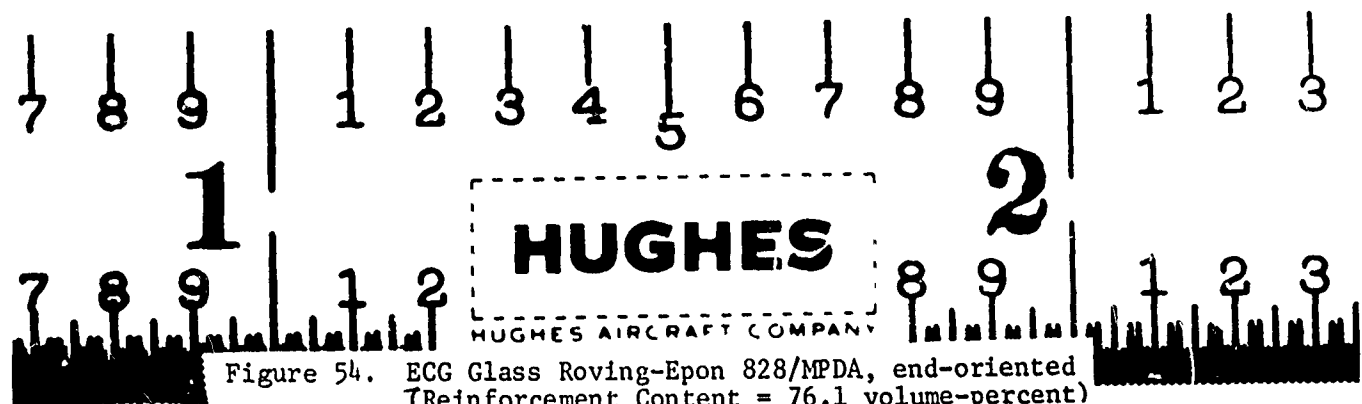
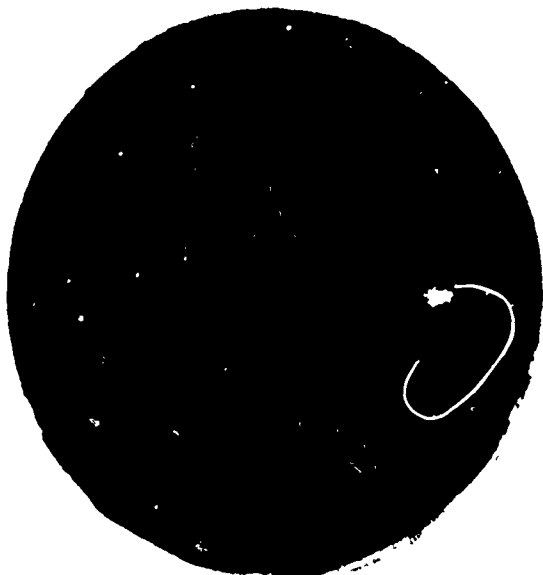
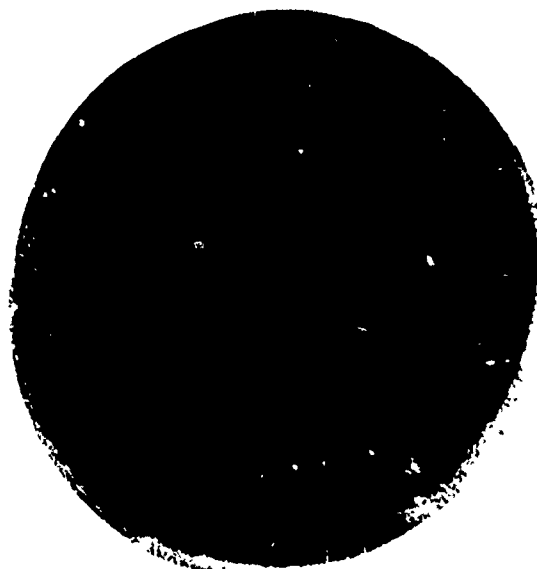


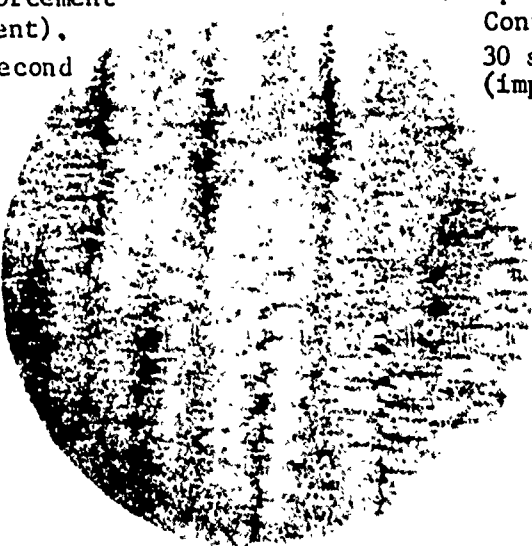
Figure 54. ECG Glass Roving-Epon 828/MPDA, end-oriented  
(Reinforcement Content = 76.1 volume-percent)



a. Specimen No. UD-20A (Reinforcement Content = 76.7 volume-percent),  
30 seconds at 300 meters/second  
(impact angle, 90°)



b. Specimen No. UD-20B (Reinforcement Content = 76.1 volume-percent),  
30 seconds at 300 meters/second  
(impact angle, 90°)



c. Unexposed Control

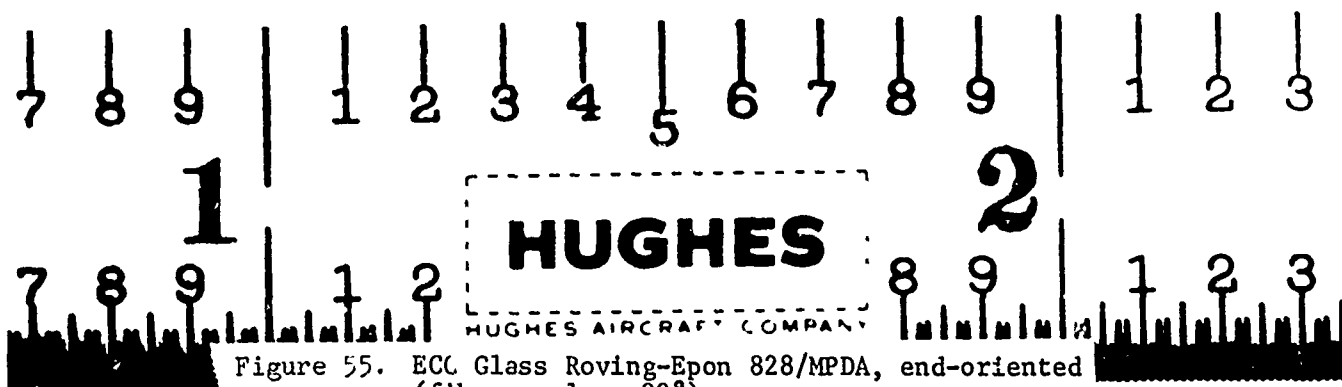
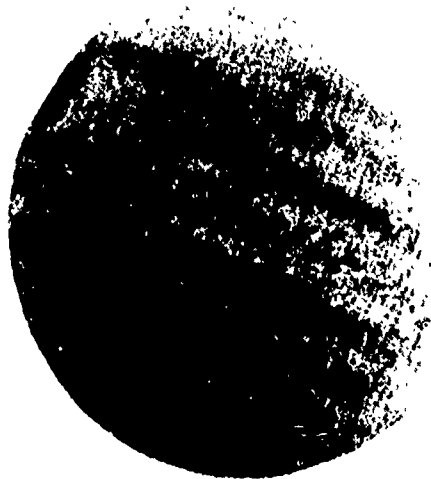


Figure 55. ECC Glass Roving-Epon 828/MPDA, end-oriented  
(fiber angle = 90°)

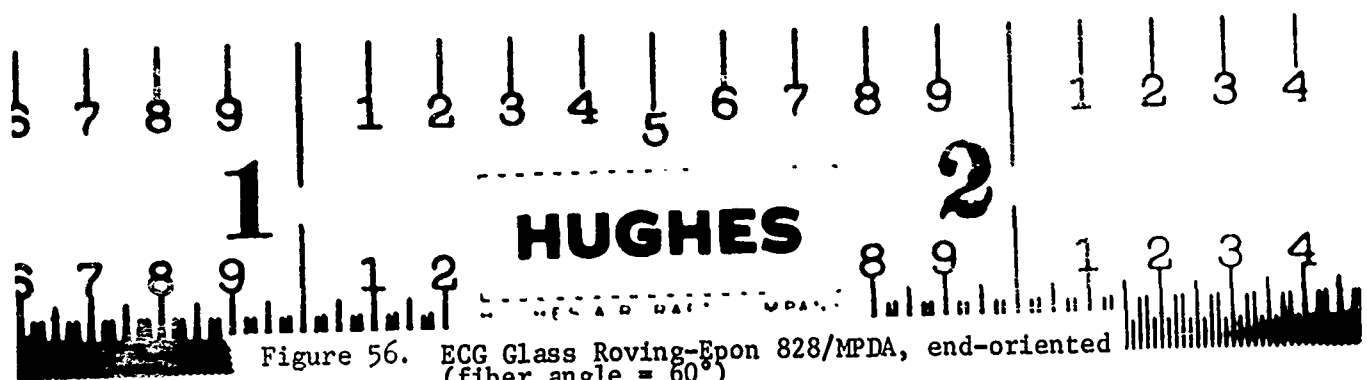


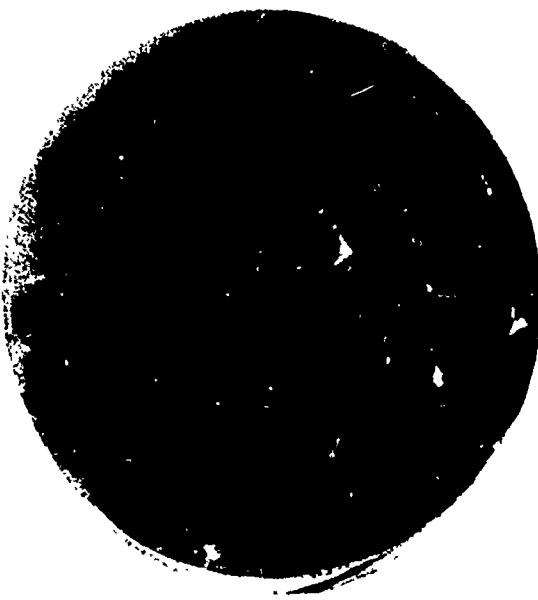
a. Specimen No. UD-20C (Reinforcement Content = 76.7 volume-percent).  
53 seconds at 300 meters/second  
(impact angle, 60°)

b. Specimen No. UD-20D (Reinforcement Content = 76.1 volume-percent).  
53 seconds at 300 meters/second  
(impact angle, 60°)

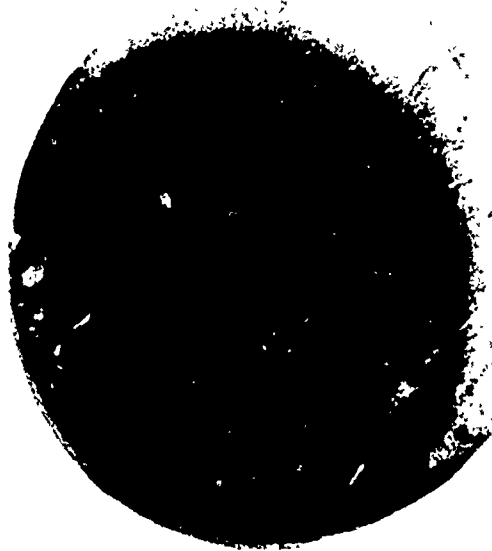


c. Unexposed Control

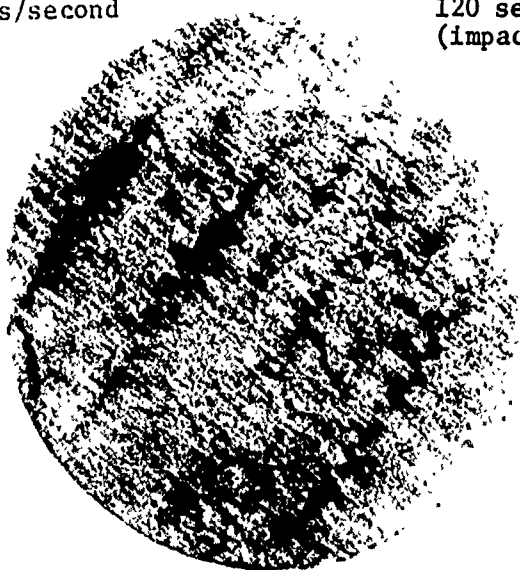




a. Specimen No. UD-20E (Reinforcement Content = 76.7 volume-percent).  
120 seconds at 300 meters/second  
(impact angle, 45°)



b. Specimen No. UD-20F (Reinforcement Content = 76.1 volume-percent),  
120 seconds at 300 meters/second  
(impact angle, 45°)



c. Unexposed Control

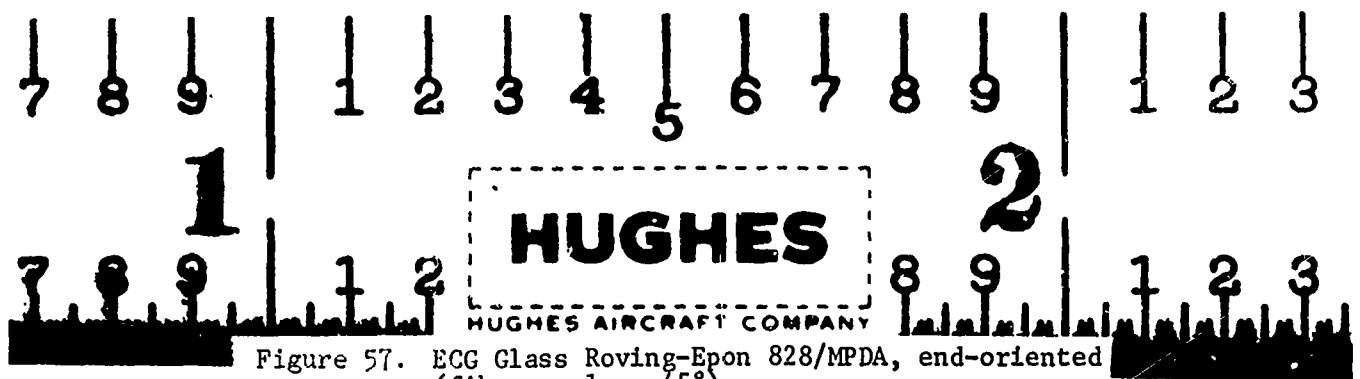
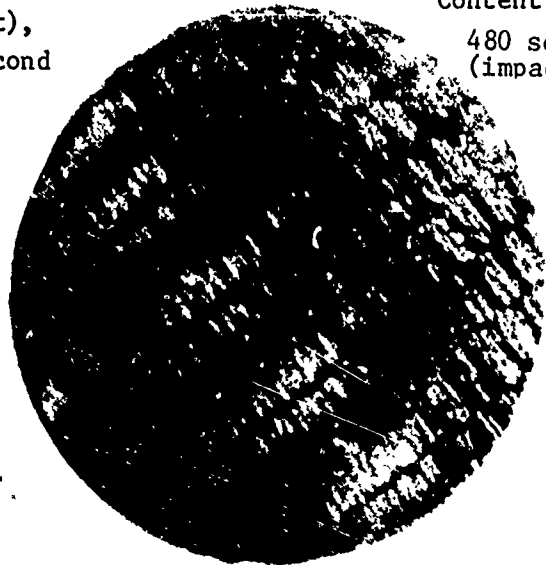


Figure 57. ECG Glass Roving-Epon 828/MPDA, end-oriented  
(fiber angle = 45°)



a. Specimen No. UD-20G (Reinforcement Content = 76.7 volume-percent), 480 seconds at 300 meters/second (impact angle, 30°)

b. Specimen No. UD-20H (Reinforcement Content = 76.1 volume-percent), 480 seconds at 300 meters/second (impact angle, 30°)



c. Unexposed Control

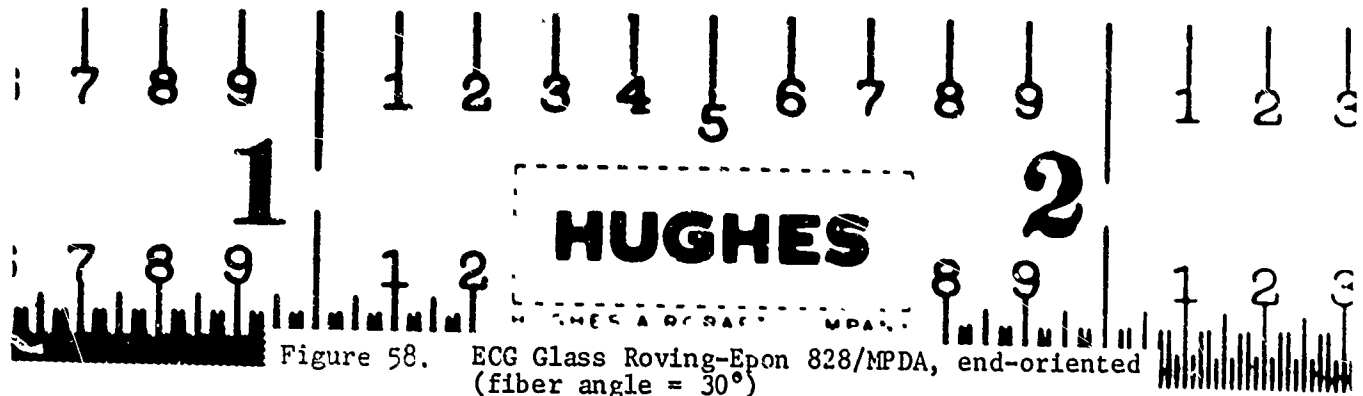


TABLE 8. EFFECT OF FIBER ANGLE AND IMPACT ANGLE ON RELATIVE RAIN EROSION  
RESISTANCE OF EPON 828/MPDA-NOMEX, END-ORIENTED COMPOSITES  
(ALL SPECIMENS TESTED AT 333 METERS/SECOND)

Specimen Code	Reinforcement Content, volume-percent	Void Content, percent	Fiber and Impact Angle, degrees.	Exposure Time, sec	Weight Loss, mg	Erosion Depth, mils	Appearance	Figure Refs.
N-12A	35.2	2.3	90	30	101	2.1	Deeply eroded locally	59
N-12B	35.4	2.4	85	30	29	-0.3	Deeply eroded locally	59
N-12C	35.2	2.3	85	30	98	3.0	Deeply eroded locally	59
N-12D	35.4	2.4	80	32	34	-0.5	Deeply eroded locally	59
N-12E	35.2	2.3	80	32	101	2.2	Deeply eroded locally	59
N-12F	35.4	2.4	75	34	34	-0.2	Deeply eroded locally	59
N-12G	35.2	2.3	75	34	88	1.9	Deeply eroded locally	60
N-12H	35.4	2.4	70	38	39	0.2	Deeply eroded locally	60
N-12I	35.2	2.3	70	38	135	5.0	Deeply eroded locally	60
N-12J	35.4	2.4	65	44	35	1.3	Deeply eroded locally	60
N-12K	35.2	2.3	65	44	169	5.7	Deeply eroded locally	60
N-12L	35.2	2.3	60	53	130	7.7	Deeply eroded locally	60
N-13A	40.6	2.1	90	30	26	0	Deeply eroded locally	61
N-13B	40.5	1.9	90	30	55	-0.1	Deeply eroded locally	61
N-13C	40.6	2.1	85	30	36	-0.3	Deeply eroded locally	61
N-13D	40.5	1.9	85	30	43	-0.5	Deeply eroded locally	61
N-13E	40.6	2.1	80	32	45	0.2	Deeply eroded locally	61
N-13F	40.5	1.9	80	32	61	0.7	Deeply eroded locally	61
N-13G	40.6	2.1	75	34	44	-0.5	Deeply eroded locally	61
N-13H	40.5	1.9	75	34	67	2.2	Deeply eroded locally	62
N-13I	40.6	2.1	70	38	55	0.7	Deeply eroded locally	62
N-13J	40.5	1.9	70	38	87	2.4	Deeply eroded locally	62
N-13K	40.6	2.1	65	44	50	1.8	Deeply eroded locally	62
N-13L	40.5	1.9	65	44	54	1.4	Deeply eroded locally	62
N-13M	40.6	2.1	60	53	52	0.1	Deeply eroded locally	62
N-13N	40.5	1.9	60	53	63	2.0	Deeply eroded locally	62
N-14A		90	30		28	-0.3	Deeply eroded locally	63
N-14B		85	30		34	-0.1	Deeply eroded locally	63
N-14C	45.8	2.7	75	34	50	1.8	Deeply eroded locally	63
N-14D		75	70	38	62	6.2	Deeply eroded locally	64
N-14E		70	65	44	75	6.8	Deeply eroded locally	64
N-14F		65	60	53	104	4.5	Deeply eroded locally	64
N-14G		60	60	52	52	4.3	Deeply eroded locally	64

Each specimen with the fiber angle other than 90 degrees was tested with the specimen holder at the same angle and aligned in the specimen holder so that the raindrop velocity vector was parallel to the fiber direction.

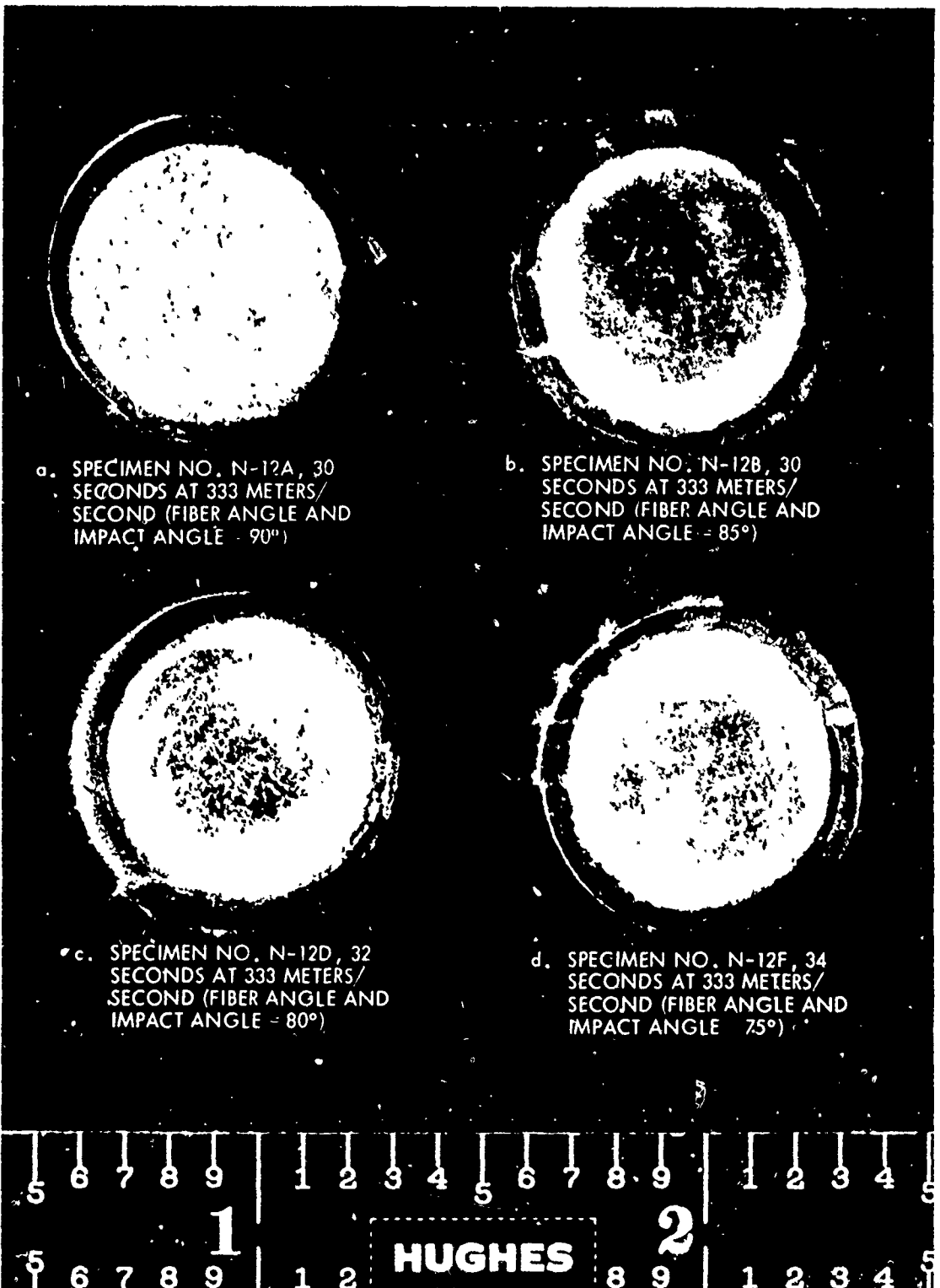
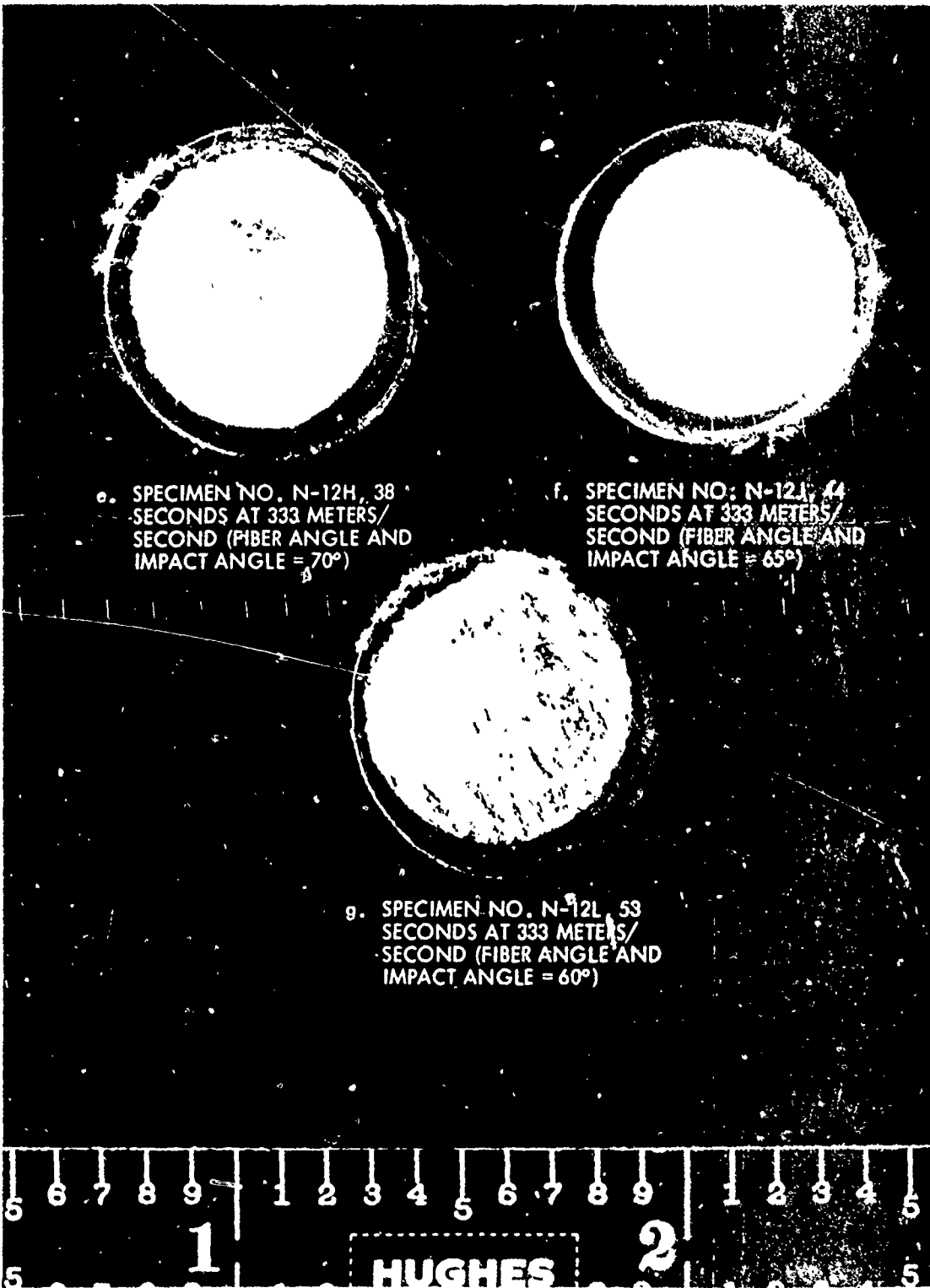
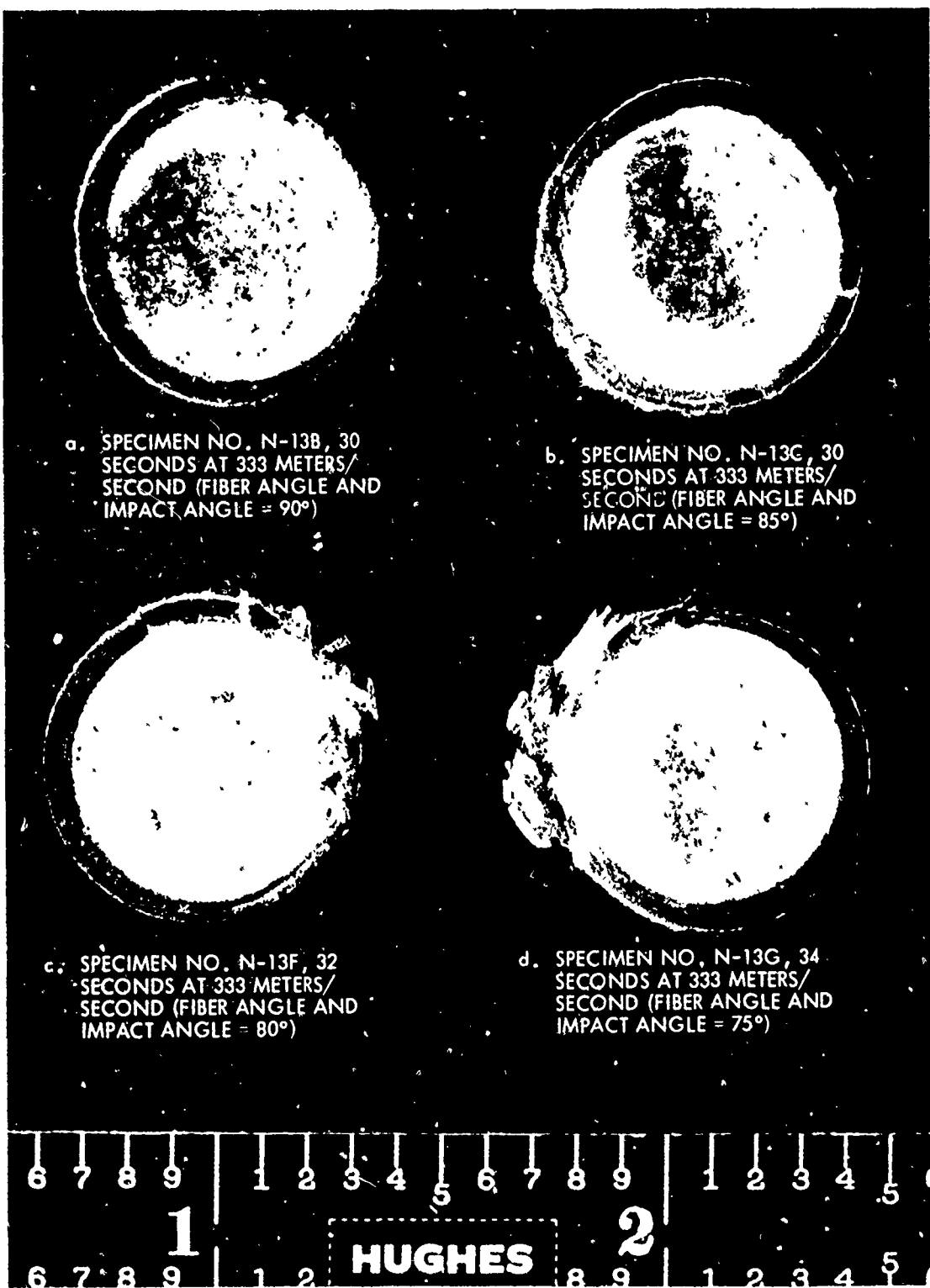
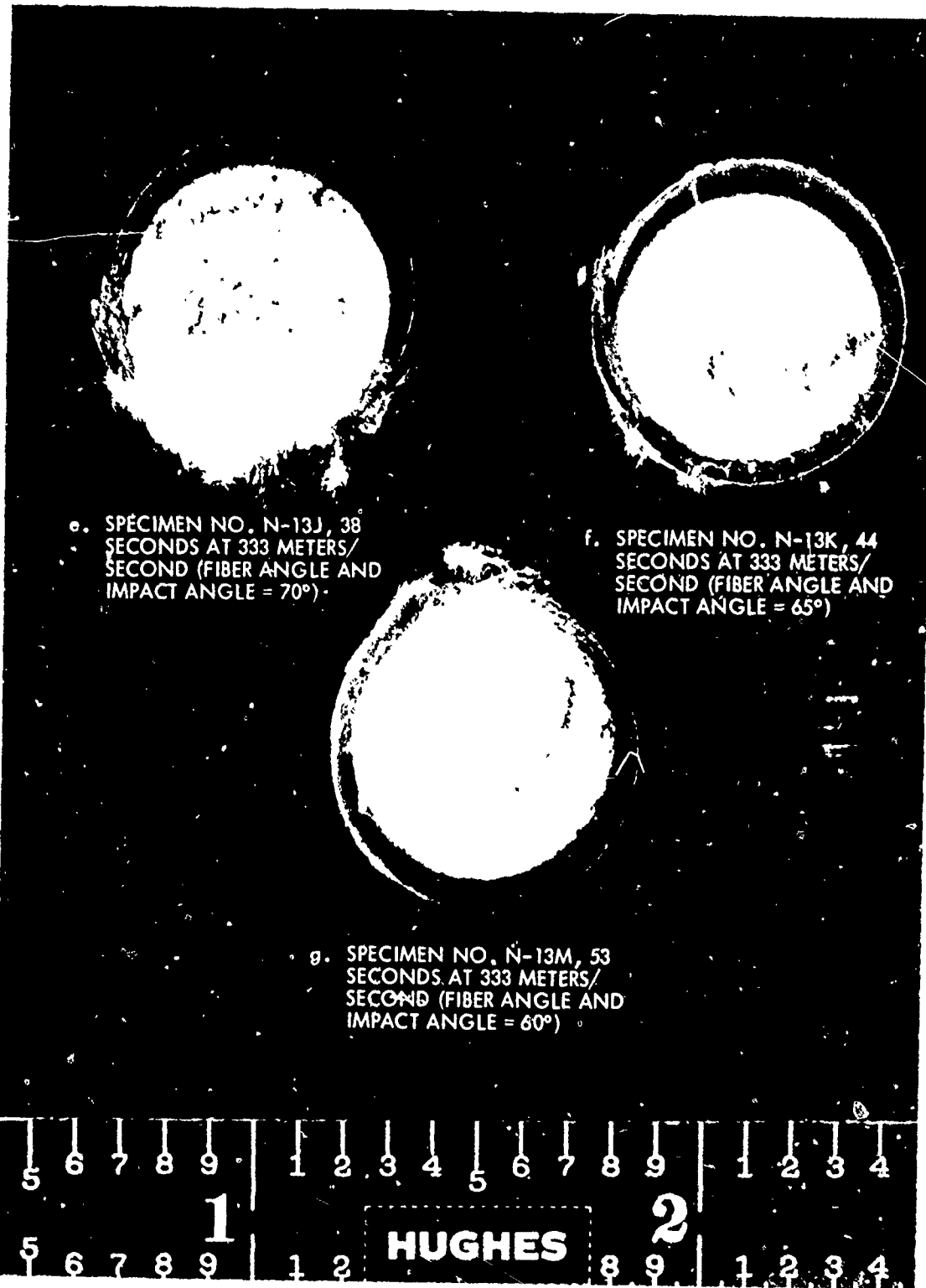


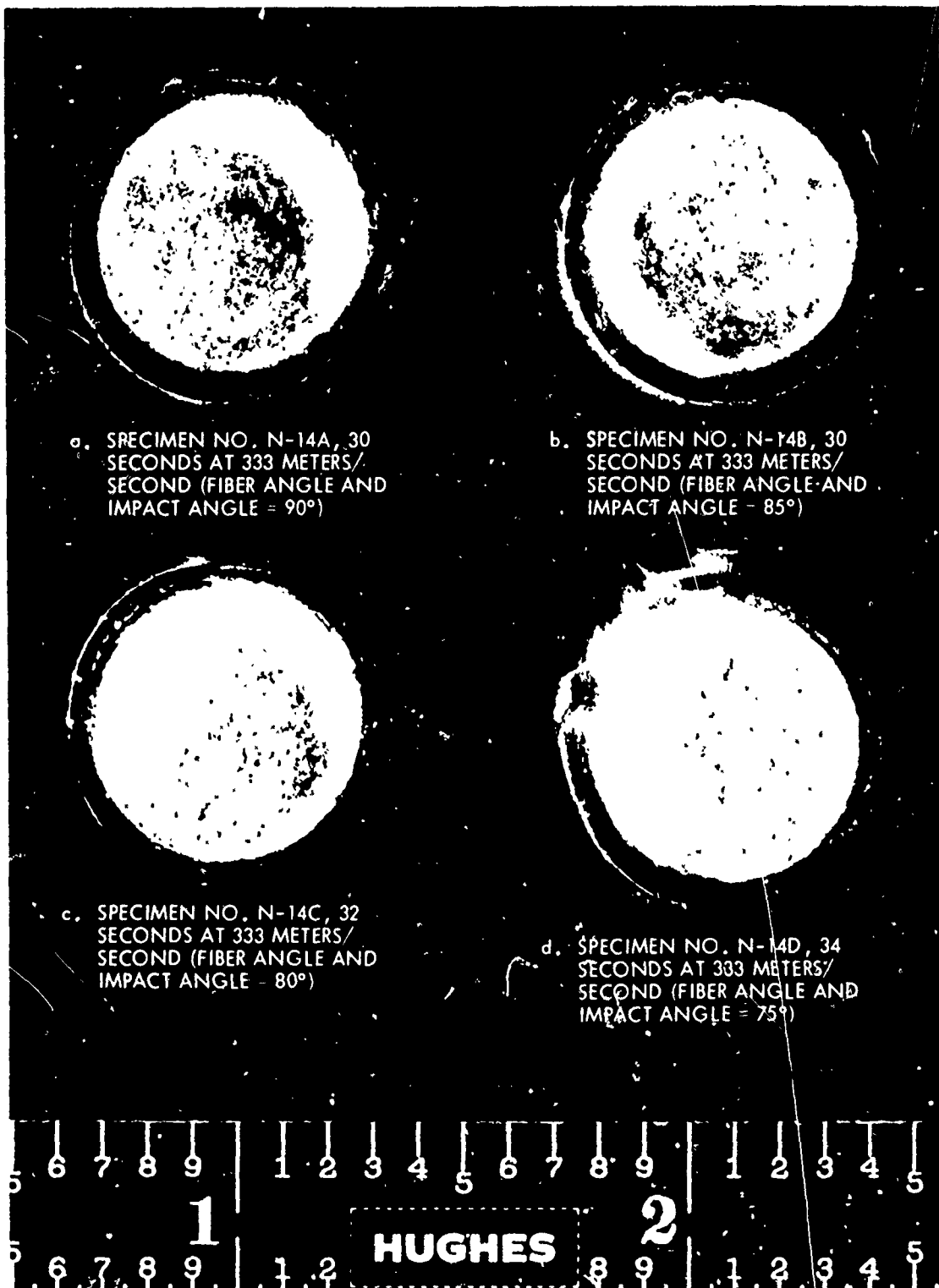
Figure 6. Novex 1200 center wire - 4 mm (28 MPa) at 333 m/s  
charge reinforcement content = 1.0% of explosive.



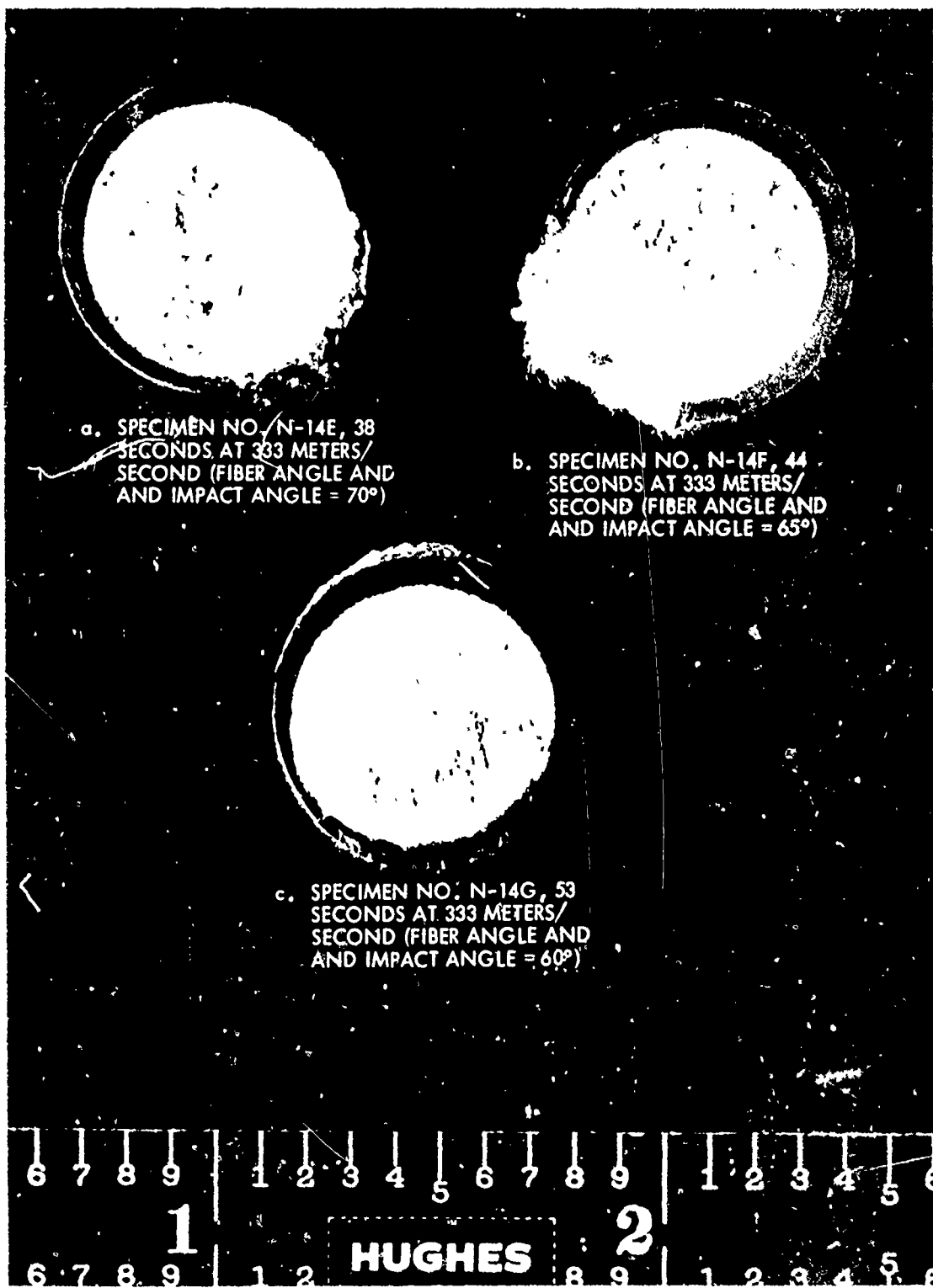


Impact Test No. 1200 done on a Hughes 28 MPDA, cylinder  
strength reinforced concrete, 40,000 psi, specimen





Impact strength 12 m/demeter, at 333 MPDA, end corrected  
reinforcement content 1.5% by weight.



a. SPECIMEN NO. N-14E, 38  
SECONDS AT 333 METERS/  
SECOND (FIBER ANGLE AND  
AND IMPACT ANGLE = 70°)

b. SPECIMEN NO. N-14F, 44  
SECONDS AT 333 METERS/  
SECOND (FIBER ANGLE AND  
AND IMPACT ANGLE = 65°)

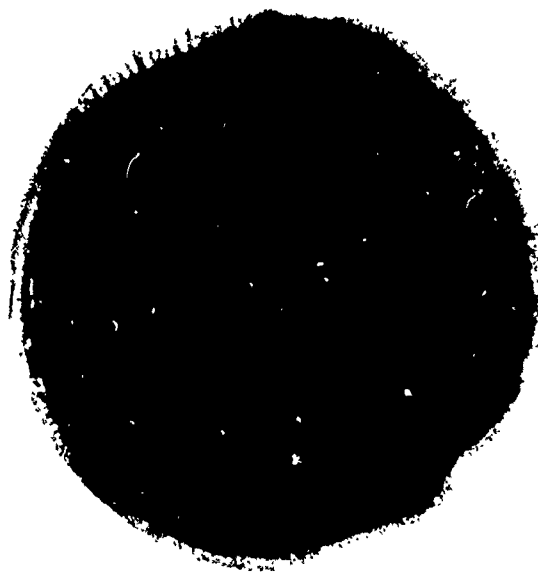
c. SPECIMEN NO. N-14G, 53  
SECONDS AT 333 METERS/  
SECOND (FIBER ANGLE AND  
AND IMPACT ANGLE = 60°)



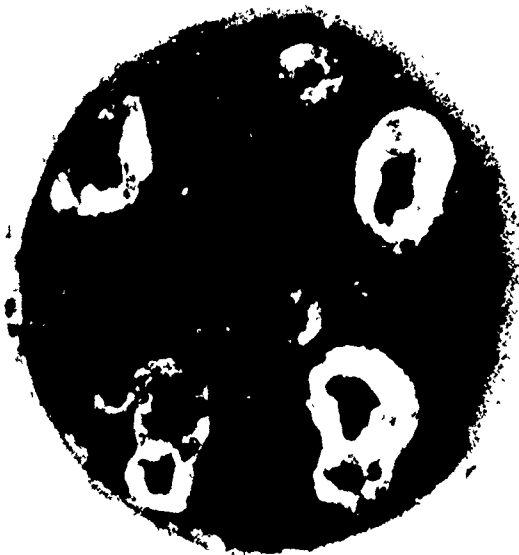
TABLE 9. EFFECT OF GLASS CLOTH FINISH AND DIELECTRIC FILLER ON RAIN EROSION RESISTANCE OF END-ORIENTED, FIBER-REINFORCED COMPOSITES (ECC-EPON 828/MPDA)

Specimen Code	Material Description	Reinforcement Content, volume-percent	Void Content, percent	Velocity, meters/sec	Exposure Time, sec	Weight Loss, mg	Erosion Depth, mils	Appearance	Figure Refs
UD-21A	ECC 37 1/0 glass yarn, starch-oil sizing with Epon 828/MPDA	77.0	0	333	30	12	0.1	Scattered pitting	65
UD-21B					30	76	0.2	Deeply eroded locally	
UD-22A	ECC glass roving, 801 sizing with Epon 828/MPDA	77.1	0	333	30	54	0.2	Deeply eroded locally	66
UD-22B					30	2	0.1	Very slightly eroded	
UD-23A	ECC glass roving, 801 sizing, Epon 828 filled with rutile titanium-dioxide (30 PHR)	77.3	-	333	30	*	-	Completely eroded away except edge	67
UD-23B					20	547	6.8	Very deeply eroded and fractured	

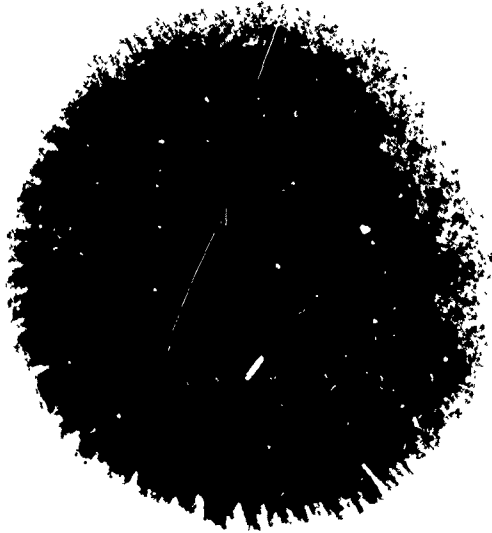
\*Weight loss could not be determined.



a. Specimen No. UD-21A, 30 seconds  
at 333 meters/second



b. Specimen No. UD-21B, 30 seconds  
at 333 meters/second



c. Unexposed Control

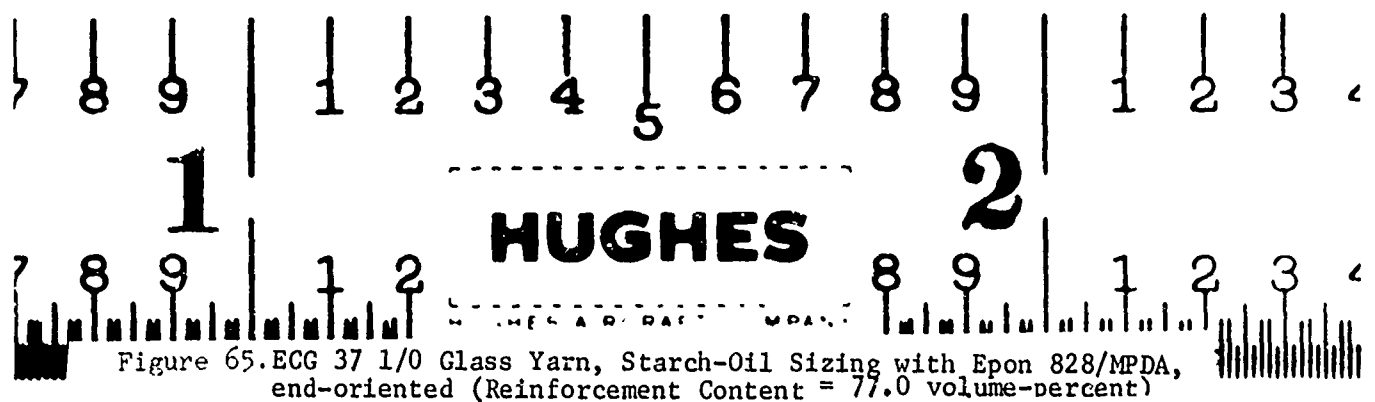
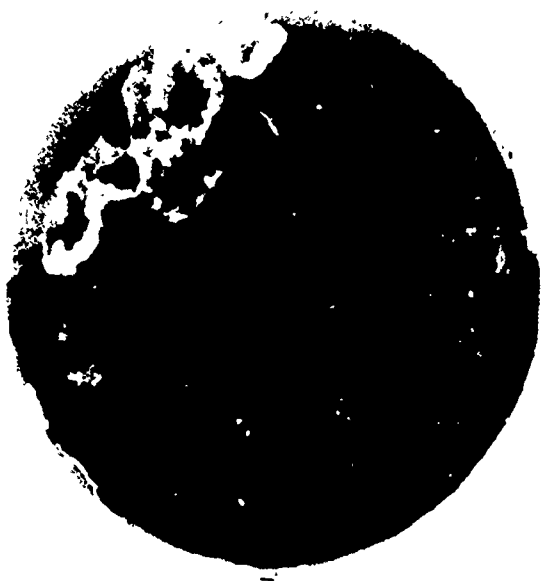
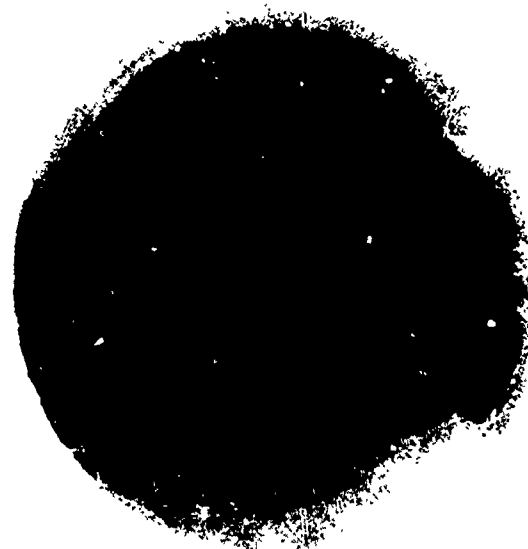


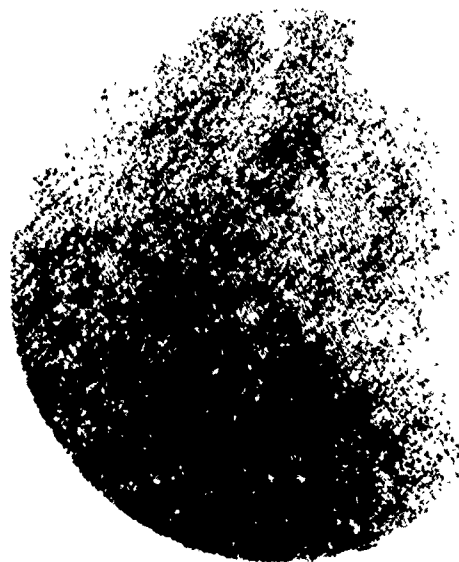
Figure 65. ECG 37 1/0 Glass Yarn, Starch-Oil Sizing with Epon 828/MPDA, end-oriented (Reinforcement Content = 77.0 volume-percent)



a. Specimen No. UD-22A, 30 seconds  
at 333 meters/second



b. Specimen No. UD-22B, 30 seconds  
at 333 meters/second



c. Unexposed Control



Figure 66 ECG Glass Roving, 801 Sizing, with Epon 828/MPDA, end-oriented  
(Reinforcement Content = 77.1 volume-percent)



a. Specimen No. UD-23A, 30 seconds  
at 333 meters/second



b. Specimen No. UD-23B, 20 seconds  
at 333 meters/second



c. Unexposed Control

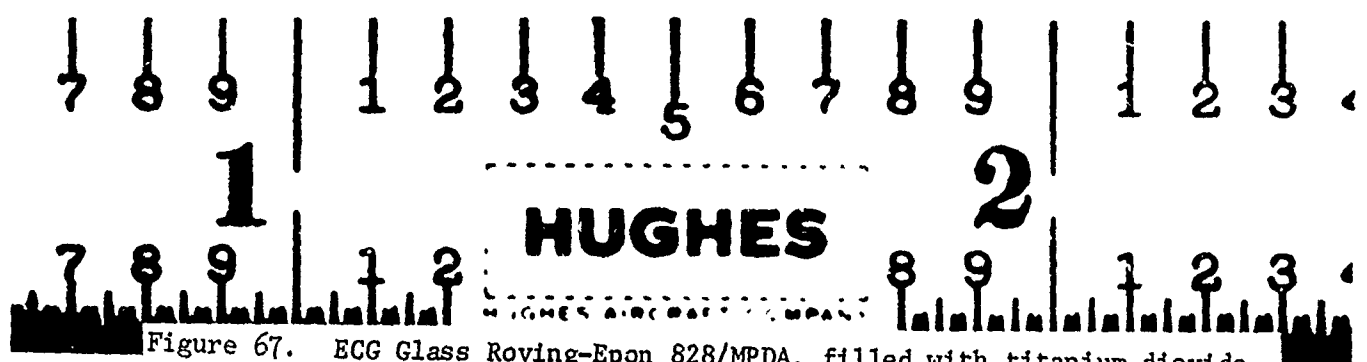


Figure 67. ECG Glass Roving-Epon 828/MPDA, filled with titanium dioxide,  
end-oriented (Reinforcement Content = 77.3 volume-percent)

work had indicated that an excess of MPDA gave superior rain erosion resistance). From an examination of the specimens, it appears that a stoichiometric amount of fresh MPDA yields a more rain erosion resistant composite than the same amount of old MPDA (Figures 40 and 41). No increase in erosion resistance was noted by increasing the hardener content above the stoichiometric amount. The spread in test results for specimens cut from a single composite (Figures 36, 37, 38 and 41) casts doubt on the uniformity of the test conditions during rain erosion testing.

#### Effect of Fiber Loading (Nomex-Epon 828/MPDA)

Previously, it was concluded from weight loss data only that higher fiber loadings were desirable. However, examination of the exposed specimens shows an increased tendency to crack with increased fiber loadings. The results seemed to indicate poor bonding between the matrix and the Nomex fibers. The same effect was observed, however, for Nomex-epoxy composites made from Nomex which had been plasma-treated to increase adhesion to the matrix.

#### Effect of the Fiber Angle and Impact Angle

In general, examination of the exposed epoxy-glass specimens corroborated the weight loss data. The  $90^\circ$  end-oriented specimens all experienced approximately the same amount of damage for the various angles and test times. However, the specimens with fiber angles other than  $90^\circ$  were severely eroded when tested at an angle and orientation such that the raindrop velocity vector was parallel to the fiber direction. Both the  $60^\circ$  and  $45^\circ$  specimens (Figures 56 and 57) were deeply eroded, while a large portion of each of the  $30^\circ$  specimens was broken off as a result of the test. While some of the erosion may be due to specimen configuration, the results indicate that the rain erosion resistance of end-oriented epoxy-glass specimens decreases with decreasing impact angle.

The test results for end-oriented, Nomex-epoxy composites (Figures 59 - 64) with fiber loadings in the range of 35-45 volume-percent indicate the degree of rain erosion to be independent of fiber angle and impact angle over the range of  $90^\circ$  to  $60^\circ$ .

### Effect of Glass Finish and Dielectric Filler

Epoxy-glass specimens were prepared, in one case, from E glass roving finished with 801 sizing and, in the other case, from E glass yarn finished with starch-oil sizing. The test results were inconclusive (Figures 65 and 66) and indicate that the test conditions may vary widely from test to test.

Tests were also run on end-oriented, glass fiber-reinforced, titanium dioxide filled specimens. The erosion resistance (Figure 67) was substantially less than that of typical, unfilled epoxy-glass specimens.

### ELECTRICAL PROPERTIES

The dielectric constant and loss tangent were determined at 9.28 gHz for four types of end-oriented plastics composites shown to have good rain erosion resistance. All of the composites tested contained Epon 828/MPDA as the matrix and were reinforced unidirectionally with the following fibers:

- ECG glass roving, 73.7 volume-percent
- Nomex yarn, 1200 denier, 50.7 volume-percent
- Dacron yarn, 1100 denier, 55.4 volume-percent
- PRD-49 Type IV yarn, 380 denier, 63.4 volume-percent

Each test specimen consisted of a circular disk nominally one-half wavelength thick by 2.135 inches in diameter. The faces of each specimen were machined flat and parallel to within 0.001 inch. Two types of specimen were machined from each composite, one with the fibers perpendicular to the specimen axis and the other with the fibers parallel to the specimen axis. For the latter type, it was necessary to bond together two sections of the original composite. The PRD-49 composite of the latter type could not be machined.

The electrical measurements were made in a resonant cavity dielectricometer at a frequency of 9.28 gHz. Two readings were taken on each specimen, with the specimen inverted for the second reading. The results, summarized in Table 10 show little effect of fiber orientation on the dielectric constant for the Nomex-epoxy. However, both the Dacron-epoxy and the glass-epoxy composites appear to have a somewhat higher dielectric constant with the reinforcing fibers perpendicular to the specimen axis.

TABLE 10. DIELECTRIC PROPERTIES OF UNIDIRECTIONAL,  
FIBER-REINFORCED PLASTICS COMPOSITES  
(FREQUENCY = 9.28 GHz)

Specimen Description	Fiber Orientation*	Dielectric Constant	Loss Tangent
Nomex-epoxy	A	3.533 3.536**	0.022 0.022**
	B	3.541 3.542**	0.020 0.020**
Dacron-epoxy	A	3.142 3.148**	0.015 0.015**
	B	2.998 2.998**	0.016 0.016**
PRD-49-epoxy	A	3.803 3.854**	0.025 0.029**
	B	— —	— —
E glass-epoxy	A	5.301 5.296**	0.017 0.017**
	B	5.103 5.105**	0.017 0.017**

\*A specimens: fibers perpendicular to specimen axis  
 B specimens: fibers parallel to specimen axis  
 \*\*Values obtained with specimen inverted

#### AFML WHIRLING ARM TEST RESULTS

The PRD-49-Type III - Epon 828/menthane diamine composite tested by Dornier (Figure 34) was also tested in the AFML whirling arm apparatus. The appearance (Figure 68) after only 5 minutes exposure to one inch/hour rainfall at 500 mph (1.8 mm raindrop size) corroborated the Dornier results which indicated poor rain erosion resistance. There was a substantial difference in degree of erosion in the two pairs of samples which can probably be attributed to an apparent difference in fiber loading. The airfoils that appear to have a higher fiber loading were more erosion resistant as shown in Figure 68.

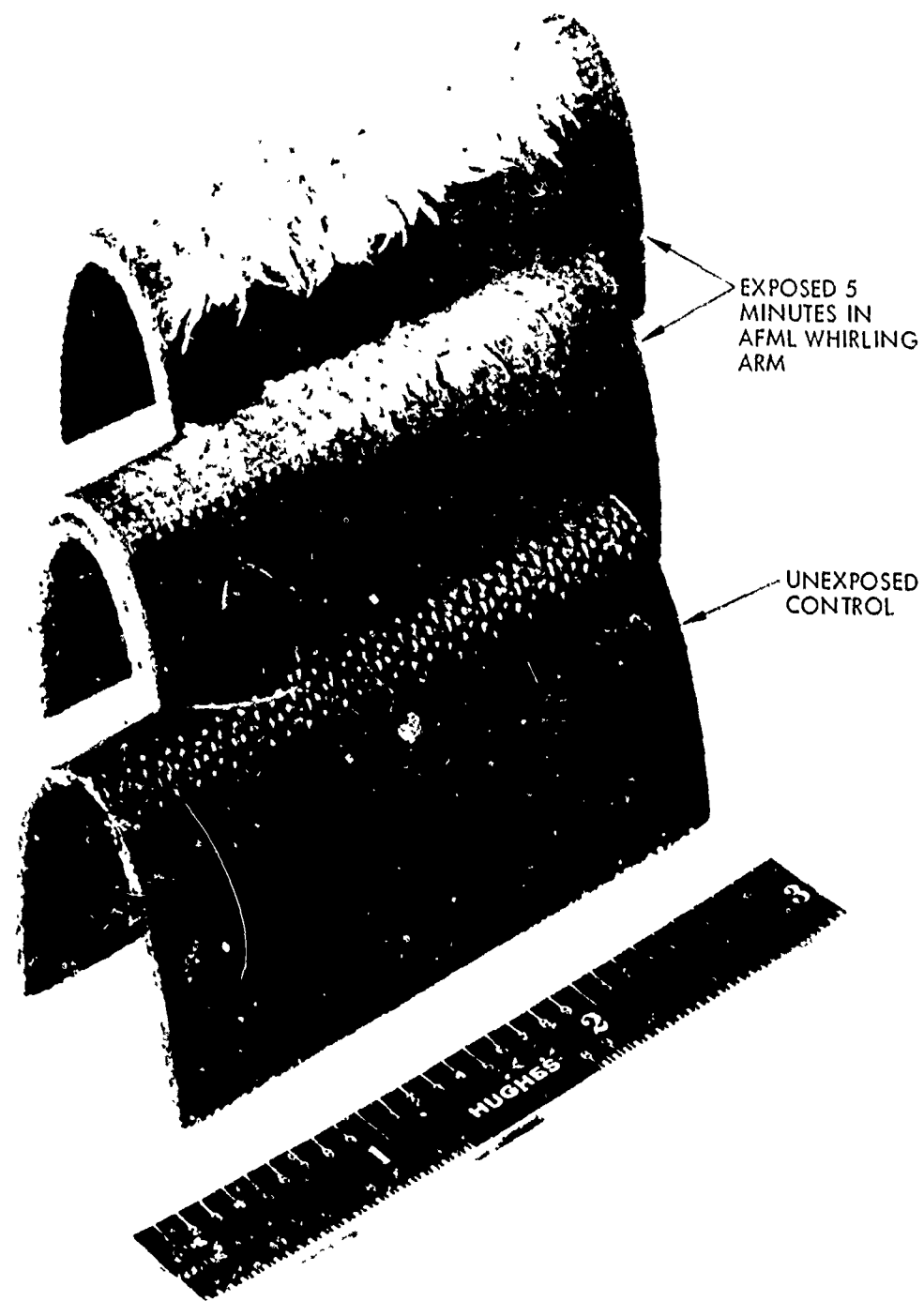


Figure 68. PRD-19 Type III, Epon 828-methane diamine (MMI) artool specimens.

## RADOME FABRICATION

Two small radome structures similar to those currently being used on a Navy military aircraft were fabricated from a single layer of a PRD-49 Type III 3-D fabric and Epon 828/menthane diamine. The fabrication process consisted of the wet layup, vacuum-bagging and curing of the resin-reinforcement system in a female plaster mold. The finished radomes, shown in Figure 69, have an approximate wall thickness of 0.050 inch.

Though the results of rain erosion tests on this material (Figures 34 and 68) did not indicate outstanding rain erosion resistance, this construction probably typifies the type of radome structure that will be used in future aircraft radar applications. The relatively thin wall thickness will allow application in broadband systems, while the proper choice of fiber, reinforcement configuration and fiber loading should allow the achievement of the required rain erosion resistance.

## CONCLUSIONS AND RECOMMENDATIONS FOR FUTURE WORK

Several main conclusions can be drawn from the test results to date:

- End-oriented, fiber-reinforced plastics are superior in rain erosion resistance to all other plastics composites tested.
- Polymeric fibers such as Nomex and Dacron are superior to glass fibers (e.g., E glass and S glass) either in the form of end-oriented fibers or as three-dimensional fabrics.
- Flexibilized matrices are superior to rigid matrices when reinforced with end-oriented glass fibers; however, polymeric fibers such as Nomex impart good erosion resistance to both rigid and flexible matrices.
- At impact angles and fiber angles other than 90°, unidirectional fiber-reinforced epoxy-glass composites have less rain erosion resistance; the rain erosion resistance of end-oriented epoxy-Nomex is virtually unaffected by impact angle.

The above test results, coupled with the requirement for relatively thin-walled, broadband radome structures, dictate that future work be concentrated on thin, 3-D (multidimensional) constructions. Such constructions will undoubtedly be woven from polymeric fibers and will contain a high volume fraction of tightly packed fibers.

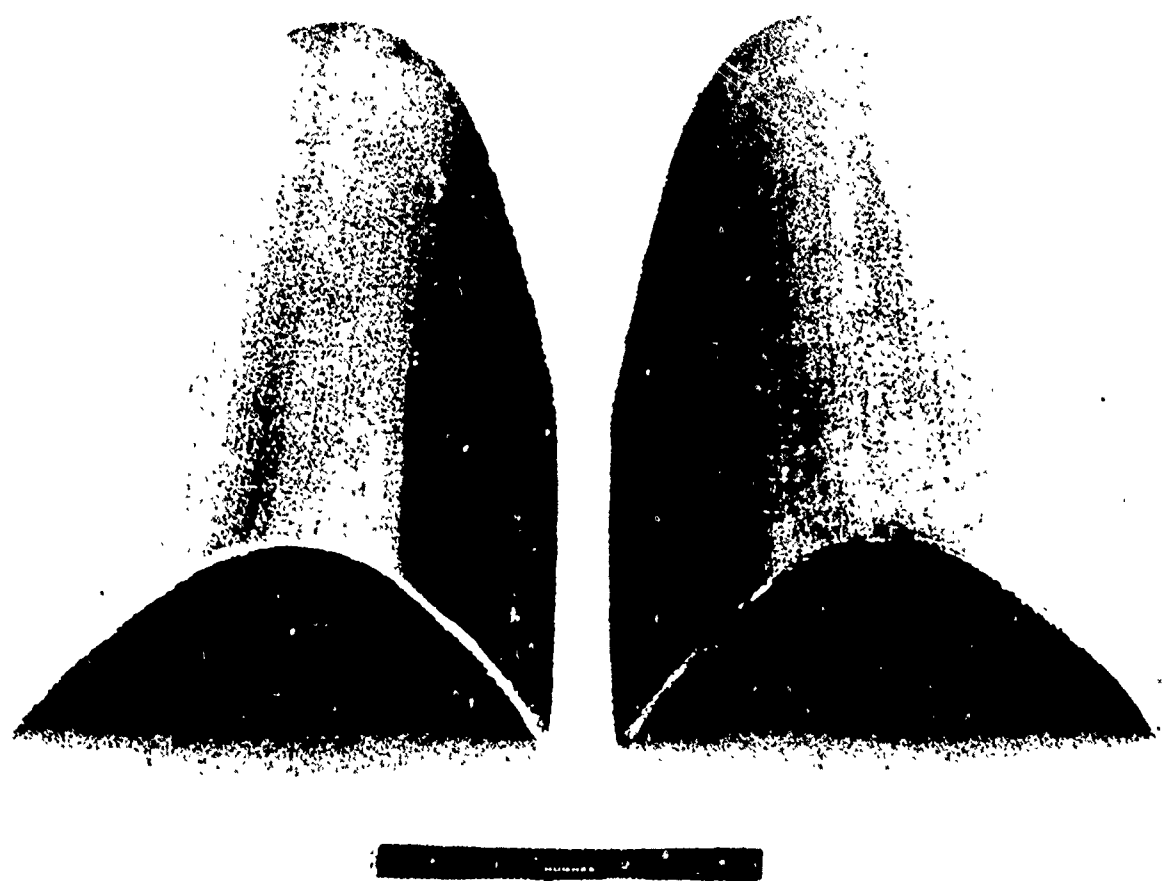


Figure 69. Experimental radome structures fabricated from 3-D PRD-49/epoxy